SIMULATION OF SURFACE WATER TEMPERAURE AND ICE EXTENT IN LAKE ONTARIO AND LAKE ERIE USING A DYNAMIC RESERVOIR SIMULATION MODEL (DYRESM)

by

R.C. McCrimmon[1], W.M. Schertzer[2]
and A.M. Sawchuk[3]

NWRI Contribution No. 88-32

[1] 3481 Galena Crescent
MISSISSAUGA, Ontario
L5A 3L7

[2] Project Leader: NWRI Climate Studies
National Water Research Institute
Canada Centre for Inland Waters
BURLINGTON, Ontario L7R 4A6

[3] University of Toronto (Scarborough Campus)
TORONTO, Ontario

EXECUTIVE SUMMARY

As part of the NWRI commitment to the Canada Climate Program to define the climatology of the lake responses to climate changes, an examination of the simulation capability for water surface temperature was undertaken. Accurate estimation of this parameter is crucial since formulations for some of the major air/water exchange parameters in heat balance analyses such as radiation exchange, evaporation and scaling transformations are functions of the water temperature. Direct temperature observations by lakewide ship measurements, airborne radiometer technique (ART) overflights or recently by satellite technology are either time consuming or expensive to undertake and do not provide the required temporal resolution for simulations. In this study, atmospheric variability is incorporated within a dynamical reservoir simulation model to simulate the water temperature. Agreement between observed and computed temperatures is exceptional and tested with 31 years of data from both Lake Ontario and Lake Erie.

MANAGEMENT PERSPECTIVE

This investigation was undertaken as part of the NWRI-Climate Studies on the Lower Great Lakes in support of the Canada Climate Program. The DYRESM model was initialized using a heat flux model developed at NWRI under the climate studies program and run using a long-term climate data base collated at NWRI. DYRESM was demonstrated to provide highly accurate estimations of the daily surface water temperature for the Lower Great Lakes over the period 1966-1983. Since water surface temperature is a primary parameter used in the study of the physical, chemical and biological characteristics of lakes, the accuracy of the model simulations represent a significant advance for studies requiring temperature estimates over short time scales or for periods not represented by ship cruises or by satellite digital data.

ABSTRACT

The one-dimensional dynamic reservoir simulation model, DYRESM, was used to simulate the physical response of Lake Ontario from 1967-1982 and Lake Erie from 1967-1983 to inflow/outflow and meteorological conditions. The model simulates the daily vertical lakewide average temperature profile and the fraction of ice cover. Emphasis was placed on comparisons between simulated and observed water surface temperatures and fractional ice cover. Relatively good agreement was achieved for the water surface temperatures for both lakes. Reasonable agreement for the ice cover fractions was also achieved for both lakes except for four years for Lake Ontario during which the amount of ice cover was over simulated. The suspect cause of the over-simulation of ice was the lack of ice dynamics and variable ice thickness in the ice component of DYRESM.

The results contained herein describe research conducted within the NWRI Climate Studies DSS Contract KW405-5-1182.

PERSPECTIVES DE GESTION

Ces recherches ont été entreprises dans le cadre des études climatologiques INRE des Grands lacs inférieurs, pour le Programme climatologique canadien. Le modèle DYRESM a été conçu à partir d'un modèle de flux thermique, mis au point à l'INRE dans le cadre du programme d'études climatologiques, et exploité à l'aide d'une base de données climatologiques à long terme, réunies à l'INRE. Le DYRESM a donné des estimations très exactes de la température quotidienne de l'eau de surface des Grands lacs inférieurs pendant la période 1966-1983. Étant donné que la température à la surface de l'eau est un paramètre essentiel pour l'étude des caractéristiques physiques, chimiques et biologiques des lacs, l'exactitude des simulations du modèle constitue un progrès significatif dans les recherches nécessitant des estimations de température pour des échelles de courte durée, ou pour des périodes non représentées par des campagnes de navires ou par les données numériques d'un satellite.

RÉSUMÉ POUR LA DIRECTION

Dans le cadre de la participation de l'INRE au Programme climatologique canadien visant à caractériser la climatologie des réactions d'un lac aux variations climatiques, on a entrepris des recherches sur les possibilités de simulation pour la température de surface de l'eau. Une évaluation exacte de ce paramètre est primordiale, car les formulations de certains des principaux paramètres d'échange air/eau dans les analyses de bilan thermique, comme l'échange radiatif, l'évaporation et les transformations d'échelle, sont fonction de la température de l'eau. Les mesures directes de température, à bord de navires sur toute l'étendue du lac, par des survols avec des radiomètres aéroportés, ou récemment à l'aide de satellite, sont très coûteuses en temps et en argent, et ne fournissent pas les données temporelles nécessaires aux simulations. Dans cette étude, la variabilité atmosphérique est incorporée dans un modèle de simulation dynamique de réservoir, afin de simuler la température de l'eau. La corrélation entre les températures observées et celles calculées est exceptionnelle; elle a été vérifiée à l'aide de données d'une période de 31 ans pour le lac Ontario et le lac Érié.

RÉSUMÉ

Le modèle de simultation dynamique unidimensionnel de réservoir, le DYRESM, a été utilisé pour simuler la réaction physique du lac Ontario de 1967 à 1982, et du lac Érié de 1967 à 1983, aux valeurs d'entrée/sortie et aux conditions météorologiques. Le modèle simule le profil vertical de la température quotidienne moyenne à la largeur du lac, et la fraction de couverture de glace. On a beaucoup insisté sur la comparaison entre les températures de la surface de l'eau, simulées et observées, et la fraction de couverture de glace. Les températures de surface de l'eau accusaient une corrélation relativement bonne pour chacun des deux lacs. Il y avait également corrélation raisonnable pour les fractions de couverture de glace dans les deux lacs, excepté une période de quatre années dans le cas du lac Ontario, pendant laquelle la quantité de couverture de glace se trouvait sursimulée. La cause probable de ce phénomène était l'absence de dynamique glaciale et de variabilité de l'épaisseur de glace dans la composante glaciale du DYRESM.

Les résultats présentés ici décrivent des recherches effectuées dans le cadre des études climatologiques INRE, sous contrat MAS KW405-5-1182.

SUMMARY AND CONCLUSIONS

This project investigates the accuracy of simulating the lakewide average thermal structure response and ice formation/ablation of Lake Ontario and Lake Erie to inflow/outflow and meteorological conditions on a daily basis using the dynamic reservoir simulation model, DYRESM. The availability of model input data and observations for simulation comparisons allowed use of DYRESM over the period of 1967-1982 for Lake Ontario and 1967-1983 for Lake Erie. The model accounts for surface energy exchanges due to shortwave and longwave radiation fluxes and to evaporative and sensible heat fluxes. It simulates mixing due to density instabilities, wind energy, diffusion, inflow and outflow in order to predict a daily vertical temperature profile and ice cover fraction. The accuracy of the model was assessed by comparing the simulated water surface temperatures and ice cover fractions with observations. A Lake Ontario and Lake Erie validated DYRESM could be used as a predictive management tool or to provide needed information for water quality models.

The conclusion of this project, based upon the comparisons of simulated and observed water surface temperature and ice extents, is that DYRESM is capable of simulating lakewide average conditions for both Lake Ontario and Lake Erie. Relatively good agreement between simulated and observed surface water temperatures was achieved for

both lakes. Fractional ice cover simulations were also relatively good for Lake Erie. The fractional ice cover simulations of Lake Ontario, however, were in reasonable agreement with observations for only 75 percent of the years, the remaining years being too high. The oversimulation of ice cover was related to a lack of ice dynamics in DYRESM and to variable ice thicknesses during partial ice cover. These factors appear important for Lake Ontario which rarely attains 100 percent ice cover. Conditions in Lake Erie more closely resemble the DYRESM ice model conditions and hence better simulations were accomplished.

Future applications of DYRESM to the Great lakes include using it as a predictive management tool. Also, the model could be used to calculate values of water temperature or ice cover on days for which observations are not available. The results of the model could also be used to simulate physical processes of a lake and the results could then be used in a water quality model which normally does not take account of physical aspects of the lake.

Research into the accuracy of the simulated vertical temperature profiles should be investigated. It is possible that the simulated profiles could be improved by further model calibration. This in turn could further improve the simulated water surface temperatures.

DYNAMICAL SIMULATION MODELLING OF SURFACE WATER TEMPERATURE AND ICE EXTENT ON THE LOWER GREAT LAKES

INTRODUCTION

Water quality responses of lakes can be influenced by prevailing meteorological conditions which have an effect on lake stratification (Lam, Schertzer and Fraser, 1983). Computation of the complete annual thermal cycle and boundary conditions are often hampered by insufficient information regarding overlake conditions. Surface water temperature is a fundamental parameter which is incorporated within formulations of the air/water heat exchange and generally heat gains and losses to the lake due to ice formation and decay are difficult to estimate. More accurate simulation of water surface temperature and reasonable indications of fractional ice extent may help to improve the predictive capability of water quality models of large lakes.

In this study, a dynamic reservoir simulation model (DYRESM) is applied to Lake Ontario and Lake Erie. DYRESM is a one-dimensional model which has been tested on lakes of varying sizes (e.g. Ivey and Patterson, 1984, Patterson and Hamblin, 1984, Imberger and Patterson, 1981).

GOALS AND OBJECTIVES

The basic goal of this study is to apply DYRESM to Lake Ontario and Lake Erie over the period 1967 to 1983 to simulate lakewide hydrometeorological conditions. In fulfilment of the contract objectives, required hydrometeological and limnological data have been collated and stored in computer data bases. The DYRESM model has been calibrated for Lake Ontario and Lake Erie conditions and simulated results for heat flux and stratification components have been stored for future analysis.

The purpose of the following report is to describe the formulations within DYRESM and to provide a summary of the simulated water surface temperature and fractional ice extent for Lake Ontario and Lake Erie.

DYNAMIC RESERVOIR SIMULATION MODEL (DYRESM)

The dynamic reservoir simulation model, DYRESM, was originally developed to predict the vertical variation of temperature and salinity in medium sized reservoirs (Patterson et al., 1978). An ice/snow model was added to DYRESM by Patterson and Hamblin (1984) for ice and snow simulations. This also allowed for temperature simulations during ice periods. DYRESM is a one-dimensional model based on

lakewide averaged values but is capable of simulating partial ice cover and its effects on heating rates.

The one-dimensionality of DYRESM is based on a Lagrangian layer structure composed of as many as 150 slab-like layers. Each layer is of variable thickness and is assumed to be homogeneous throughout. To simulate changes in a reservoir the layers can change their volume, temperature/salinity and vertical location but not their relative position. For example, to model inflow, certain layers are thickened or inserted and any layers overlying them are shifted upwards because of the underlying increase in volume. Similarly, outflow is simulated by layer depletion or removal and the downwards shifting of overlying layers. Layers can also be amalgamated to simulate mixing. Besides renumbering and vertically moving layers, only the layers directly affected by the kinematics are operated upon. This makes for an economic operation.

The computer code is composed of a relatively simple mainline program, DYRESM, which calls the necessary subprograms to simulate different processes. More specifically, DYRESM controls the input, output, daily loop, sub-daily loop and calculates fixed parameter values. Within the daily loop, inflow and outflow are simulated using subroutines INFLOW and OUTFLO respectively. In the sub-daily loop deep mixing is simulated in subroutines FCT and DIFUSE, surface mixing in MIXER and meteorological forcing, ice formation and ablation in subroutine HEATR. DYRESM also uses service routines DENSITY, RESINT

and THICK to calculate the density, surface area and volume (or thickness) of layers and to ensure that layer volumes stay within prescribed limits. A flow chart of DYRESM is presented in Figure 1.

The initial step of DYRESM is to read in the fixed data, which includes storage, surface area and length at different depths, the initial temperature and salinity profiles, simulation and print control parameters, and calibrated parameter values. The daily loop is then initiated by reading in daily inflow, outflow and meteorological data. After reading this data the sub-daily forcing-mixing-diffusion loop is entered. Meteorological forcing, surface mixing and deep-mixing are simulated with a sub-daily time step between one quarter hour and six hours. The smaller time step, which is calculated in subroutine HEATR based on the rate of transfer of thermal energy at the surface, is required to better simulate mixing time scales. The sub-daily loop begins with the meteorological forcing computations performed by HEATR, follows with epilimnetic mixing using MIXER and ends with the turbulent diffusion simulation using FCT and DIFUSE. After this sub-daily loop is finished, the daily loop is re-entered and INFLOW and OUTFLO are called by DYRESM. The last function of DYRESM is to print out the results of the day's simulation. A more detailed description of the model will be presented below.

DYRESM also calculates interpolation coefficients, (used in subroutine RESINT), from the input storage-depth and surface

area-depth relationships. The service subroutine RESINT is used to calculate layer volumes and surface areas from layer heights or to calculate layer heights and surface areas from volumes. Therefore, when layer volumes or heights are changed by an operation, then RESINT will be called.

After the initial temperature profile is read by DYRESM, the subroutines DENSITY and THICK are called. DENSITY calculates the density of the water in each layer based upon its temperature using the formula

$$\begin{aligned} \text{DENSITY} = {} & 0.9998395 + 6.7914*10^{-5}*T - 9.0894*10^{-6}*T^2 \\ & + 1.0171*10^{-7}*T^3 - 1.2846*10^{-9}*T^4 \\ & + 1.1592*10^{-11}*T^5 - 5.0125*10^{-14}*T^6 \end{aligned} \quad (1)$$

where T is the water temperature (°C) and the density is in units of kg/L. Subroutine THICK is used to ensure that layers do not exceed a volume, V_{max}, in order to maintain a reasonable resolution, and are not smaller than a volume, V_{min}, to limit the number of layers required. Imberger and Patterson (1981) found that reasonable values are $V_{max} = S/N$ and $V_{min} = 2V_{min}$ where S is the lake capacity and N is the maximum number of layers of 150. When a layer is larger than V_{max} it is divided into an appropriate number of layers, all less than V_{max}. When a layer is less than V_{min}, it is amalgamated

with its smallest neighbour to form one layer, then rechecked against V_{min} and V_{max}.

Subroutine HEATR

DYRESM enters the daily loop after the above detailed preliminary calculations and reads the daily data. Immediately after this the sub-daily forcing-mixing-diffusion loop is initiated with the calling of subroutine HEATR. HEATR performs the meteorological forcing computations, which consist of calculating: transfer of heat at the lake surface due to the shortwave radiation incident on the surface, evaporative heat flux, conductive heat flux and longwave absorption heat flux. The daily data required for this subroutine are:

SW = Incident short wave radiation ($KJ/m^2/d$)

SRAT = Sunshine ratio (sunshine hours/daylight hours)

T4 = Average daily air temperature (°C)

SVPD = Average daily air vapour pressure (mb)

U6 = Average daily wind speed (m/s)

RAIN = Daily total precipitation (mm)

ETW = Water extinction coefficient (1/m)

HEATR also performs the ice formation and ablation computations, which are based upon the heat fluxes at the surface and at the water/ice interface. All of the calculated sources and sinks of heat at the surface are proportioned over each time period and then applied over the entire day. The daily input of shortwave radiation, however, is assumed to apply only over the last 12 hours of a day and, therefore, is divided by 48 and applied equally over each of the 48 quarter hour time periods of a half day. The input of total daily precipitation is divided equally and applied over each of the 96 quarter hour time periods in a day.

The evaporative and conductive heat fluxes are based on the fluxes of moisture, E, and heat, H, given as:

$$E = -C_w*U6(f-f_s)*p \qquad (2)$$

$$H = -C_H*U6(T-T_s)*p*C_p \qquad (3)$$

in which C_H and C_w are the bulk transfer coefficients, T is temperature, f is the humidity, p is density, C_p is the specific heat of water and subscript s refers to the surface. These fluxes are based upon bulk aerodynamic formulae. The constants C_H and C_w range from $1.3*10^{-3}$ to $1.5*10^{-3}$. A value of $1.4*10^{-3}$ was assumed by Imberger and Patterson (1981). The formulations of equations 2 and 3 are coded in DYRESM as:

$$XEV = -3.51*U6*(SVPO-SVPD) \qquad (J/m^2/s) \qquad (4)$$

$$XCO = R*XEV = 2.282*U6*(T_S-T4) \qquad (J/m^2/s) \qquad (5)$$

where XEV is the evaporative heat flux, XCO is the conductive heat flux, T4 is the average daily air temperature, SVPD is the average daily vapour pressure, SVPO is the average daily saturation vapour pressure at T_S and R is the Bowen ratio. DYRESM assumes a positive heat flux is directed towards the lake surface.

Longwave radiation heat fluxes are both emitted from the water surface and absorbed at the water surface. The emitted radiation is:

$$QW = -5.53*10^{-8}*(T_S+273)^4 \qquad (6)$$

where QW is the emitted longwave radiation ($J/m^2/s$). The longwave radiation absorbed in the water is the sum of the radiation emitted by clouds plus a fraction of the emitted radiation being re-radiated back to the earth. The incoming longwave flux estimates of Sawchuk and Schertzer (1987) are used in this study.

Shortwave radiation SW, used in this analysis, is also computed using formulations described by Sawchuk and Schertzer (1987). Penetration of the shortwave radiation within the water column is modelled after Beers Law

$$q(z) = SW*e^{-n_1 z} \tag{7}$$

where n_1 is the bulk extinction coefficient and z is the depth. In order to account for the reduction of shortwave radiation due to ice and snow cover, the actual shortwave radiation reaching the water surface q(z) is modelled using:

$$q(z) = ALW*SW(1-FICE)*e^{(-X_w z)}+SW*AL*FICE*e^{(-X_i h_i)} \tag{8}$$
$$*e^{(-X_w z)}*e^{(-X_s h_s)}$$

where FICE is the fraction of the water surface covered by ice, subscripts i, s and w refer to ice, snow and water respectively, X is the extinction coefficient (1/m) (for ice=1.5, for snow=14), ALW is the albedo of the water (=1.0), AL is the albedo of the ice or snow, and h is the component thickness (m).

These meteorological heat fluxes are also used in the ice formation and ablation computations. The ice/snow model is based upon two conditions which incorporate the necessary heat fluxes including the meteorological heat fluxes.

The first condition, surface flux condition, sums all heat fluxes at the surface to determine the surface temperature and the amount of ice or snow melting, if any. The heat flux at the surface of the ice

or at the surface of the snow, when there is snow cover, is computed after Maykut and Untersteiner (1971) as:

$$q_o = \frac{K_i K_s (T_f - T_o) + I_o [K_i h_s + K_s h_i - \frac{K_i (1-e^{(-X_s h_s)})}{X_s} - \frac{K_s (1-e^{(-X_i h_i)}) e^{(-X_s h_s)}}{X_i}]}{K_i h_s + K_s h_i} \quad (9)$$

where q_o is the heat flux at the surface of the upper snow or ice layer, K_x is the thermal conductivity of ice for x=i and snow for x=s, T_o is the surface temperature, T_f is the freezing temperture of water and I_o is the non-reflected shortwave radiation intensity at the surface. The change in the surface temperature required to balance q_o with the meteorological fluxes due to absorbed and emitted longwave radiation, conduction and evaporation is calculated and implemented. However, if there is a heat gain and the temperature is raised to the melting point then any remaining heat is used for melting at the surface. Ice formation at the surface is assumed not to occur and only the snow thickness can increase by precipitation.

The second condition, ice/water interface flux condition, is the basis for ice formation and ablation at the ice/water interface. It uses the heat flux in the ice which depends upon the conditions at the surface, and the heat flux from the water to the ice which depends

upon the conditions in the water. The heat flux in the ice, q_f, is calculated as

$$q_f = q_o - I_o \left(1 - e^{-(X_s h_i + X_i h_i)}\right) \tag{10}$$

The heat flux from the water to the ice, q_w, was specified as a parameter in the Maykut and Untersteiner (1971) model. Patterson and Hamblin (1984), however, assumed q_w to be the sum of laminar and turbulent transport fluxes, which essentially links the ice formation and ablation to the underlying water. q_w is calculated as

$$q_w = -K_w \frac{dT_w}{dz} \Big|_{z=0} + C_s \rho_w C_p U (T_w - T_f) \tag{11}$$

where, K_w is the molecular conductivity, z is the distance from the interface, C_s is the sensible heat transfer coefficient C_s = 0.0014 (Hamblin, 1985), C_p is the specific heat of water and U is the speed of flow in the top water layer. Ice formation or ablation is then calculated using

$$q_f - q_w = \rho_i L_i \frac{dh_i}{dt} \tag{12}$$

where L_i is the latent heat of fusion of ice and t is time.

With an assumed minimum ice thickness, partial ice cover is also simulated. If the ice thickness is less than the minimum thickness, then the existing volume of ice is transformed into a smaller area with an equivalent volume at the minimum thickness. Therefore, as ice forms or melts, the fraction of ice cover will increase or decrease respectively. Only when the entire surface is covered at the minimum thickness can the ice thickness increase.

A minimum ice thickness of 10 cm has been used for medium sized northern lakes (Patterson and Hamblin, 1984). Factors, such as, surface wind stress or ice underflow, most likely affect the value of minimum ice thickness but such relationships have not been incorporated in the model. Since Lake Ontario and Lake Erie are large lakes, a larger minimum ice thickness of 20 cm was used (Hamblin, 1985, per comm).

The time step used in HEATR and MIXER is calculated in HEATR. The minimum time step is set at 900 seconds or one quarter hour. The maximum time step is six hours due to the six hour wind speed components used. In order to prevent the turbulent velocity scale, w*, and the mixed layer mean velocity, U, from becoming too large in subroutine MIXER, the change in surface temperature before MIXER is called is limited to 3°C. The conductive, evaporative and longwave heat fluxes are each calculated for one quarter hour and summed to determine a change in heat in the surface layer. Then, if appropriate, the heat increase due to shortwave radiation applied over a

quarter hour is added. Since the input data is in the form of a daily average, it is assumed that a temperature change due to the above heat sources will be the same for each subsequent quarter hour period. Therefore, if delT is the calculated temperature change in the surface layer over one quarter hour, then the time step is limited to

$$n_q\ (T) = 3.0/delT \tag{13}$$

where n_q is the integer number of quarter hour periods with a minimum of one. The time step, n_q, must also satisfy the mean velocity criterion of

$$n_q\ (U) = 0.1h/u^{*2} \tag{14}$$

where h is the mixed layer depth from the previous time step, u* is the current wind shear velocity and U is the mixed layer mean velocity. This criterion is used to ensure the mean velocity increase is limited to 0.1 m/s over the previous value. The temperature increment for each layer over n_q quarter hours is then calculated and added to the existing temperature.

The surface layer is adjusted at the end of HEATR to account for precipitation and evaporation. The precipitation is a daily input and the water level change due to evaporation, WLOST, is also calculated daily as

$$WLOST = XEV/L \quad (15)$$

where L is the latent heat of evaporation ($2.453*10^9$ J/m^3).

Subroutine MIXER

Subroutine MIXER is called after HEATR to simulate mixing in the epilimnion. If surface cooling occurred in HEATR, then the density of the surface layer may have become greater than that of underlying layers, causing the density structure to become unstable. To maintain a stable structure MIXER performs layer amalgamation for the surface layer with less dense underlying layers.

If layer amalgamation is performed then the center of gravity will be lowered, releasing potential energy. This potential energy per unit area is the buoyancy flux, APE. If this energy flux is sufficient, then further mixing is performed, which increases the mixed layer thickness. MIXER then combines any residual energy with the wind power flux to attempt further mixing. Layer amalgamation is performed until the available energy is less than the energy required to mix with the next layer. Any residual energy is then stored for use in the next mixing event.

If after the mixing phases the interface is too thin then it will be unstable to shear. Subroutine KH is called to account for the

formation of the Kelvin-Helmholtz billows at the interface. If the billows are large enough, KH forms at least six layers over the shear zone and mixes from the interface outwards to form a linear density gradient across the billow thickness.

The last function of MIXER is to amalgamate layers of equal density irrespective of the volume constraints. The purpose of this procedure is to reduce the computations that will be required in the diffusion calculations that follow MIXER.

Diffusion Subroutines

Using subroutines FCT and DIFUSE, the final step of the sub-daily loop simulates the mixing in the hypolimnion by turbulent diffusion. The constant flux model

$$\frac{dT_i}{dt} = \frac{1}{p_i A_i} * \frac{d}{dz}\left(A_i p_i E \frac{dT_i}{dz}\right) \qquad (16)$$

is the form of the diffusion equation being solved where p is the density, A is the layer surface area, E is the eddy diffusivity and subscript i denotes the layer number. The vertical diffusion coefficient is calculated as

$$E = a_1 * H^2/(T_M * S) \qquad (17)$$

where a_1 is a vertical transport constant, H is the lake depth, T_M is a mixing time scale and S is a stability factor. The diffusion constant a_1 is actually a function of the basin shape, stratification and forcing history but through experience (Imberger and Patterson, 1981) a constant value of 0.048 produces good results provided the basin shape is not too contorted. the stability factor is calculated as

$$S = \frac{H}{P}\frac{dp}{dz} \qquad (18)$$

where $\frac{dp}{dz} = \frac{p_i - p_{i+1}}{h_{i+1} - h_i}$

h = height to centre of layer i

p_i = density of layer i

P = difference in density from top to bottom of reservoir

H = total lake depth

FCT is used to calculate equation (17) and the right side of equation (16) for each layer. DIFUSE is then used to determine the redistribution of heat by ensuring no reversals in the temperature gradient occur. This is accomplished by amalgamating two layers when the slope of T changes sign across the two layers.

The mixing time scale, T_m, employed in FCT when solving equation (17) is calculated as

$$T_m = E/(P_s + P_w) \tag{19}$$

where P_s is the rate of working of the inflowing water, P_w is the rate of working of the wind and E is the potential energy locked in stratification.

Subroutine INFLOW

Subroutines FCT and DIFUSE are called for each quarter hour period in the sub-daily time step. The sub-daily loop is then repeated until the entire day has been covered.

After the completion of the forcing-mixing-diffusion loop, the daily loop continues with the insertion of the daily inflow using subroutine INFLOW. The basic procedure for inserting the inflow is to first compare the inflow density with the surface layer density. If the inflow density is less than the surface layer density, the inflow is mixed with this layer. If the inflow density is greater than the surface layer density, the inflow continues downward and entrains water from the surface layer, decreasing the density and increasing the volume of the inflow. The new inflow density is then compared to

the next layer density. This process is repeated until a layer with a greater density is reached. The inflow is then inserted at the mid-point of this layer.

The entrainment from the layer, Q_d (m^3/d), is calculated as

$$Q_d = Q((H/HO)^{5/3}-1) \tag{20}$$

where Q is the inflow at the top of the layer, HO is the initial flowing depth at the top layer and H is the present flowing depth. The parameters H and HO are calculated in INFLOW using the drag coefficient, the slope of the incoming river and the half angle of the river cross-section. Details of the above are given in Imberger and Patterson (1981). The inflow is then mixed with the layers within a thickness 2d where

$$d = \frac{Q}{B}\left(1 - \frac{e}{L}\right)\frac{1}{e} \tag{21}$$

where B and L are the reservoir width and length at the level of insertion and e is the length of inflow intrusion. Restricting the entrance thickness to 2d insures that the inserted fluid is in static equilibrium with the fluid in the layers which it pushes ahead itself (Imberger and Patterson, 1981).

Subroutine OUTFLO

Following the inflow calculations, subroutine OUTFLO is called to withdraw the daily outflow. OUTFLO is capable of simulating withdrawal from submerged offtakes and as overflow. However, when overflow is simulated, which is especially used in lake applications, the point of withdrawl is fixed at the surface and the upper half of the withdrawl thickness, d_T, is restricted to zero outflow. Therefore, all overflow is apportioned over a bottom thickness, d_B. The withdrawal for each layer is calculated and withdrawn and the layers and surface level are shifted downwards due to the volume decrease.

The final step of the daily loop is to print the results of the daily calculations. The daily loop is repeated for the followng days until the end of the simulation period.

DATA BASE

The basic input data to DYRESM include the following meteorological, hydrological and limnological parameters:

hypsometric data (depth, area, volume)	(m, m^2, m^3)
wind speed (daily average)	(m/s)
wind velocity (6-hour component along lake axis)	(m/s)

air temperature	(°C)
vapour pressure	(mb)
precipitation	(mm)
shortwave radiation	($KJ/m^2/day$)
longwave radiation	($KJ/m^2/day$)
water level	(m, ASL)
extinction coefficient	(1/m)
inflow volume and temperature	(m^3/s, °C)

Figures 2 and 3 show Lake Ontario and Lake Erie including locations from which meteorological and hydrological data were obtained. Hypsometric data are plotted in Figures 4 and 5 for Lake Ontario and Lake Erie respectively. Lake Ontario has a mean depth of 90 m, a surface area of 18484 km^2 and a volume of $0.167 \times 10^{13} m^3$. In comparison, lake Erie has a mean depth of 18.7 m, a surface area of 25320 km^2 and a volume of $0.473 \times 10^{12} m^3$.

The primary sources of data used in this report include the Atmospheric Environment Service (AES), National Climate Digital Data Service (NCOS), Water Survey of Canada (WSC), U.S. Army Corps of Engineers (U.S. Corps), U.S. Geological Survey (USGS), Water Planning and Management Branch (Canada Centre for Inland Waters, WPM).

The majority of the data utilized was collated from the long-term climatological analyses of Sawchuk and Schertzer (1987). A general summary of the data base is given below.

Meteorological Data

Wind speed, air temperature and vapour pressure longterm averages and extremes are illustrated in Figures 6, 7 and 8 for Lake Ontario and Lake Erie, respectively. Daily estimates of the overlake values were derived by Sawchuk and Schertzer (1987) according to relationships developed by Phillips and Irbe (1972) based on 6000 paired lake-land observations during the International Field Year for the Great Lakes (IFYGL). Overlake values are dependant on stability and fetch criteria.

Wind speed measurements from meteorological stations at the lake periphery were modified to a common 6 m height for application to DYRESM using the logarithmic wind profile relationship

$$u_2 = u_1 (z_2/z_1)^{1/7} \qquad (22)$$

where u is wind speed, Z are measurement heights and the subscripts represent height levels 1 and 2. Within DYRESM, daily average wind speeds are used. Illustrated in Figure 6 are 2-day averaged wind speeds and extremes for Lake Ontario and Lake Erie. The long-term means for Lake Ontario indicate a larger range in the seasonal wind regime than that of Lake Erie. Minimum wind speeds occur in the spring and summer months and maximum wind speeds occur in the fall and winter period. Figure 6 also indicates that over the long-term

analysis, a substantial variation in the range of daily wind speeds is expected. Appendix 1 illustrates that wind speed departures from the longterm means for Lake Ontario and Lake Erie.

The 6-hourly wind velocity components along the lake axis for each lake were computed using hourly wind speed and direction by applying the Theisson polygon method on data from Kingston, Toronto Island, Trenton, Rochester, and Buffalo in Lake Ontario and meteorological stations Cleveland, Detroit, Erie, Toledo and Buffalo for Lake Erie.

Overlake air temperature and extremes for the longterm analysis is given in Figure 7 for Lake Ontario and Lake Erie. Mean air temperature maximum occur between 21-22°C for Lake Erie and about 20-21°C for Lake Ontario in the months of July and August. Mean mimimum temperatures occur in January and February for both lakes. Based on the long-term values derived by Sawchuk and Schertzer (1987) it appears that the range of air temperature on an annual and daily extreme basis is larger for Lake Erie. Appendix 2 illustrates the air temperature departures from the long-term mean for both Lake Ontario and Lake Erie.

Figure 8 illustrates the longterm summary of the overlake vapour pressure and extremes for Lake Ontario and Lake Erie based on land station dew point temperatures modified to overlake conditions (Sawchuk and Schertzer, 1987). Maximum vapour pressure occurs in the summer months and the extremes are larger for Lake Erie. Appendix 3

provides a summary of the vapour pressure departures from the long-term means.

Radiation Data

Incoming global solar radiation and incoming longwave radiation are used as inputs to DYRESM based on computations given in Sawchuk and Schertzer (1987). Longterm means of the radiation values are provided in Figures 23, 24, 25 and 26. Incoming solar radiation averages from a minimum of 2-4 $MJ/m^2/day$ in January-February to an average of 18-20 $MJ/m^2/day$ in the period June-July. Very large extremes in the values of solar radiation occur for both lakes due to the effects of over lake cloud and fog. Incoming longwave radiation shows much less variability compared to solar radiation. According to the computed longterm means (Sawchuk and Schertzer, 1987) the average incoming longwave radiation ranges from approximately 20-22 $MJ/m^2/day$ in winter to 30-34 $MJ/m^2/day$ in the June to July period.

Hydrological and Limnological Data

The hydrological and limnological inputs to DYRESM include water level, precipitation, extinction coefficient and river inflow volume and temperature.

Lakewide average surface water level was calculated using the Theisson polygon method incorporating the daily mean water levels from Bar Point, Kingsville, Erieau, Port Stanley, Port Dover, and Port Colbourne, for Lake Erie and Port Weller, Burlington Pier, Toronto, Cobourg and Kingston stations for Lake Ontario. For both lakes, these stations are biased to the north shore and an error in the lakewide mean water level may be introduced. Observed water levels by the Fisheries and Marine Service of Canada were recorded to the nearest 0.01 m. The lake depths used in DYRESM, which were calculated using the lakewide average water levels, are given in Figure 9 and 10 for Lake Ontario and Lake Erie.

Lakewide average precipitation was also computed using the Theisson polygon technique using data from AES and NOAA meteorological stations. For Lake Ontario, representative values were obtained from Hamilton, Toronto Island, Toronto Airport, Port Hope, Cobourg, Trenton, Kingston, Syracuse and Rochester. Data from the two Toronto stations and also from Port Hope and Cobourg were averaged due to their close proximity. Precipitation for Lake Erie was derived using data from Port Colbourne, Port Stanley, Pelee Island, Kingsville, Buffalo, Erie, Cleveland and Toledo. All Canadian data were recorded to the nearest 0.1 mm of water or water equivalent while all American data was recorded to the nearest 0.254 mm of water. A time series of the precipitation for Lake Ontario and Lake Erie is given in Figures 11 and 12, respectively.

Lakewide average light extinction coefficients were calculated using observed Secchi disc (30 cm disc) observations which are spatially interpolated and averaged over the lake. Lakewide mean values were determined for each survey of the lake. Interpolation through the cruise means provided daily estimates for use in DYRESM. Figures 13 and 14 show the mean vertical extinction coefficient for Lake Ontario and Lake Erie respectively. A long-term average extinction and range of value is given in each illustration. In general, summertime values of light extinction range from 0.3 to 0.5 1/m for Lake Ontario and from 0.4 to 0.5 for Lake Erie.

DYRESM requires inflow volume and corresponding temperatures as input. For this analysis it is assumed that the Detroit River is the sole input to Lake Erie and that the combined flow of the Niagara River and Welland Canal are the sole inputs to Lake Ontario. Daily inflow volumes are ploted in Figures 15 and 16 for both lakes. Included in each figure is inflow temperature which is the average of several years of data recorded by the USGS. The same temperature curves are used for each year of calculation for each lake.

Model Calibration

Lakewide surface water temperature and fractional ice-cover were the primary outputs of DYRESM for the purposes of this study. Water

temperature values summarized by Schertzer and Sawchuk (1985) using data collected from CCIW cruises, airborne radiometer observations and satellite data (AES 1985) formed the data base from which DYRESM simulations could be compared. Observed fractional ice cover for Lake Ontario 1966-1982 and for Lake Erie 1980-1983 were derived by planimetry of the Great Lakes composite ice charts (NOAA 1983). Half-monthly averages of ice cover for Lake Erie from 1967 to 1979 were obtained from NOAA (1983). A summary of observed water surface temperature and fractional ice cover for the longterm period is illustrated in Figures 17 and 18 for both lakes.

Calibration of the DYRESM model was accomplished using water surface temperatures and fractional ice cover in the period May 1972 to March 1983. For Lake Ontario this time interval represented the period of intensive measurements during the International Field Year for the Great Lakes (IFYGL) and therefore allows for detailed calibration. Fewer observations were available for calibration of DYRESM for Lake Erie, however, for both lakes, the observations for both water surface temperature and fractional ice cover were sufficient to calibrate over an annual cycle beginning in isothermal conditions, extending through the period of build-up and breakdown of the thermal structure in the summer and fall and through the ice formation and ablation stages during the first three months of 1973.

Lake Ontario Calibration

DYRESM calibration results for water surface temperature and fractional ice extent are illustrated in Figures 19 and 21 for the period May 1972 to March 1973. In terms of temperature, simulated and observed values rarely differed by more than 1°C indicating very good results. Simulations for ice cover fraction, however, showed less accuracy. During the winter of 1972/1973, the observed fractional ice extent varied significantly. Basically, in January the ice cover ranged from 0 to 35 percent; in February it varied from 20 to 70 percent and in March, all ice melted. DYRESM did not simulate ice in January but the seasonal cycle of ice increase and decrease was simulated over the February to March period. The ice model was developed by Patterson and Hamblin (1984). The absence of ice dynamics in DYRESM was expected to cause an over-simulation of ice cover but the opposite occurred suggesting that the ice model may not be the sole cause of the under-simulation. During December 1972 and January 1973, the water surface temperature was simulated slightly too warm. The resulting higher heat storage may have delayed the onset of ice formation and thus reduced the total amount of ice simulated in the calibration year.

As indicated previously, the primary parameter simulated in this study is water surface temperature. Since the calibration results indicate very good correspondence between observed and computed

temperatures, DYRESM was assumed adequately calibrated for Lake Ontario.

Lake Erie Calibration

Lake Erie is shallower than Lake Ontario and has a smaller heat storage (Schertzer, 1987). Figure 18 indicates that Lake Erie frequently achieves 100 percent ice cover over most years. After incorporating the hypsometric features (Figure 5) essentially the same version of DYRESM as used for Lake Ontario was applied to Lake Erie. Calibration testing was performed over the same period May 1972 to March 1983. A comparison between observed and computed surface water temperature and ice extent for the calibration years is included in Figures 20 and 22. Excellent agreement was achieved for the surface water temperature and generally good results were achieved for the ice model which duplicated the seasonal pattern of ice extent. Based on this test, the DYRESM model was assumed adequately calibrated for Lake Erie.

SIMULATION RESULTS AND DISCUSSION

A calibrated DYRESM model was used to simulate the water surface temperature and fractional ice extent for Lake Ontario for the period January 1967 to December 1982 and for Lake Erie from April 1967 to December 1983. Figures 19 and 20 show comparisons between simulated and observed temperatures for Lake Ontario and Lake Erie respectively while Figures 21 and 22 detail simulation results for the ice extent.

Water Surface Temperature

Comparison between simulated and observed surface water temperatures for both Lake Ontario and Lake Erie (Figures 19 and 20) show relatively good correspondence for the majority of cases. Simulations for Lake Ontario occasionally showed some underestimation of the peak temperature in summer (about 1°C) and simular 1°C over-estimation of temperature in the fall cooling phase. Lake Erie simulations show a slight tendency toward an over estimation of temperature in the heating phase with relatively accurate results at peak temperatures and in the cooling phase.

One probable cause of the discrepancies between observed and simulated water temperatures is the over-lake wind estimates. As indicated previously, overlake wind speed has been estimated using

land station data adjusted to lake conditions (Sawchuk and Schertzer, 1987) using relationships developed by Phillips and Irbe (1978). Low summer surface temperature estimates may result from too much surface wind mixing which would mix the warmer surface water with deeper cooler water, the net effect being cooler upper layer temperatures. An analysis of generated vertical temperature profiles in DYRESM in comparison with the wind history would be required in order to specify the wind-mixing coefficients more accurately. Additional sources of error may include aliasing of the data since the duration of the typical cruise is approximately 5-days. Unlike averages of layer temperatures, surface water temperatures respond more quickly to changing meteorological conditions. Figure 17 shows a composite of all available surface temperature observations for both lakes using data from CCIW cruises, ART over flights and satellite data. Much of the scatter in such a diagram occurs due to the time of observation since water surface temperature can be observed in daylight and night-time measurement programs. No differentiation was given to time of observation in constructing the average observed water surface temperature. Considering these limitations, the simulation results given in Figures 19 and 20 for both lakes is encouraging.

Fractional Ice Cover

Time series of the daily simulated ice cover fraction is compared with observations in Figures 21 and 22 for Lake Ontario and Lake Erie, respectively.

Reasonable agreement between simulated and observed values was achieved for Lake Ontario except during the years of 1970, 1976, 1977 and 1981. During these four years, ice cover was simulated between 30 to 60 percent too high. The errors in these years do not appear to be associated with the temperature model in DYRESM since the simulated temperature during the ice formation phase (Figure 19) shows good correspondence with observations. The more likely explanation lies with the limitations of the ice model. As discussed previously, the DYRESM ice model (Patterson and Hamblin, 1984) does not account for ice dynamics and assumes a constant, uniform ice thickness of 20 cm until the lake is completely covered. Due to smaller heat storage capacity smaller lakes experience faster freeze over resulting in a more uniform ice thickness. Consequently, the DYRESM ice model assumptions are likely more suitable for small lakes, and therefore, the inability of the simple model to simulate variable ice thickness under less than 100 percent ice cover conditions could account for the over simulations of ice extent in Lake Ontario. Figure 18 indicates that Lake Ontario rarely experiences 100 percent ice cover. In

general, simulations for other years are reasonably good considering the model limitations.

Simulations for Lake Erie (Figure 21 and 22) shows relatively good depiction of the seasonal progression of ice fraction increase at the beginning of the winter period and subsequent decrease in the March/April period. In most cases, the estimates of the variation of ice extent over the January to March period is accurate. Simulations for the years 1973, 1974 and 1975 demonstrate that the DYRESM ice model is able to predict the variability in the fractional ice extent in Lake Erie. The maximum departure between simulated and observed values occurred in 1983 when ice cover was underestimated by approximately 20 percent. This discrepancy is small compared to errors encountered for Lake Ontario. As indicated above, the smaller heat storage capacity and the tendency for Lake Erie to freeze over at 100 percent ice cover for most years (Figure 18) correspond more closely with the asumptions incorporated into the DYRESM ice model and, hence, the more accurate simulation results.

Surface Heat Fluxes

The surface heat flux is an important boundary condition in DYRESM since it directly affects the simulations for water surface temperature and ice extent. As discussed previously, the incoming

solar and longwave radiation estimates were used directly from Sawchuk and Schertzer (1987). Other components of the surface heat flux include reflected solar radiation, emitted longwave radiation, sensible and latent heat flux. Figures 23 to 30 illustrate the long-term means of the surface heat flux components. Detailed description of the incoming radiation fluxes is contained in Sawchuk and Schertzer (1987). A brief description of the heat flux components is given below.

The long-term mean and extremes based on daily values of the incoming solar and reflected radiation fluxes are illustrated in Figure 23 and 24 for Lake Ontario and Lake Erie. A comparison of the solar radiation values was given previously under the data base description. In terms of the reflected solar radiation, average wintertime values for Lake Erie ($6MJ/m^2/day$) are twice that of Lake Ontario ($3MJ/m^2/day$). As indicated in the discussion of fractional ice cover, Lake Erie experiences greater ice cover than Lake Ontario resulting in higher reflected solar radiation which is a function of the albedo (40-80%) calculated in DYRESM for combinations and age of ice and snow. The albedo for the ice free water surface was assumed to be 3 percent of the incoming solar radiation within DYRESM. Higher reflectories have been reported based on IFYGL studies on Lake Ontario (Nunez et al., 1972; Davies and Schertzer, 1975). DYRESM parameterizations were not changed.

The long-term mean and extremes based on daily values of the incoming and emitted longwave radiation fluxes are illustrated in Figure 25 and 26 for Lake Ontario and Lake Erie. Longwave radiation flux was described under the data base description. The emitted longwave radiation flux for the two lakes is computed based on the water surface temperature (Equation 6). The longterm mean of emitted longwave radiation ranges from approximately 24 MJ/m^2/day in winter to approximately 36 MJ/m^2/day in summer. A smaller range of values is computed for Lake Ontario.

The long-term mean and extremes of the computed sensible heat flux is given in Figure 27 and 28 for Lake Ontario and Lake Erie, respectively. The sensible heat flux shows the loss or gain of heat to the lake surface due to the temperature differences between the air and water. For Lake Ontario, DYRESM computes heat losses from the water surface to the overlying air, in general, occurring over the fall and winter months with summertime sensible heat gains to the water surface. Conditions for Lake Erie are more complex. Sensible heat losses to the overlying air generally occur in the fall and winter months and heat gains are computed for the summer months. DYRESM bulk aerodynamic formulations (Equation 4) tend to provide similar seasonal distribution in the sensible heat flux as the Bowen ratio approach (Schertzer, 1987).

The long-term mean and extremes of the computed latent heat flux are illustrated in Figures 29 and 30 for Lake Ontario and Lake Erie

based on bulk aerodynamic formulation (Equation 6). In general, Lake Ontario experiences highest evaporation during the fall and winter months with lowest evaporation occurring in the spring and summer. Based on the long-term means, condensation is expected to occur in the months of May and June. The average evaporation for Lake Erie is computed with lower values in the winter and spring months and higher values towards the late summer and fall. Condensation may occur in the spring months. The seasonal distribution in evaporation for both lakes is similar to that determined in previous studies (Elder, Boyce and Davies, 1974; Derecki, 1975; Schertzer, 1987). Figures 29 and 30 illustrate a very high variability of the daily evaporation as compared to the visual depiction of monthly means.

ACKNOWLEDGEMENTS

The authors acknowledge the helpful suggestions given by P. Hamblin and F.M. Boyce on aspects of this report. Data supplied by Water Planning and Management Branch, CCIW, Atmospheric Environment Service, Ice Central Ottawa, Marine Environment Data Services, National Climate Digital Data Center, National Ocean and Atmospheric Administration, U.S. Army Corps of Engineers, U.S. Geological Survey, is greatly appreciated.

This research was funded through the NWRI Canada Climate Program (Supply and Services Contract No. 02SE-KW405-5-1182).

REFERENCES

AES, 1985. Canadian Climatological Data, Atmospheric Environment Service, Canadian Climate Centre, Data Management Division, Downsview, Ontario.

AES, 1985b. Surface water temperatures for Lake Erie by infra-red thermometer and satellite techniques 1967-1983. Hydrometerology and Applications Division, Atmospheric Environment Service, Downsview, Ontario.

Davies, J.A., Schertzer, W.M. and Nunez, M. 1975. Estimating global solar radiation, Boundary Layer Meteorology, 9(33-52).

Derecki, J.A. 1975. Evaporation from Lake Erie. NOAA Tech. Report ERL 342-GLERL 3, Ann Arbor, Michigan, 84 p.

Elder, F.C., Boyce, F.M., and Davies, J.A. 1974. Preliminary energy budget of Lake Ontario for the period May through November 1972 (IFYGL), Proc. 17th Conf. Great Lakes Res. Internat. Assoc. Great Lakes Res., 713-724.

Hamblin, P.F., Yukon River Headwater Lakes Study, 1983-1985: Preliminary Analysis and Data Report, Unpublished Report, National Water Research Institute, Burlington, Ontario, Canada, 1985.

Ice Central Ottawa, 1967 to 1971, Ice observations, Canadian Inland Waterways, Meteorological Branch, Department of Transport, Canada.

Ice Central Ottawa, 1972 to 1983, Composite ice conditions, Great Lake Composite ice charts, Atmospheric Environment Service, Department of the Environment, Canada.

Imberger, J. and Patterson, J.C. 1981. 'A Dynamic Reservoir Simulation Model: DYRESM 5', In Fischer, H.B., Transport Models for Inland and Coastal Waters, Academic, 1981, pp. 310-361.

Ivey, G.N. and Patterson, J.C. 1984. A model of vertical mixing in Lake Erie in summer, Limnol. Oceanogr., 29(3), pp. 553-563.

Lam, D.C.L., Schertzer, W.M. and Fraser, A.A. 1983. Simulation of Lake Erie water quality responses to loading and weather variations. IWD Scientific Series 134, NWRI. Canada Centre for Inland Waters, 310 pages.

Lam, D.C.L. and Schertzer, W.M. 1987. Lake Erie thermocline model results, comparison with 1967 to 1982 data and relation to anoxic occurrences. J. Great Lakes Research, 13(4), In Press.

Marine Environmental Data Service. 1985. Water surface levels, Environment Canada, Fisheries and Marine Service.

Maykut, G.N., and Untersteiner, N. 1971. Some results from a time dependent thermodynamic model for sea ice. J. Geophys. Res., Vol. 83, pp. 1550-1575.

NCDC, 1985. Hourly surface weather observations. National Climate Digital Data Centre, Aeshville, N.C.

NOAA Technical Memorandum ERL GLERL-48, 'Lake Erie Regional Ice Cover: Preliminary Results', Great Lakes Environmental Research Laboratory, Ann Arbor, Michigan, 1983.

Nunez, M., Davies, J.A. and Robinson, P.J. 1971. Solar radiation and albedo at a Lake Ontario Tower site. 3rd Report for Gov. of Canada Contract No. HD-81276. Canada Centre for Inland Waters, 82 pages.

Patterson, J.C. and Hamblin, P.F. 1984. 'Thermal simulation of lakes with winter ice cover', National Water Research Institute, Contribution #85-29.

Pattersons, J.C., Imberger, J., Hebbert, B. and Loh, I. 1978. 'Users guide to DYRESM', Report No. EFM-3, Univ. of Western Australia.

Phillips, D.W. and Irbe, G. 1978. Lake to land comparison of wind, temperature and humidity on Lake Ontario during the International Field Year for the Great Lakes (IFYGL), CCI-2-77, Atmospheric Environment Services, Downsview, 51 pages.

Sawchuk, A.M. and Schertzer, W.M. 1987. Modelling the surface heat flux of Lake Ontario and Lake Erie 1953 to 1983. NWRI Climate Program. Interim Report DSS Contract KW405-4-1340.

Schertzer, W.M. 1987. Heat balance and heat storage estimates for Lake Erie 1967 to 1982. Journal of Great Lakes Research, Internat. Assoc. Great Lakes Res., 13(4): 454-467.

Schertzer, W.M. and Sawchuk, A.M. 1985. Summary of water surface temperature observations for Lake Ontario (1966-1984) and Lake Erie (1967-1982), NWRI Contribution 85-159, Canada Centre for Inland Waters, 46 pages.

U.S. Corps. 1985. Detroit River flows. U.S. Army Corps of Engineers. Detroit District, 477 Michigan Avenue, Detroit, Michigan, 48226.

USGS, 1984, Water Resources Data, New York, Water Year 1983, U.S. Geological Survey Water-Data Report NY-83-3, P.O. Box 1350, Albany, New York, 12201.

LIST OF FIGURES

18. Composites of available Lake Ontario and Lake Erie fractional ice cover observations 1967 to 1983.
19. Time-series of Lake Ontario simulated and observed water surface temperture 1967 to 1982.
20. Time-series of Lake Erie simulated and observed water surface temperature 1967 to 1983.
21. Time-series of Lake Ontario simulated and observed fractional ice cover 1967 to 1982.
22. Time-series of Lake Erie simulated and observed fractional ice cover 1967 to 1983.
23. Lake Ontario shortwave radiation fluxes long-term averages and ranges 1967 to 1982.
24. Lake Erie shortwave radiation fluxes long-term averages and ranges 1967 to 1983.
25. Lake Ontario longwave radiation fluxes long-term averages and ranges 1967 to 1982.
26. Lake Erie longwave radiation fluxes long-term averages and ranges 1967 to 1983.
27. Lake Ontario sensible heat flux long-term average and range 1967 to 1982.
28. Lake Erie sensible heat flux long-term average and range 1967 to 1983.
29. Lake Ontario latent heat flux long-term average and range 1967 to 1982.

30. Lake Erie latent heat flux long-term average and range 1967 to 1983.

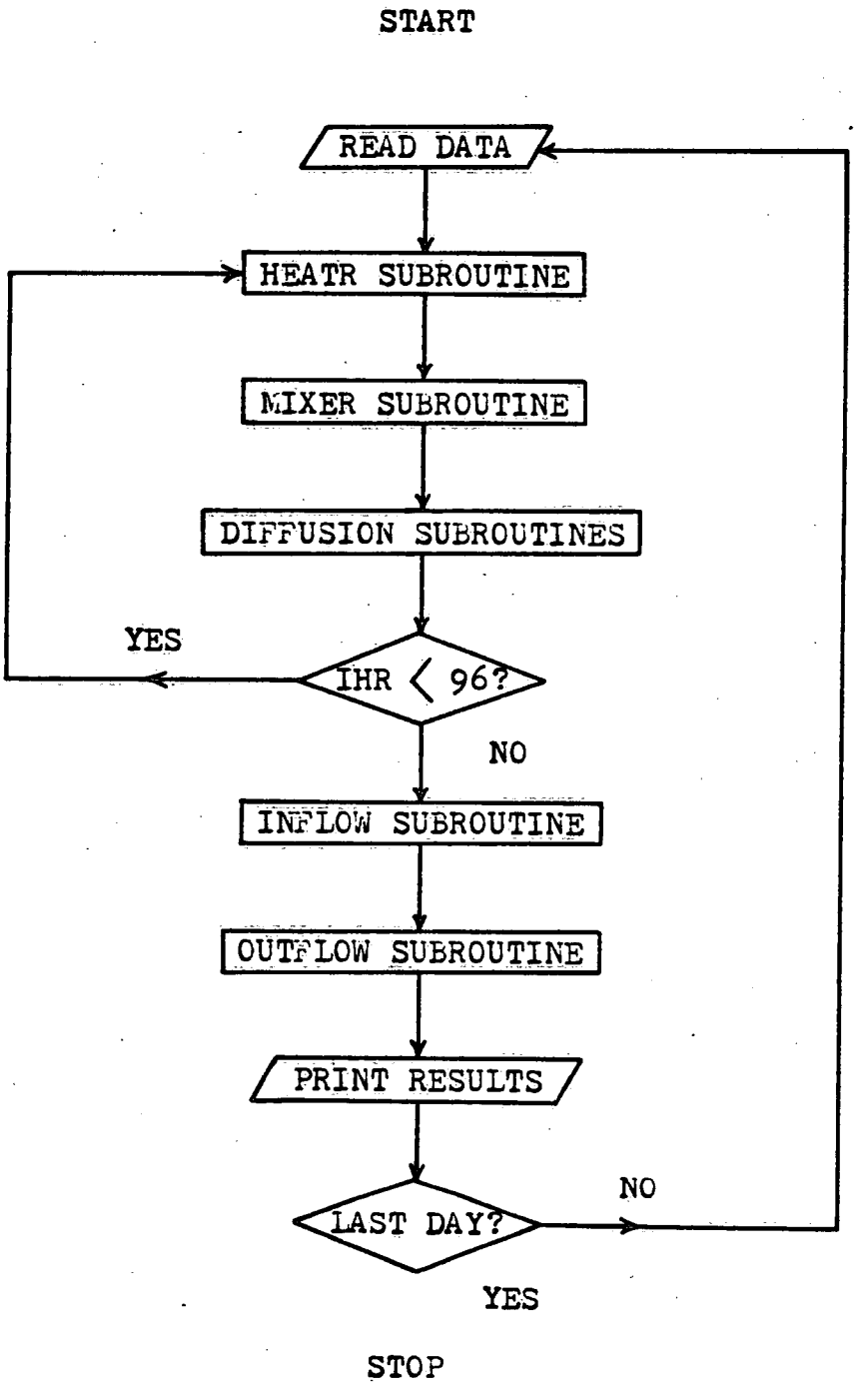

Figure 1. Flow Chart of DYRESM

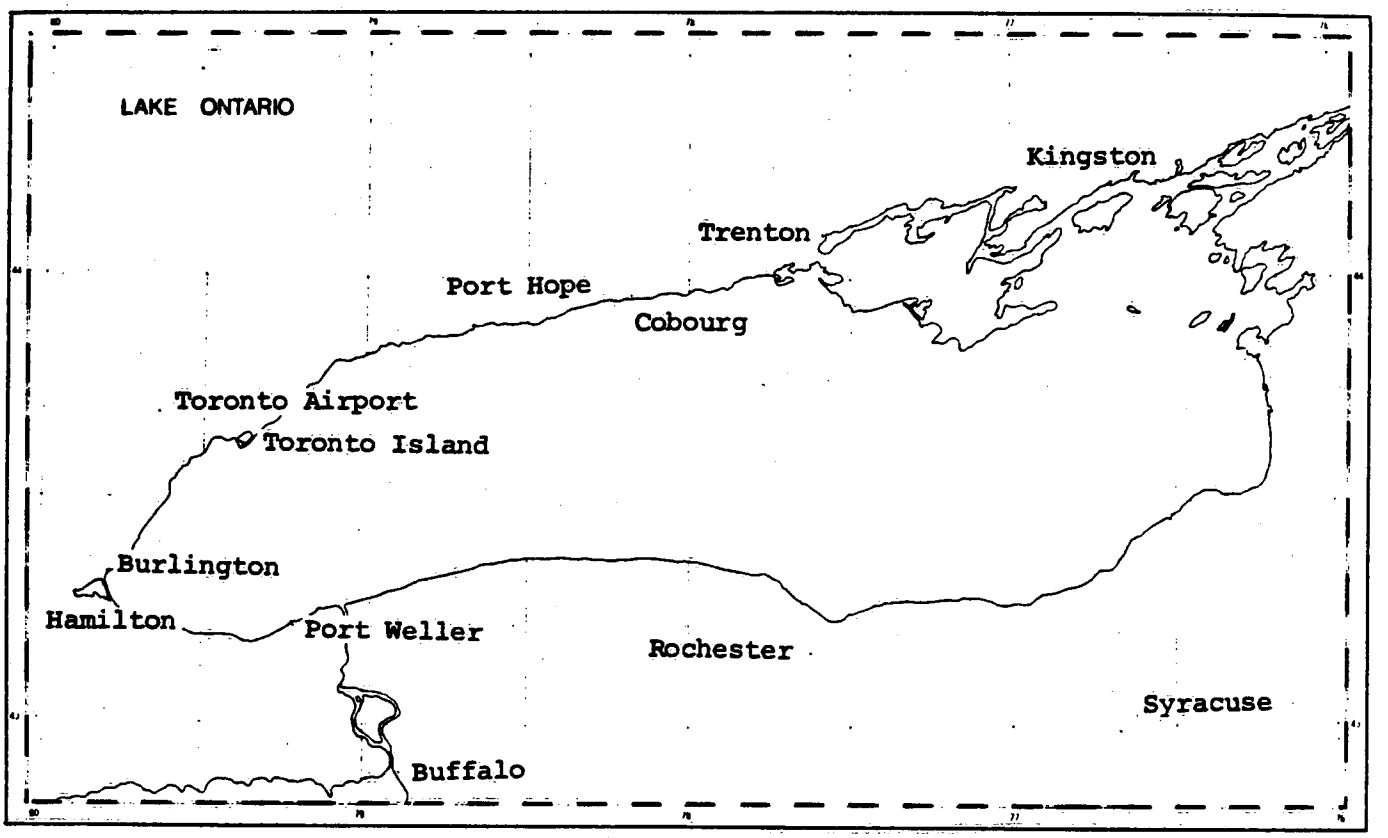

Figure 2. Map of Lake Ontario.

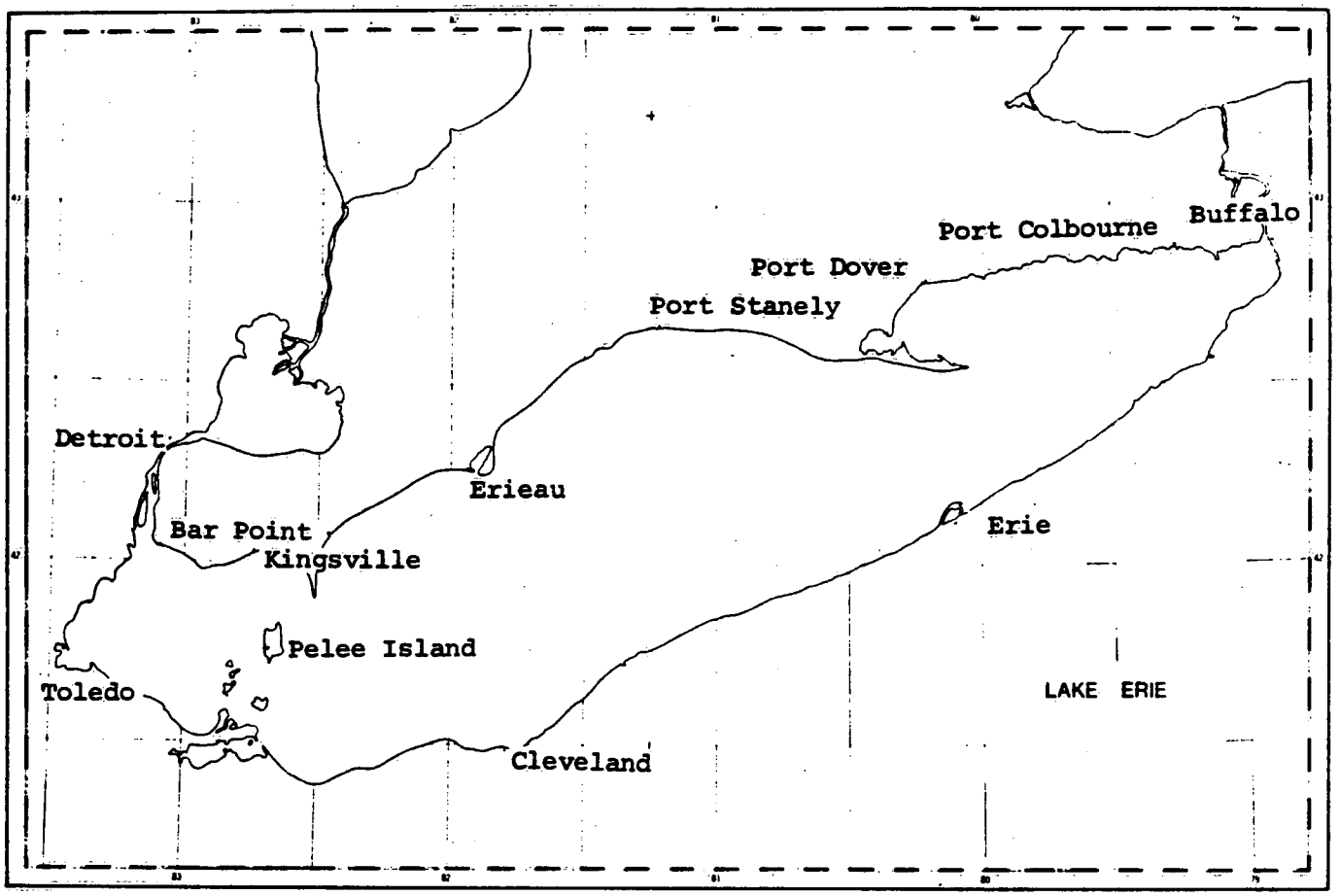

Figure 3. Map of Lake Erie.

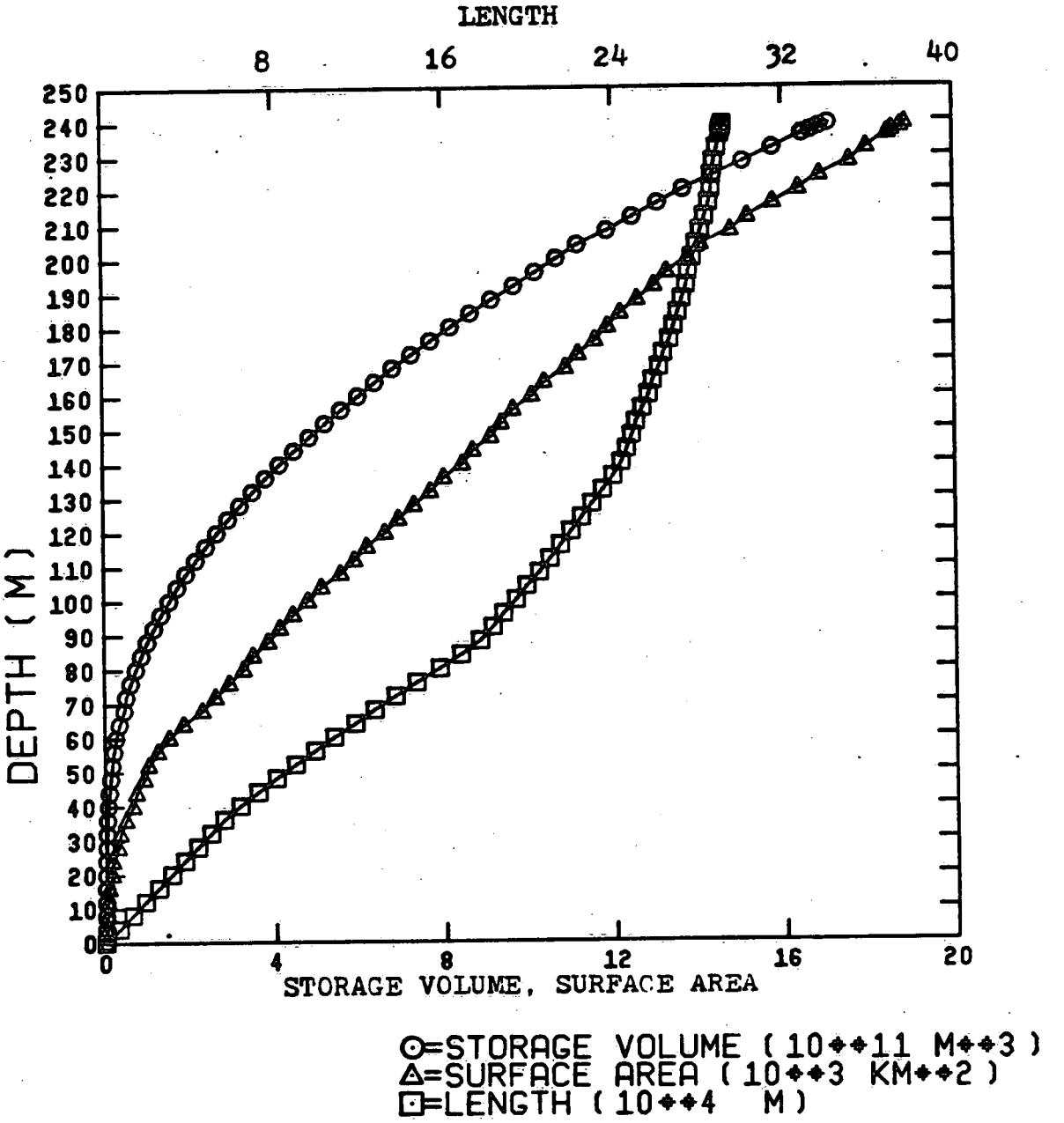

Figure 4. Lake Ontario hypsometric data.

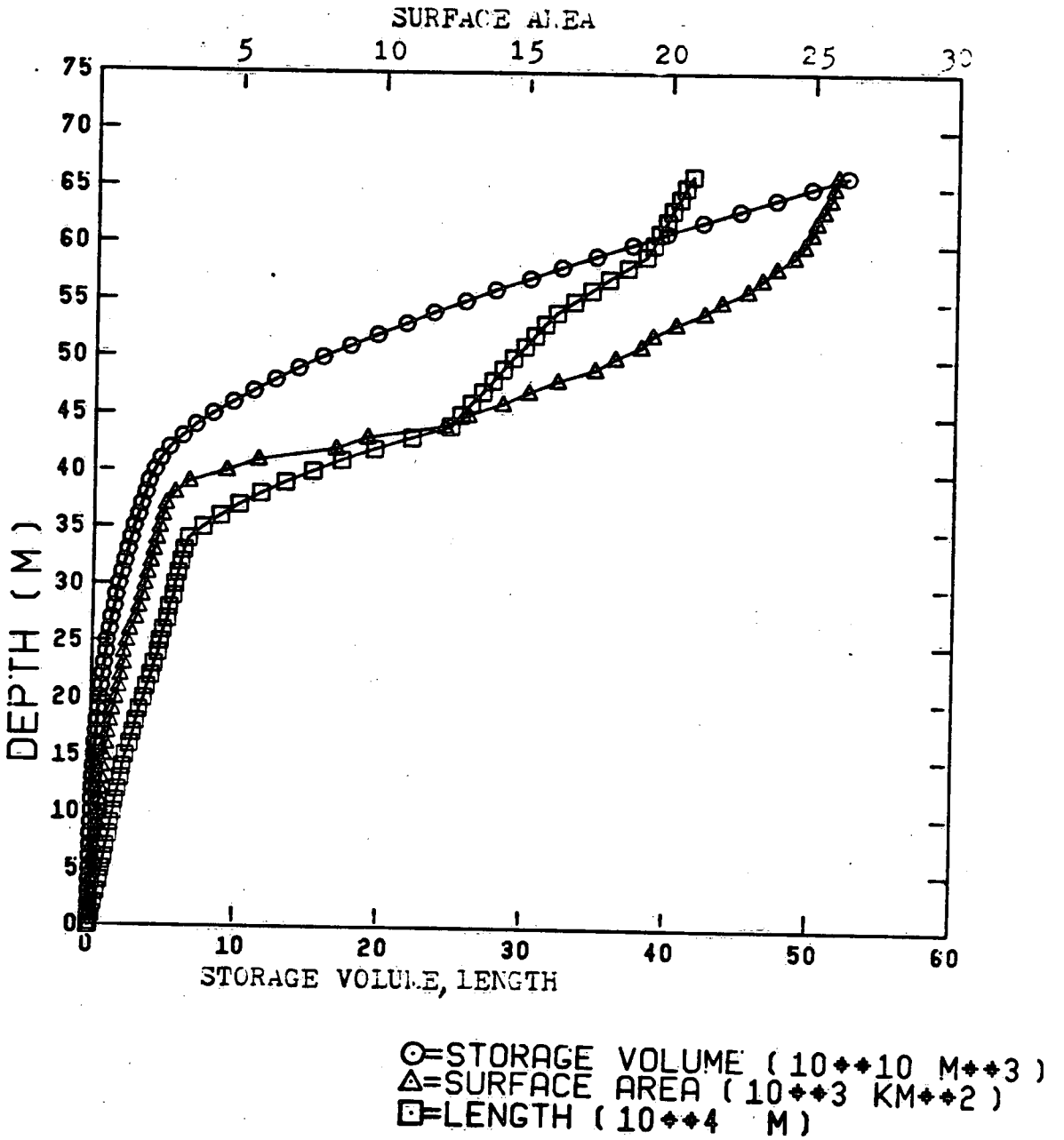

Figure 5. Lake Erie hypsometric data.

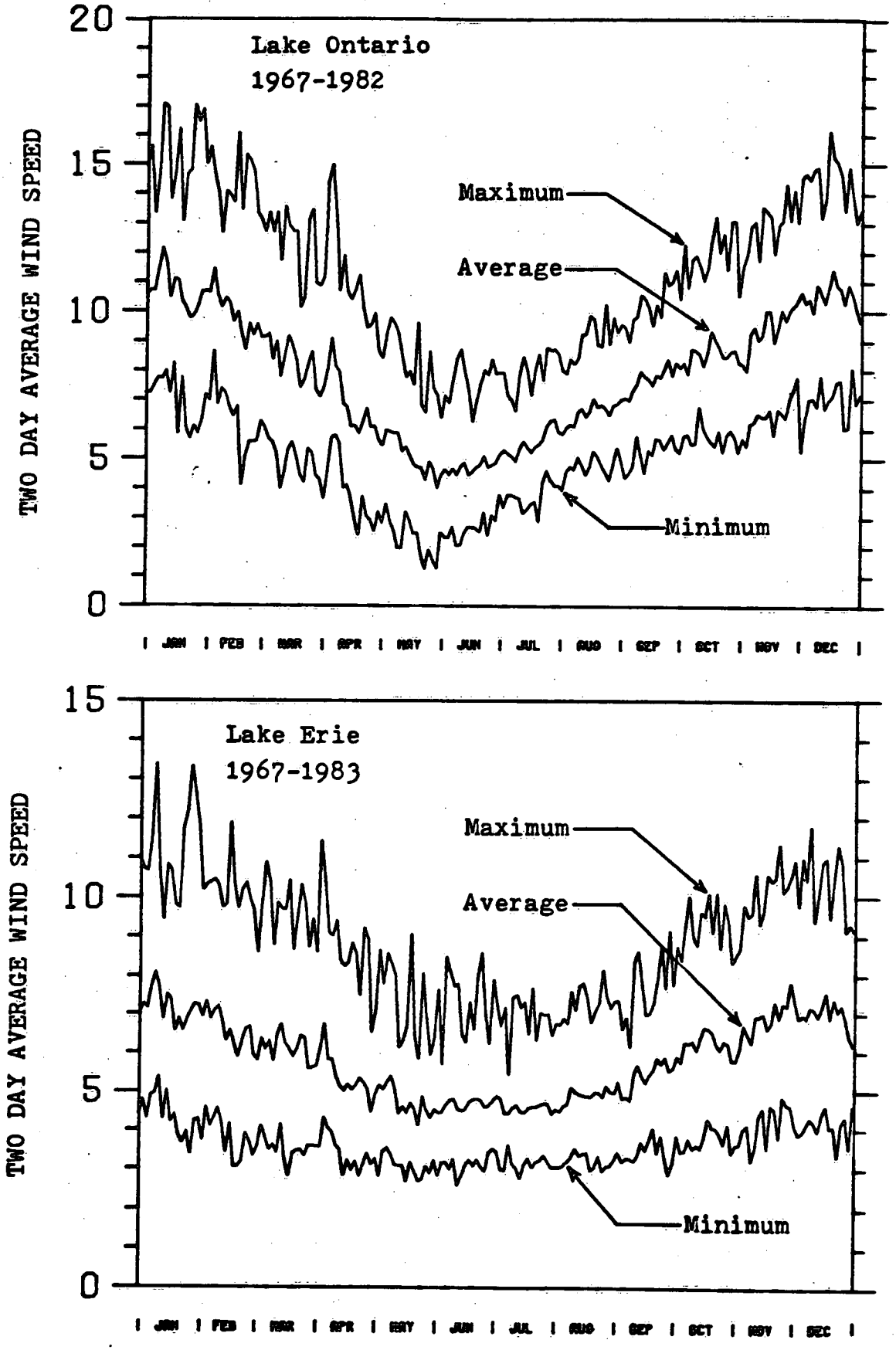

Figure 6. Longterm two day average and range of wind speed.

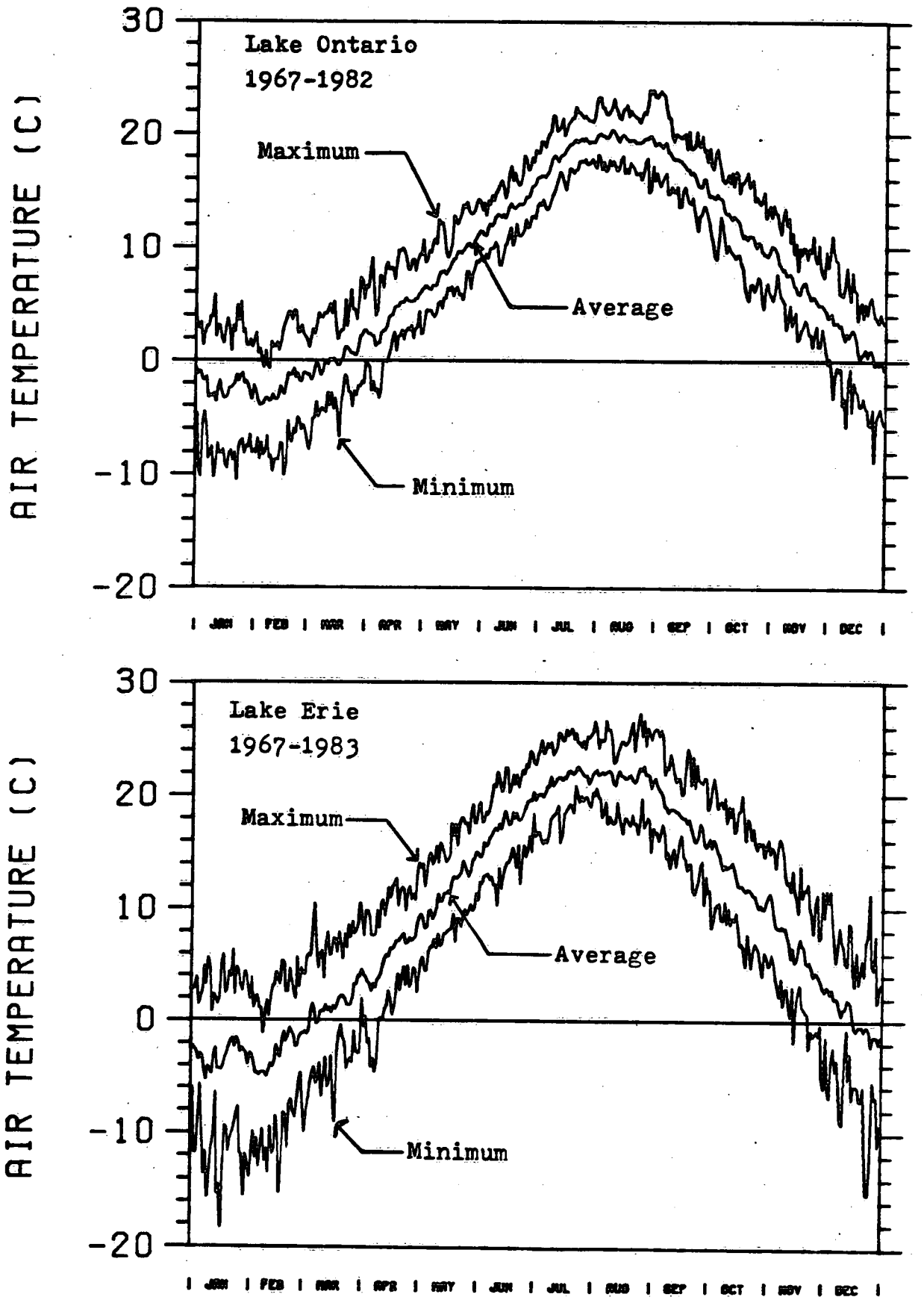

Figure 7. Longterm average and range of air temperature.

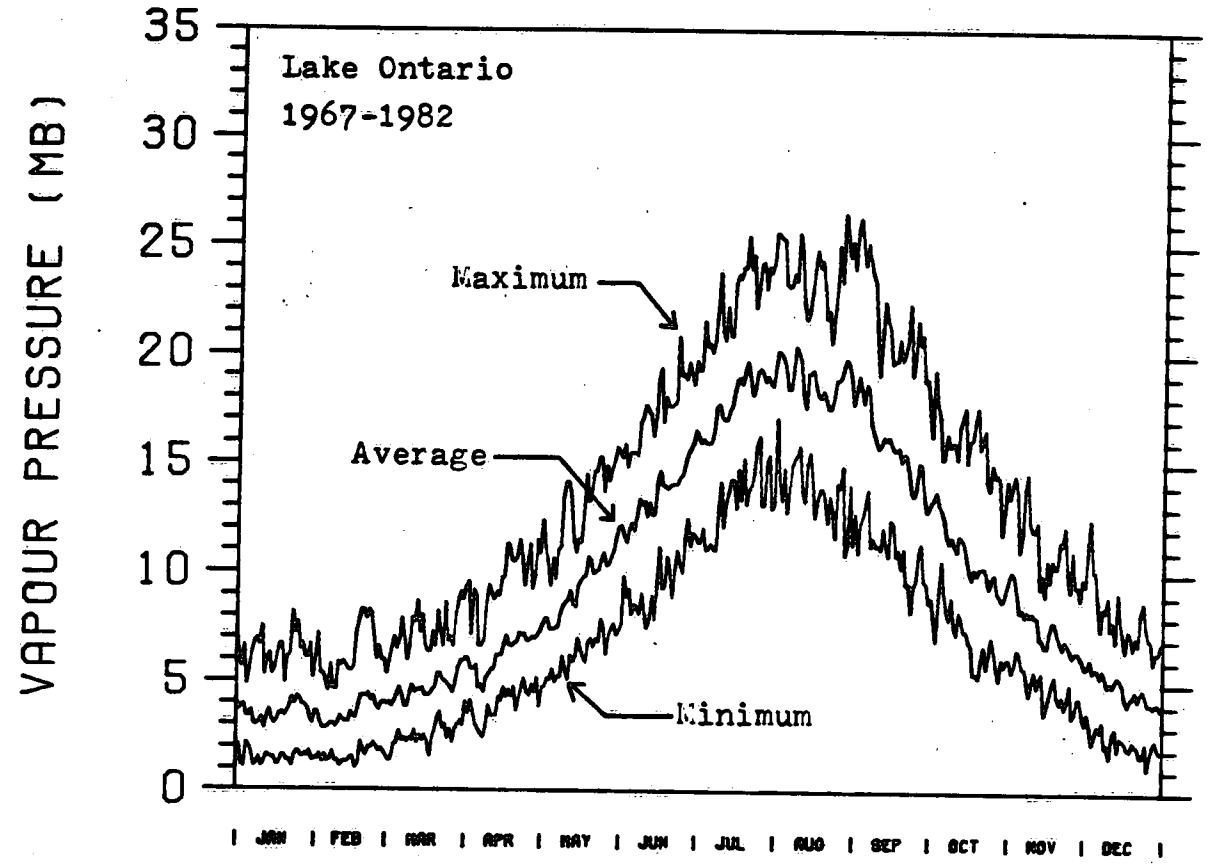

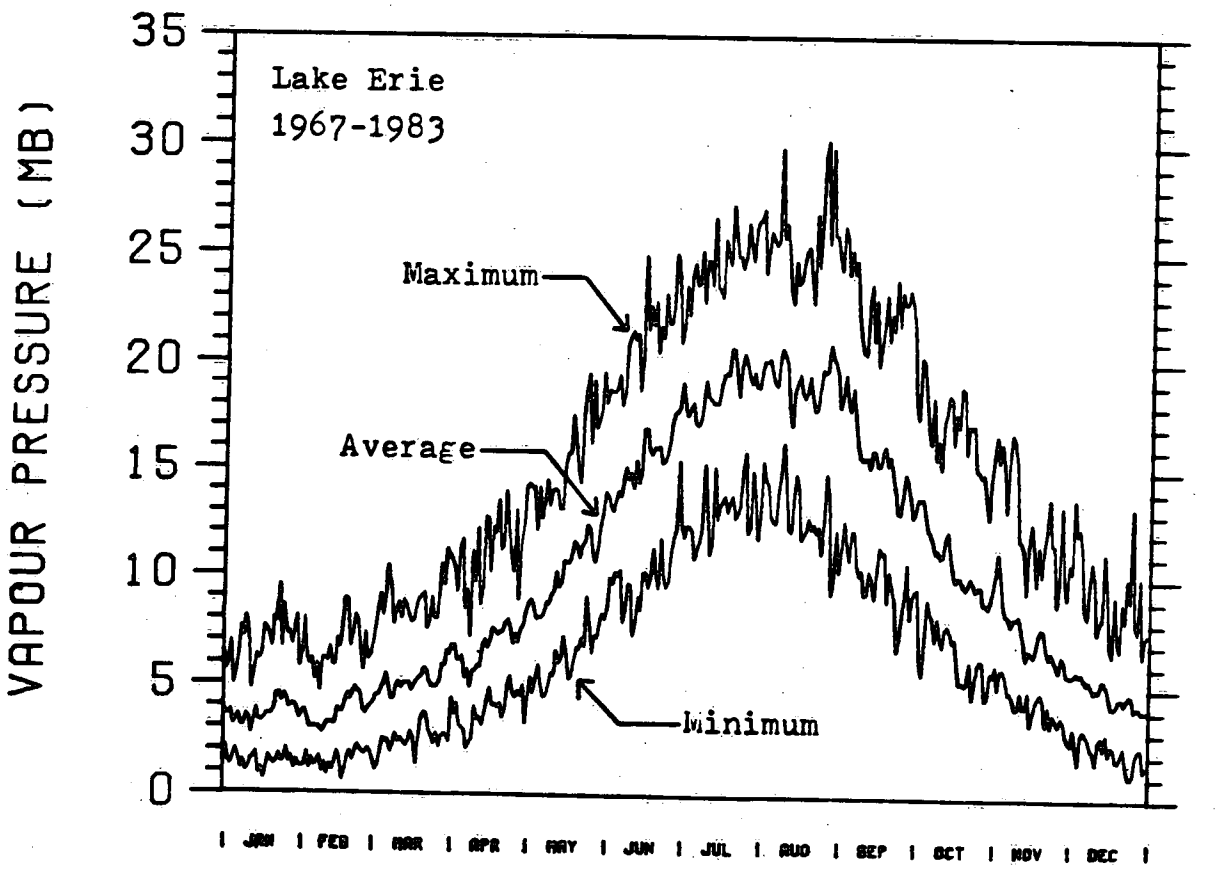

Figure 8. Longterm average and range of vapour pressure.

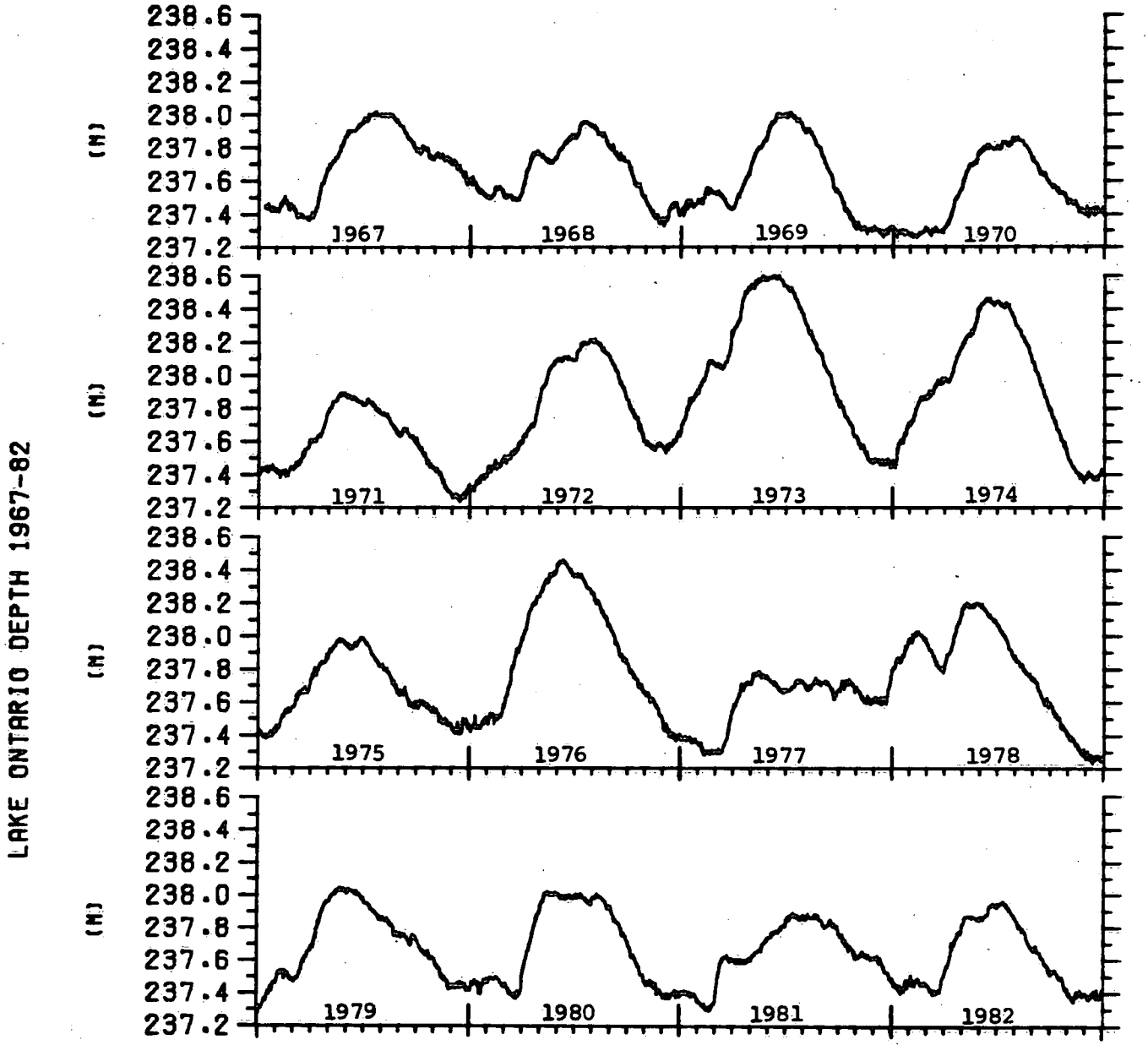

Figure 9. Time series of Lake Ontario depth 1967 to 1982.

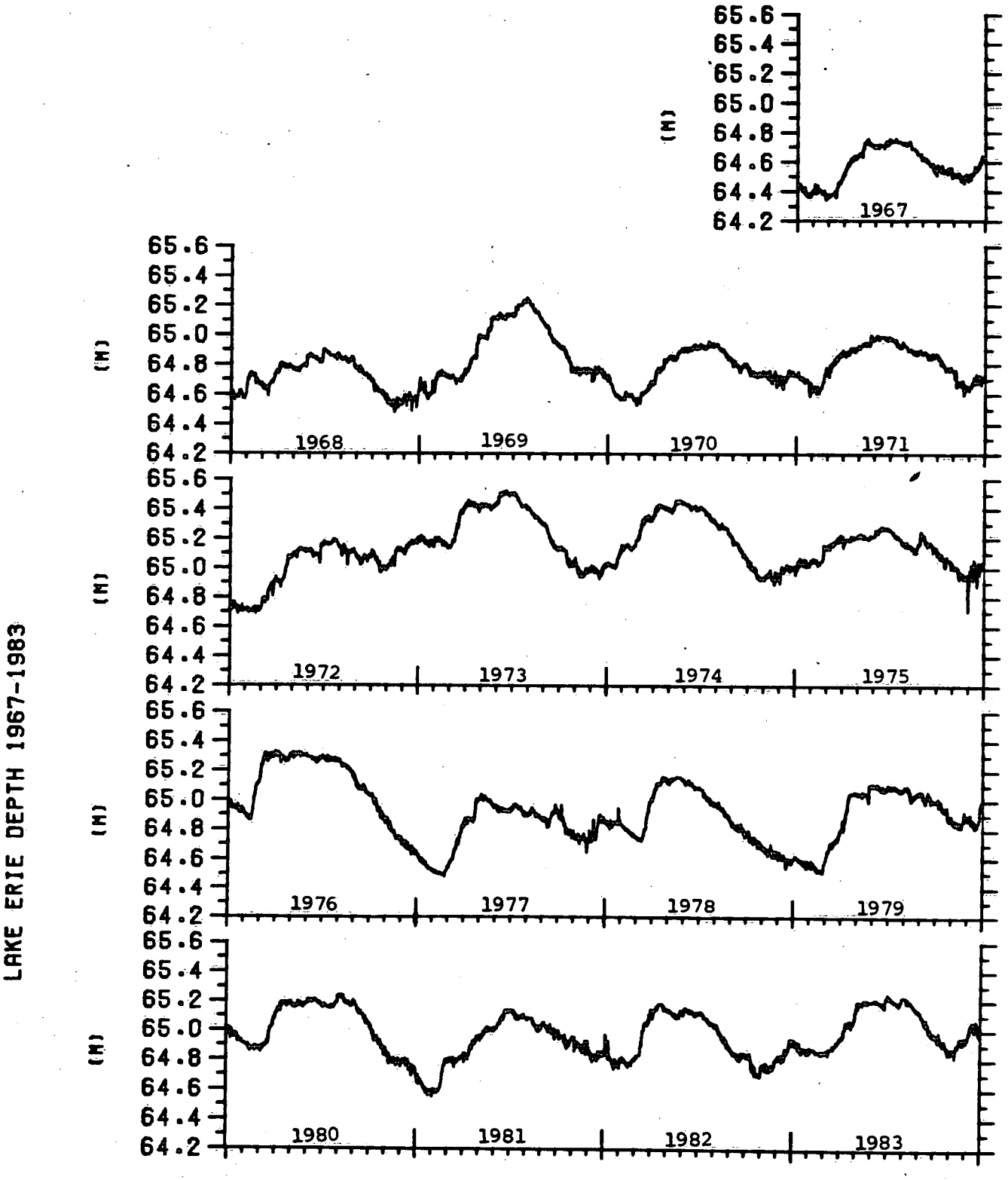

Figure 10. Time series of Lake Erie depth 1967 to 1983.

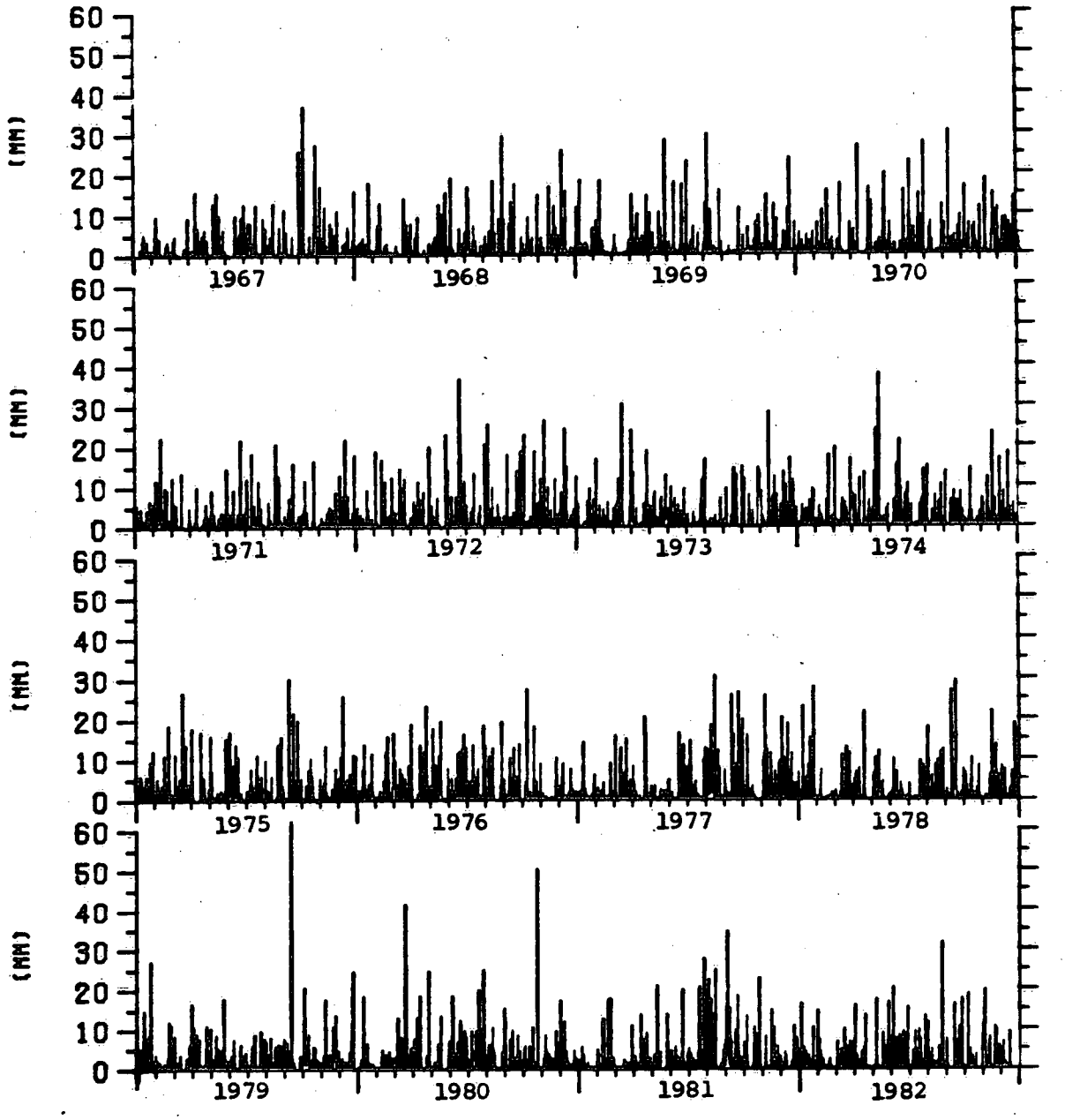

Figure 11. Time series of Lake Ontario precipitation 1967 to 1982.

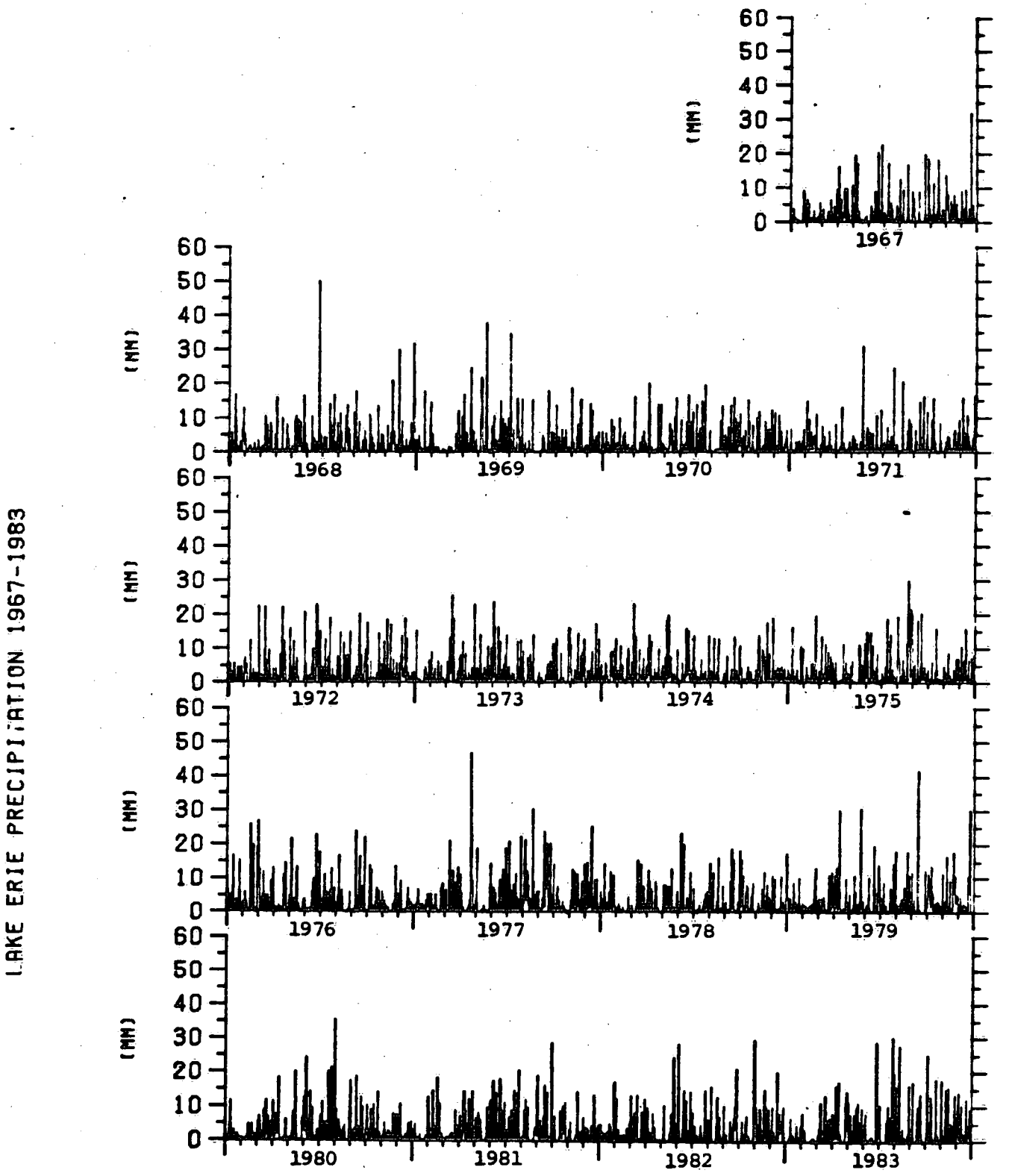

Figure 12. Time series of Lake Erie precipitation 1967 to 1983.

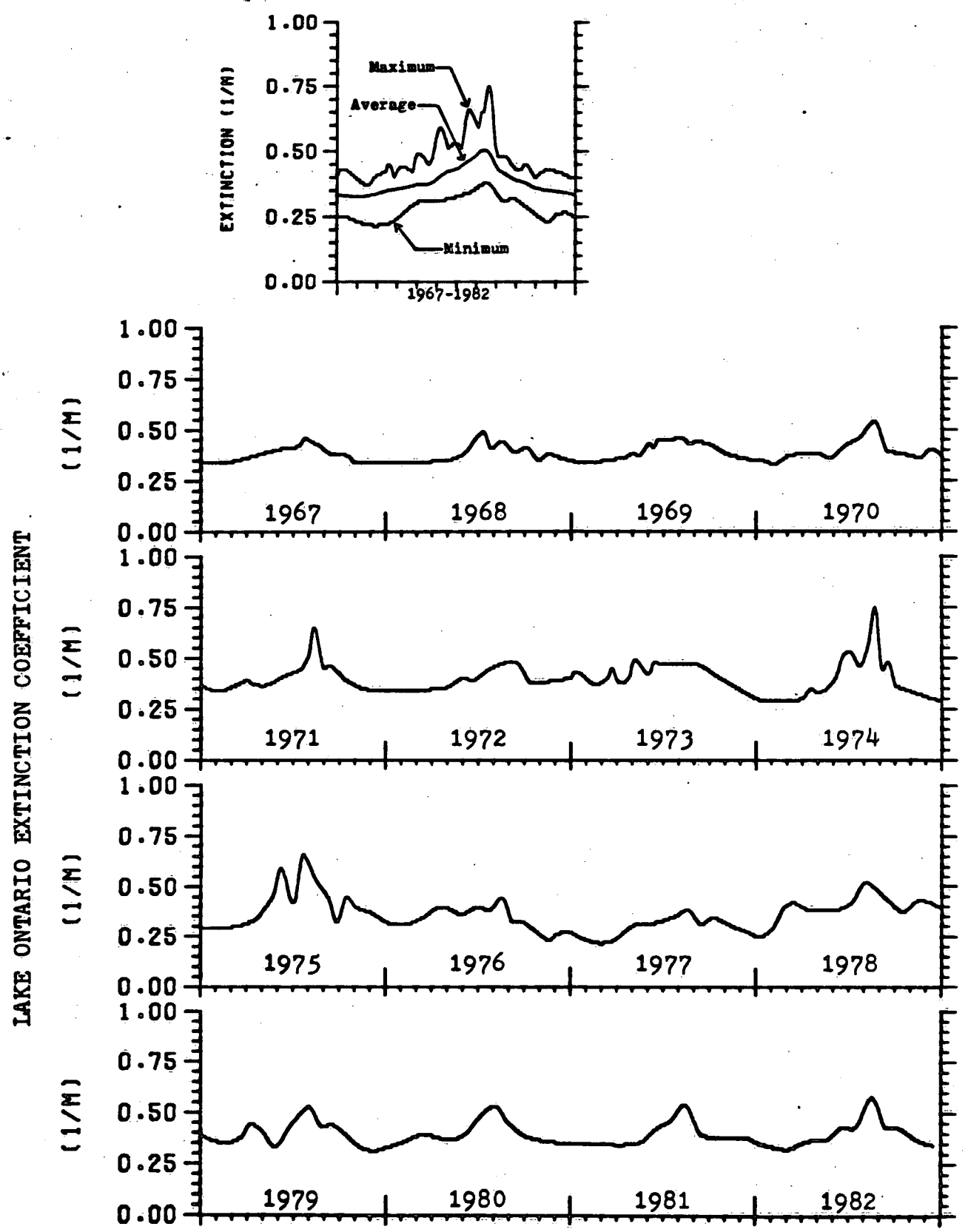

Figure 13. Time series of Lake Ontario extinction coefficient 1967 to 1982 and longterm average and range.

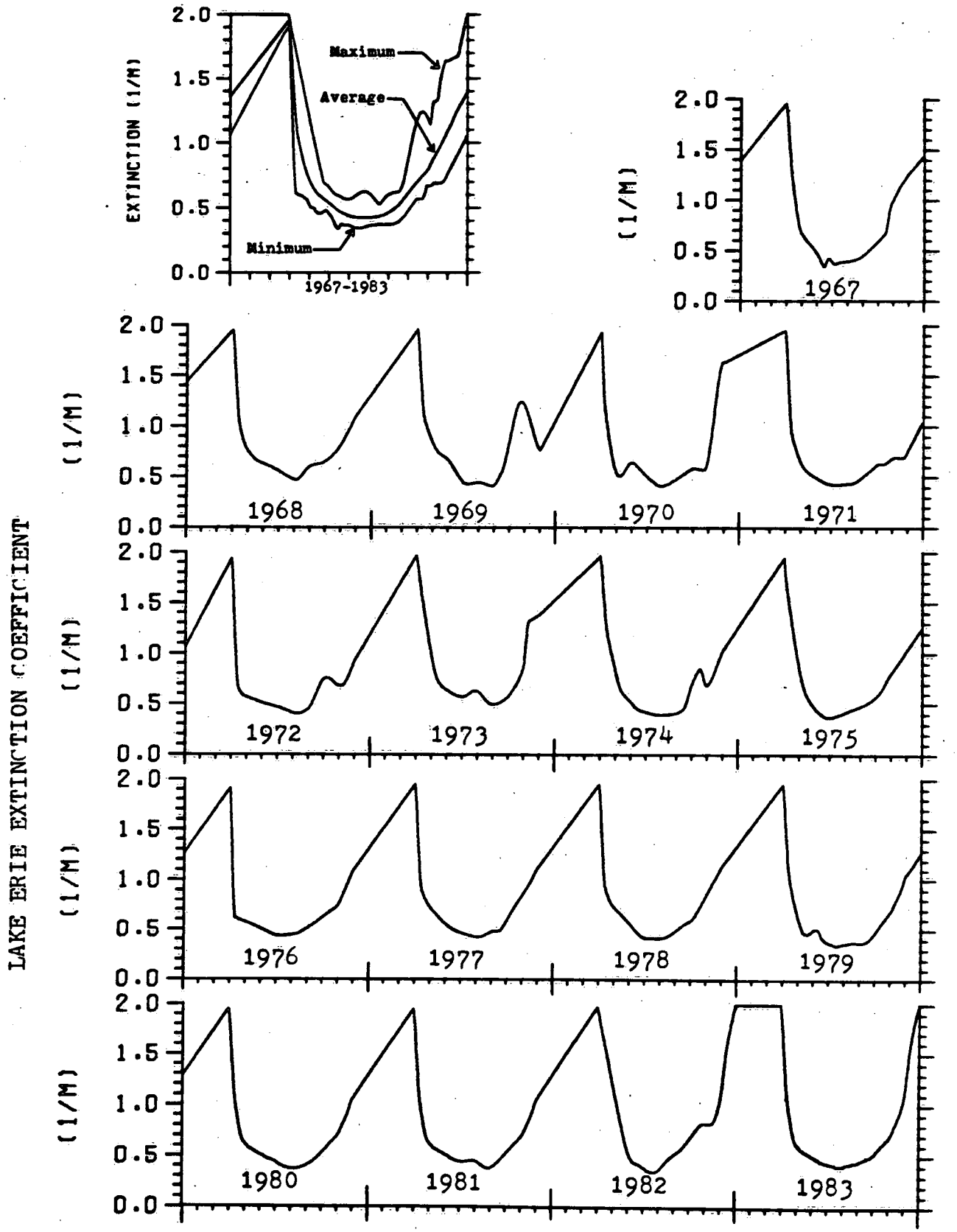

Figure 14. Time series of Lake Erie extinction coefficient 1967 to 1983 and longterm average and range.

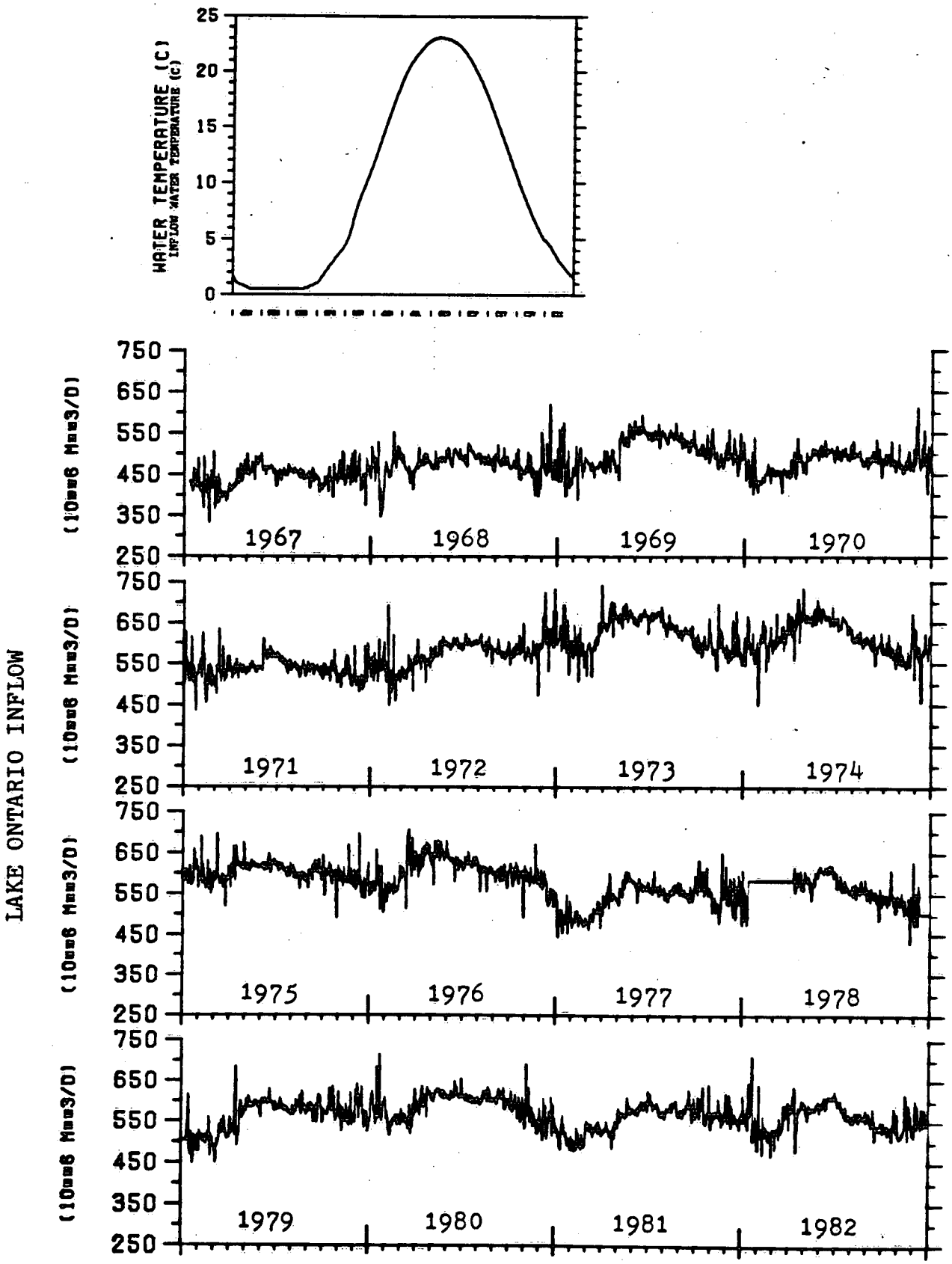

Figure 15. Time series of Lake Ontario inflow rate 1967 to 1982 and longterm average inflow temperature.

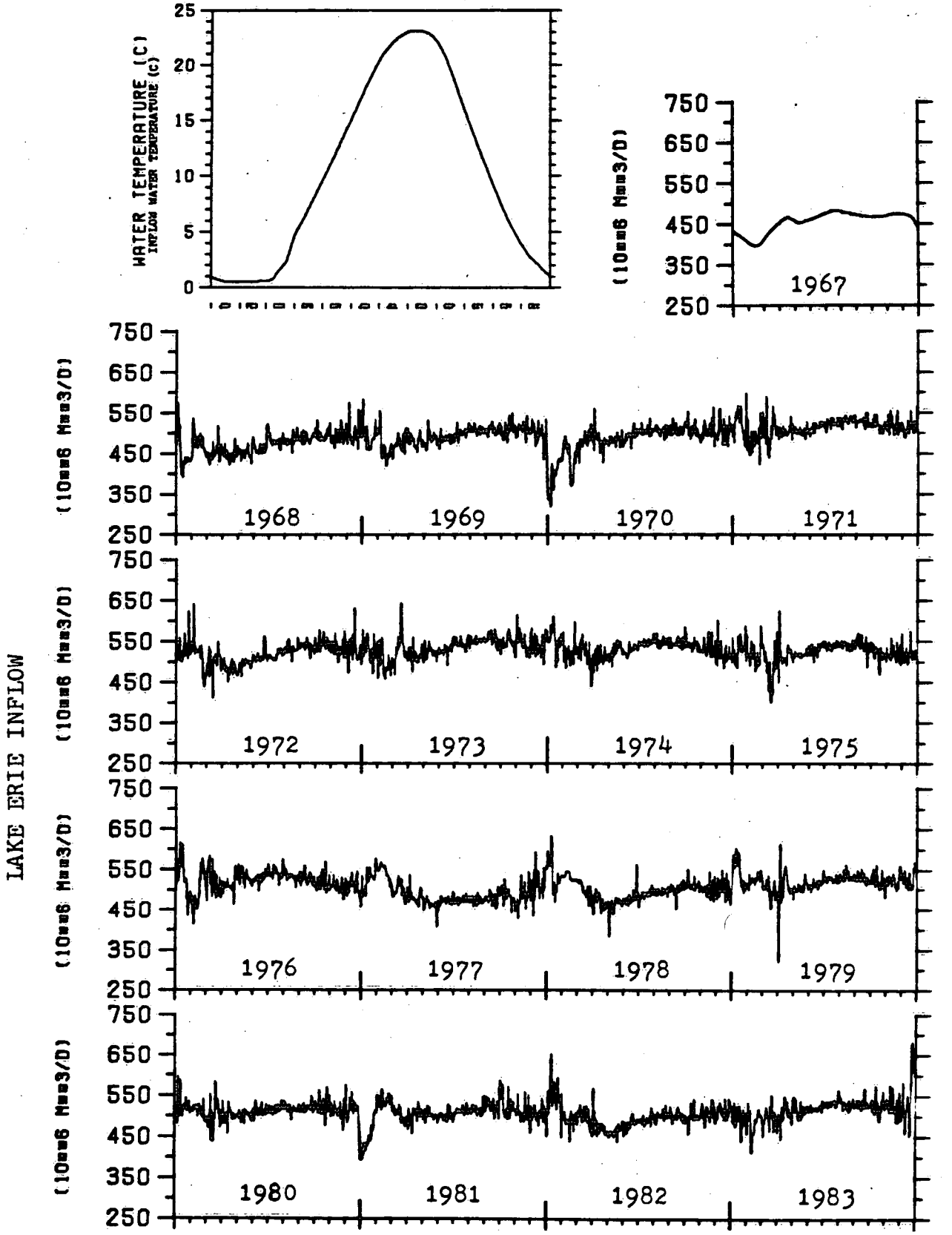

Figure 16. Time series of Lake Erie inflow rate 1967 to 1983 and longterm average inflow temperature.

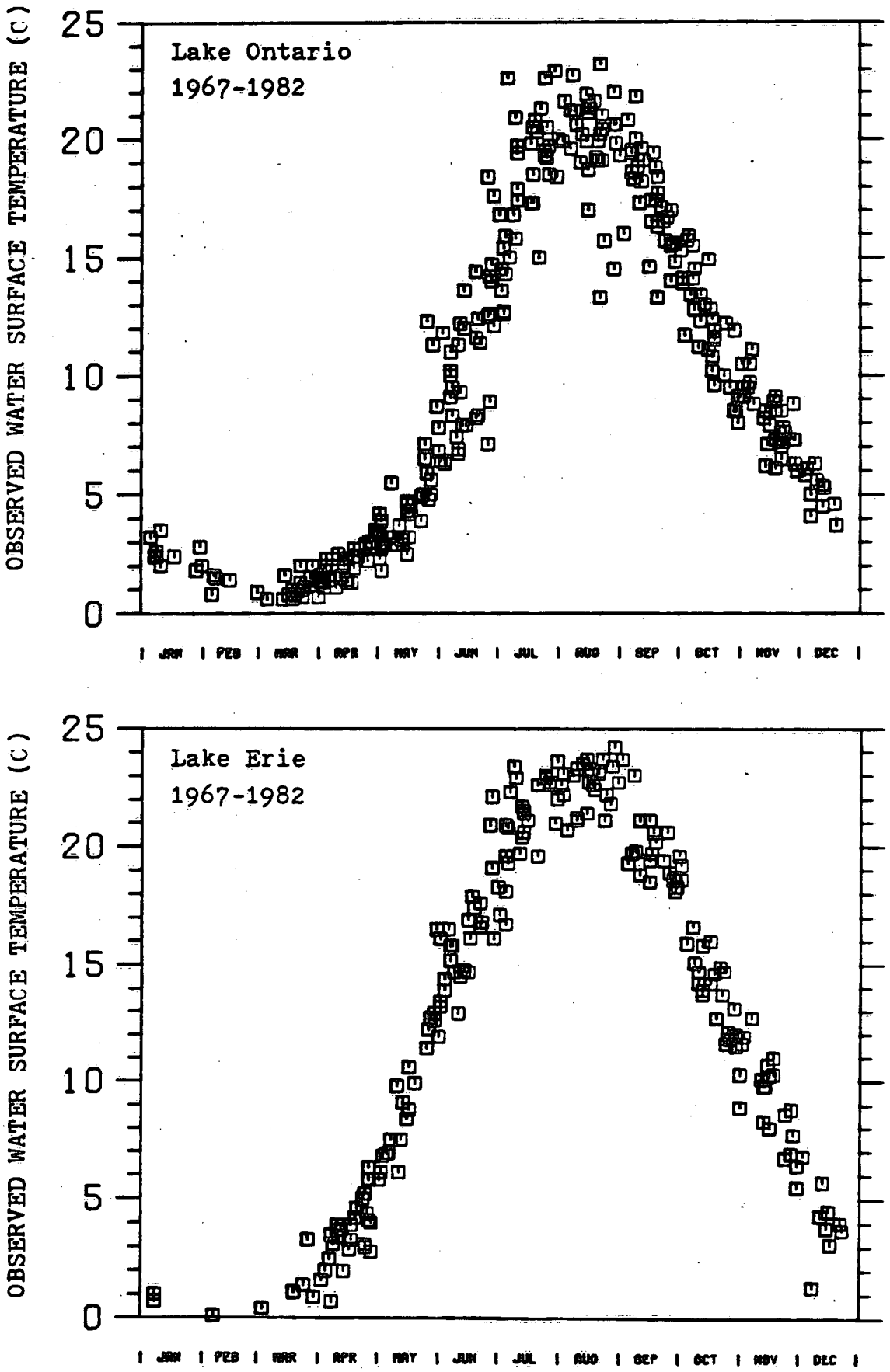

Figure 17. Composites of available Lake Ontario and Lake Erie water surface temperature observations 1967 to 1982.

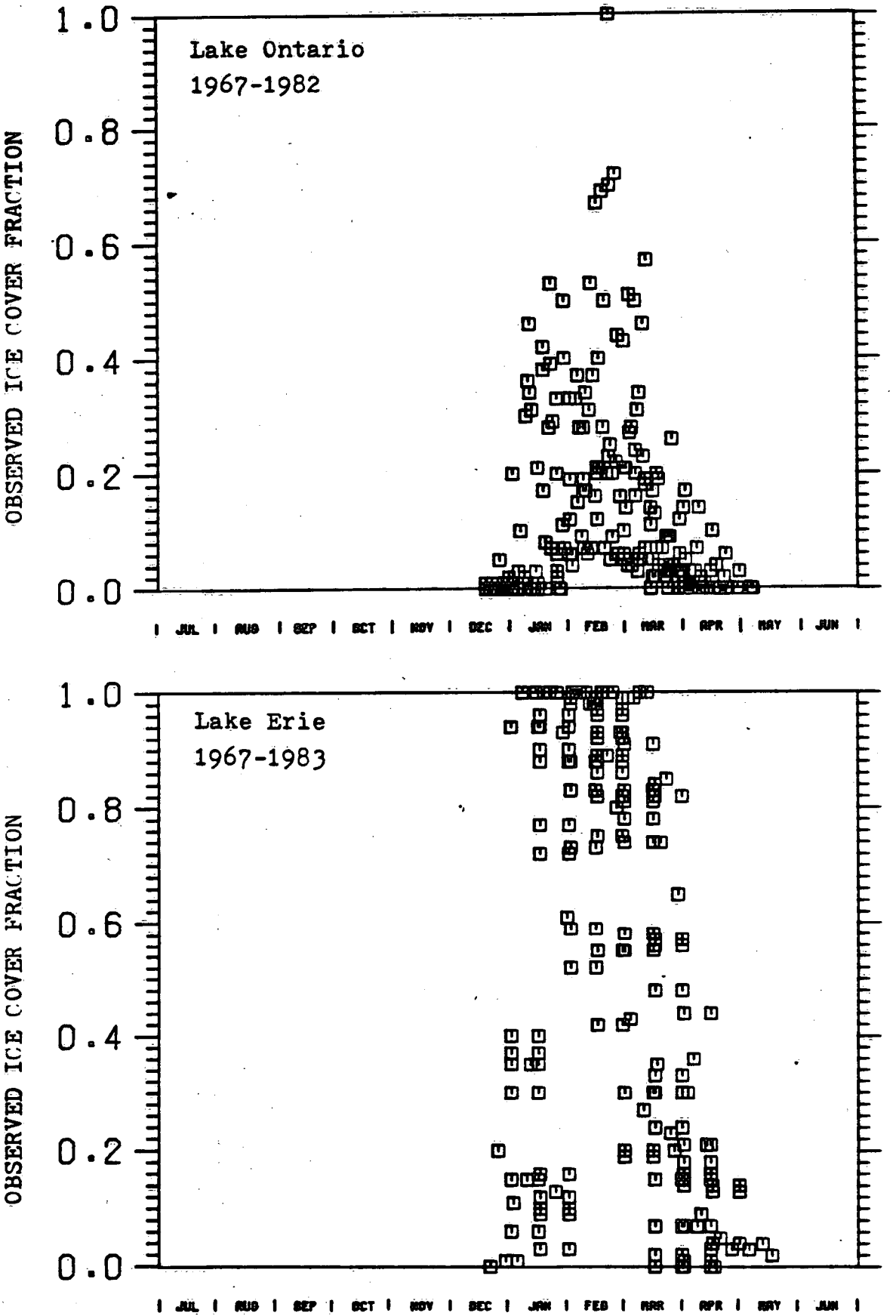

Figure 18. Composites of available Lake Ontario and Lake Erie fractional ice cover observations 1967 to 1983.

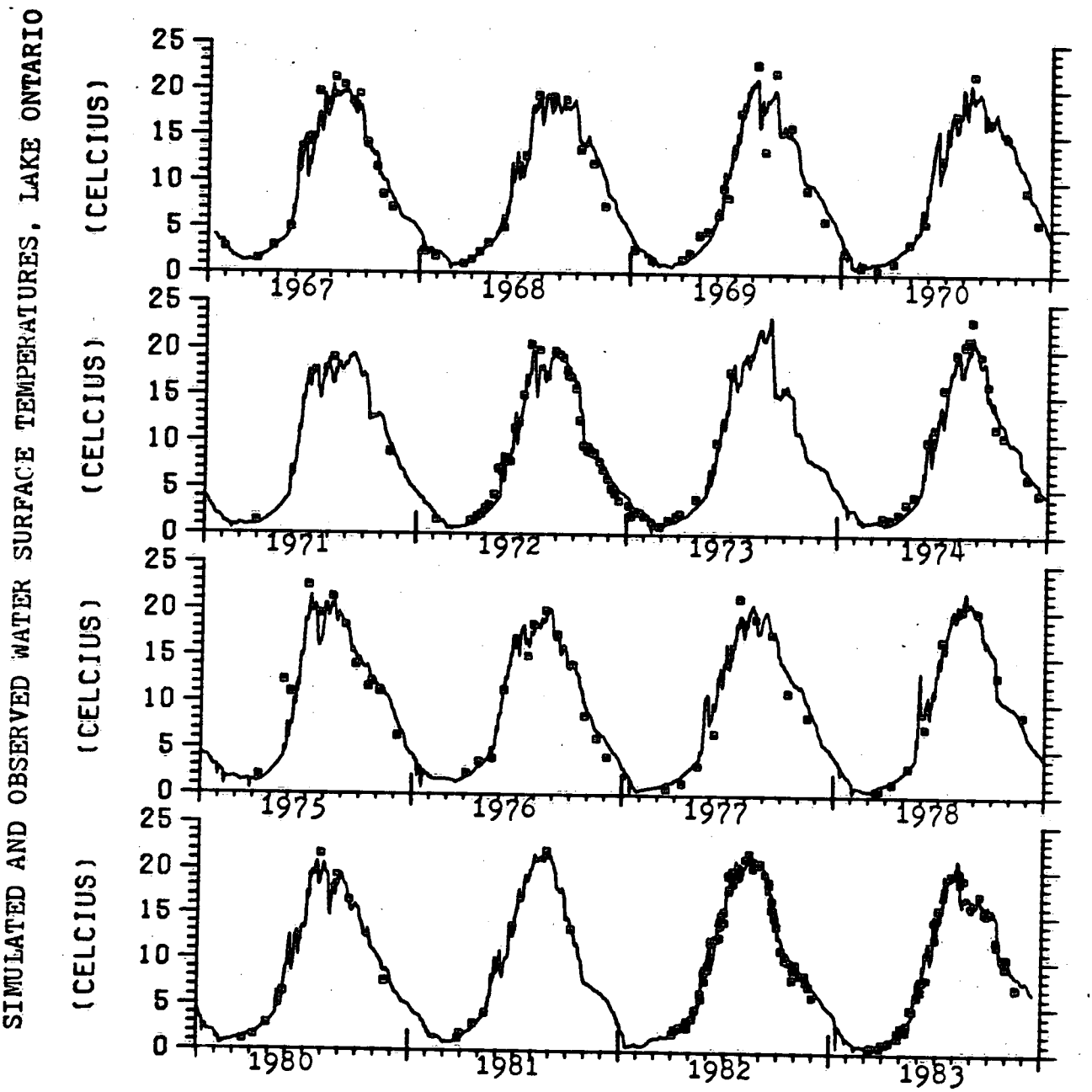

Figure 19. Time series of Lake Ontario simulated and observed water surface temperature 1967 to 1982.

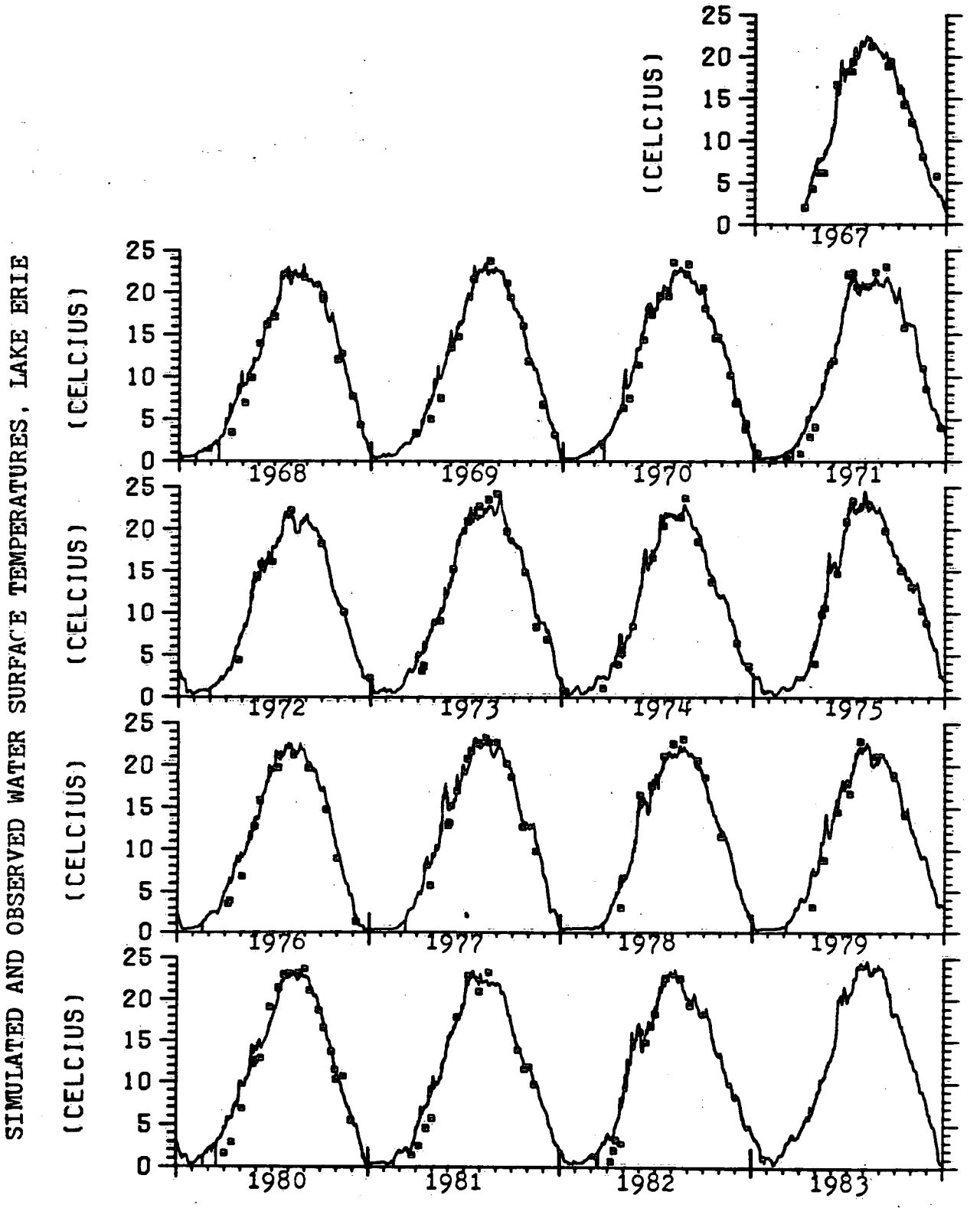

Figure 20. Time series of Lake Erie simulated and observed water surface temperature 1967 to 1983.

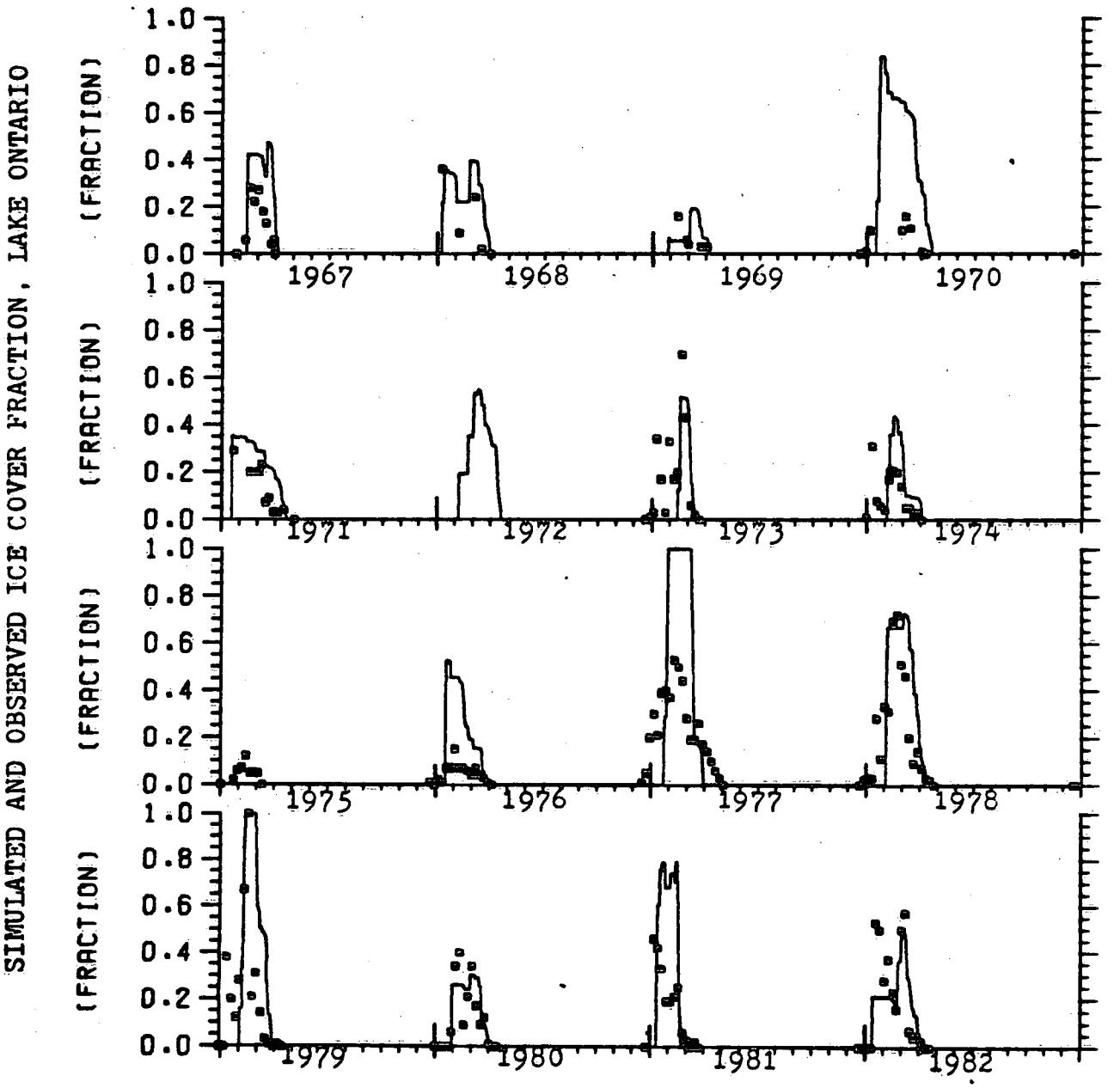

Figure 21. Time series of Lake Ontario simulated and observed fractional ice cover 1967 to 1982.

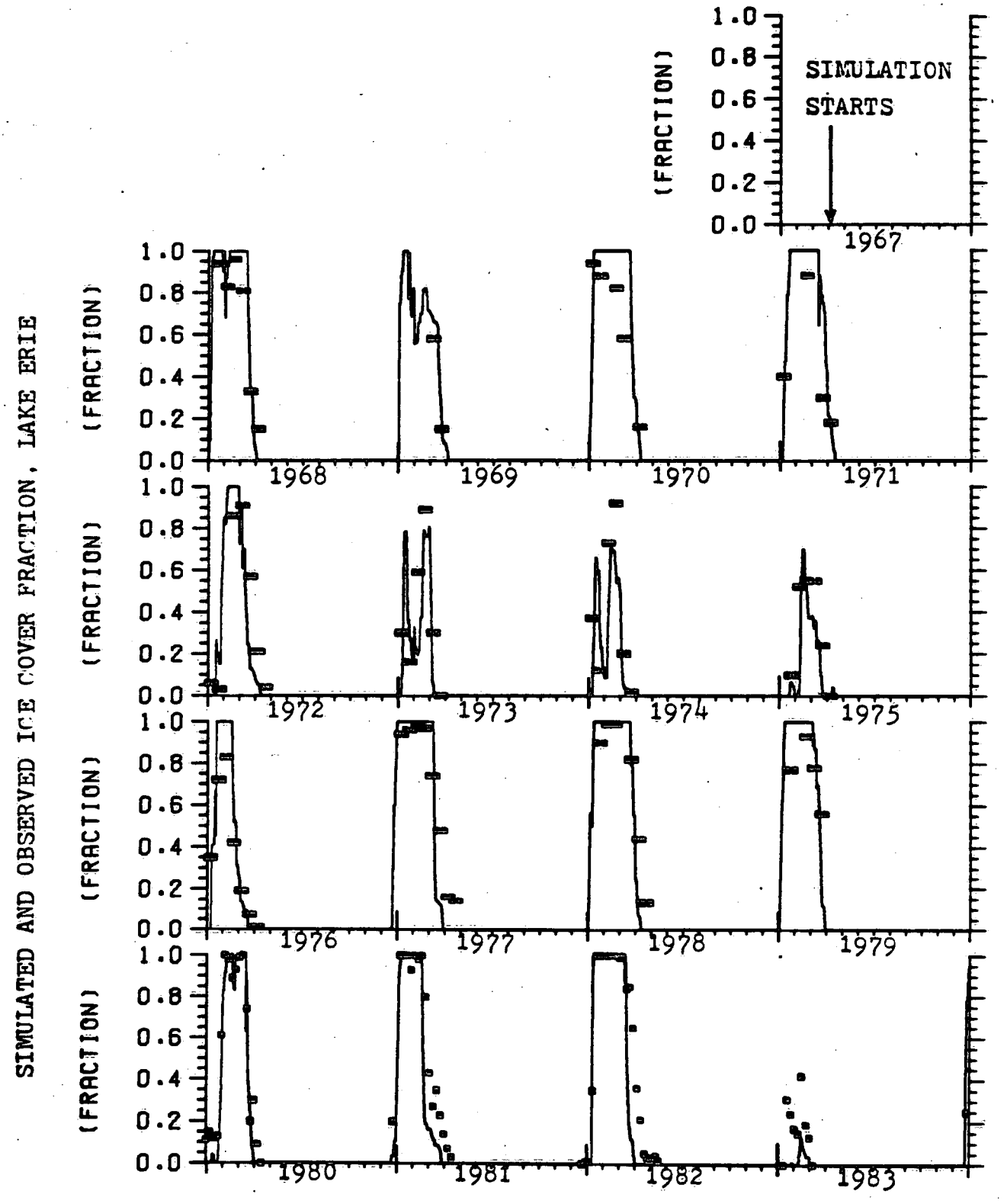

Figure 22. Time series of Lake Erie simulated and observed fractional ice cover 1967 to 1983.

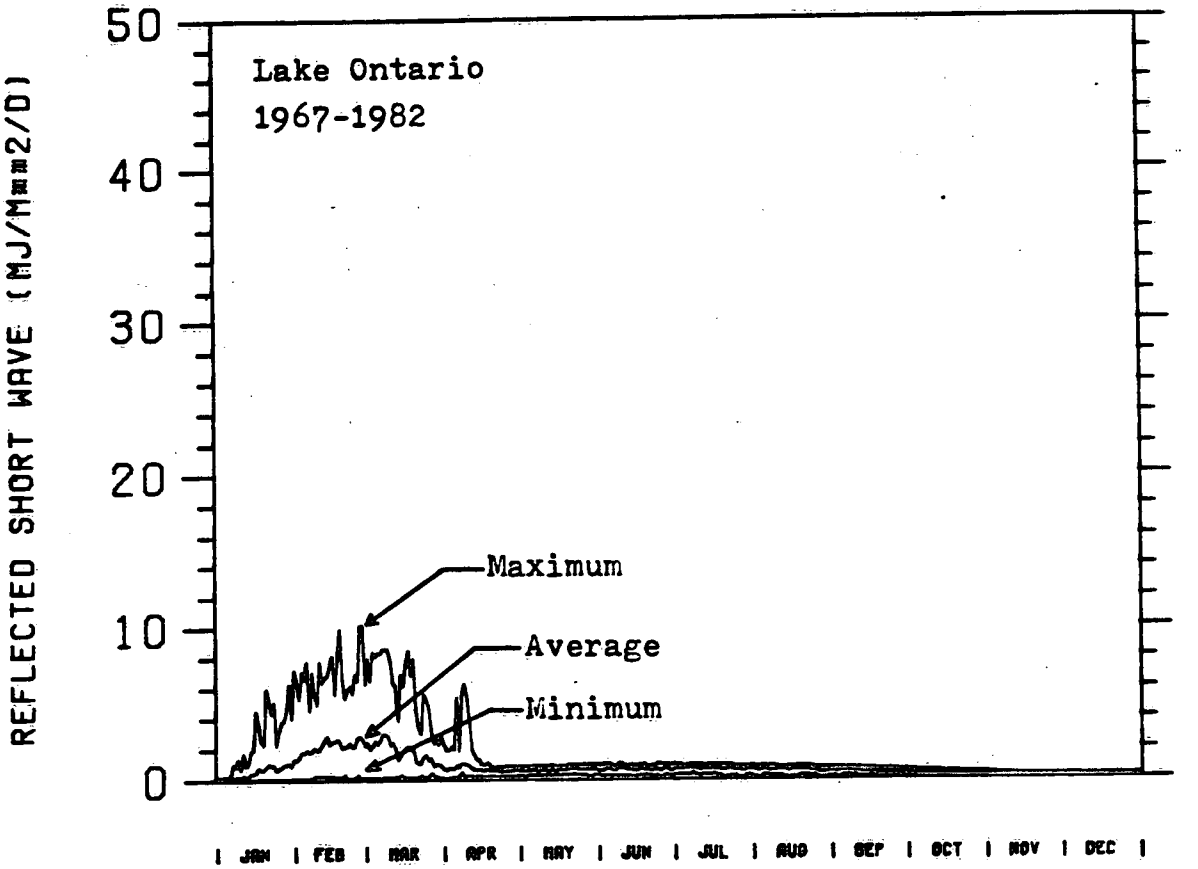

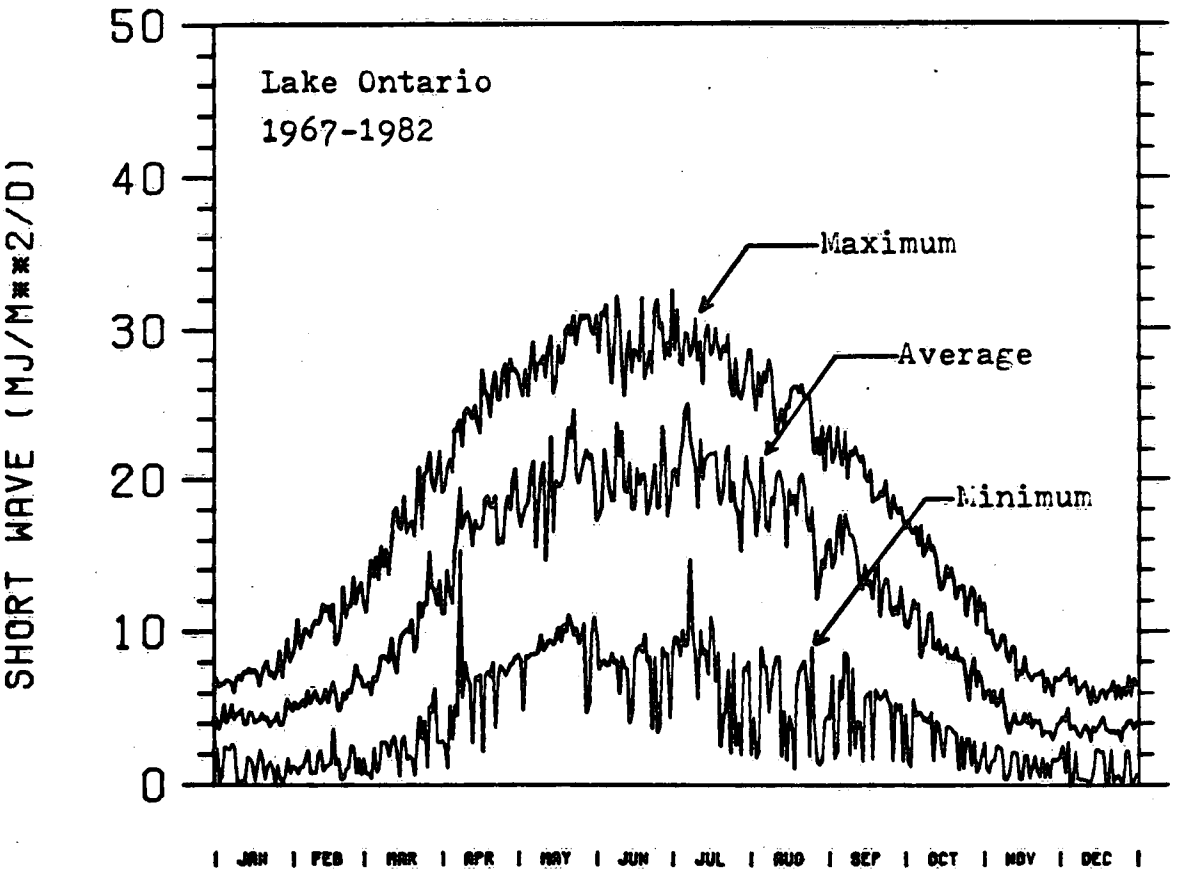

Figure 23. Lake Ontario short wave radiation fluxes longterm averages and ranges 1967 to 1982.

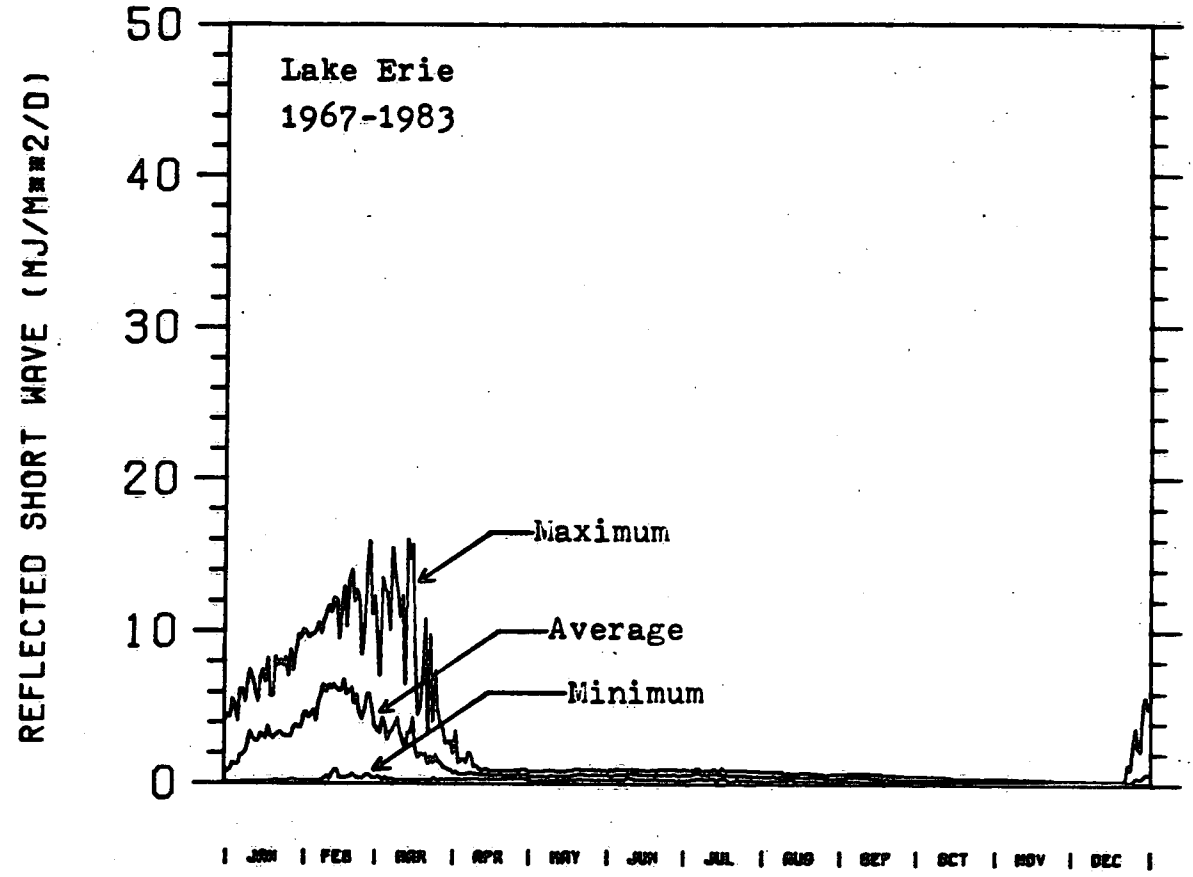

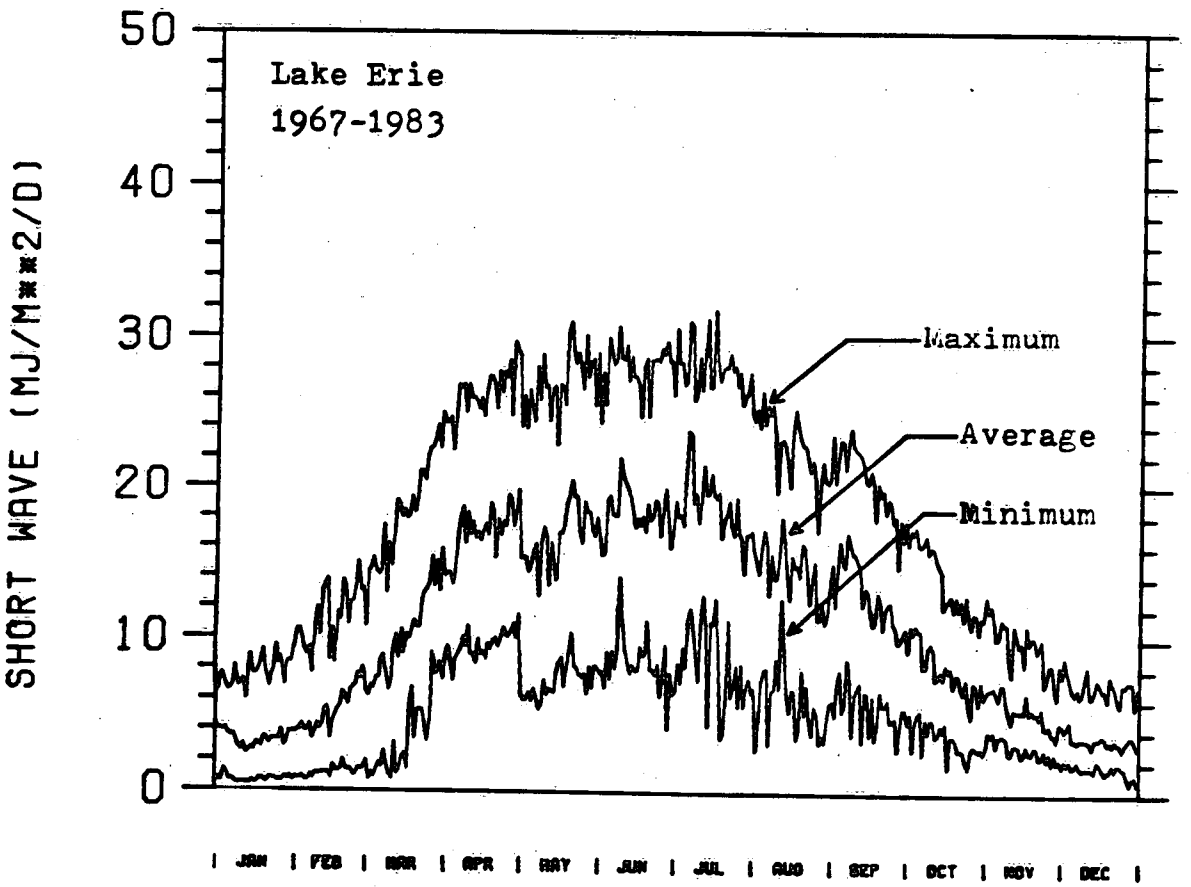

Figure 24. Lake Erie short wave radiation fluxes longterm averages and ranges 1967 to 1983.

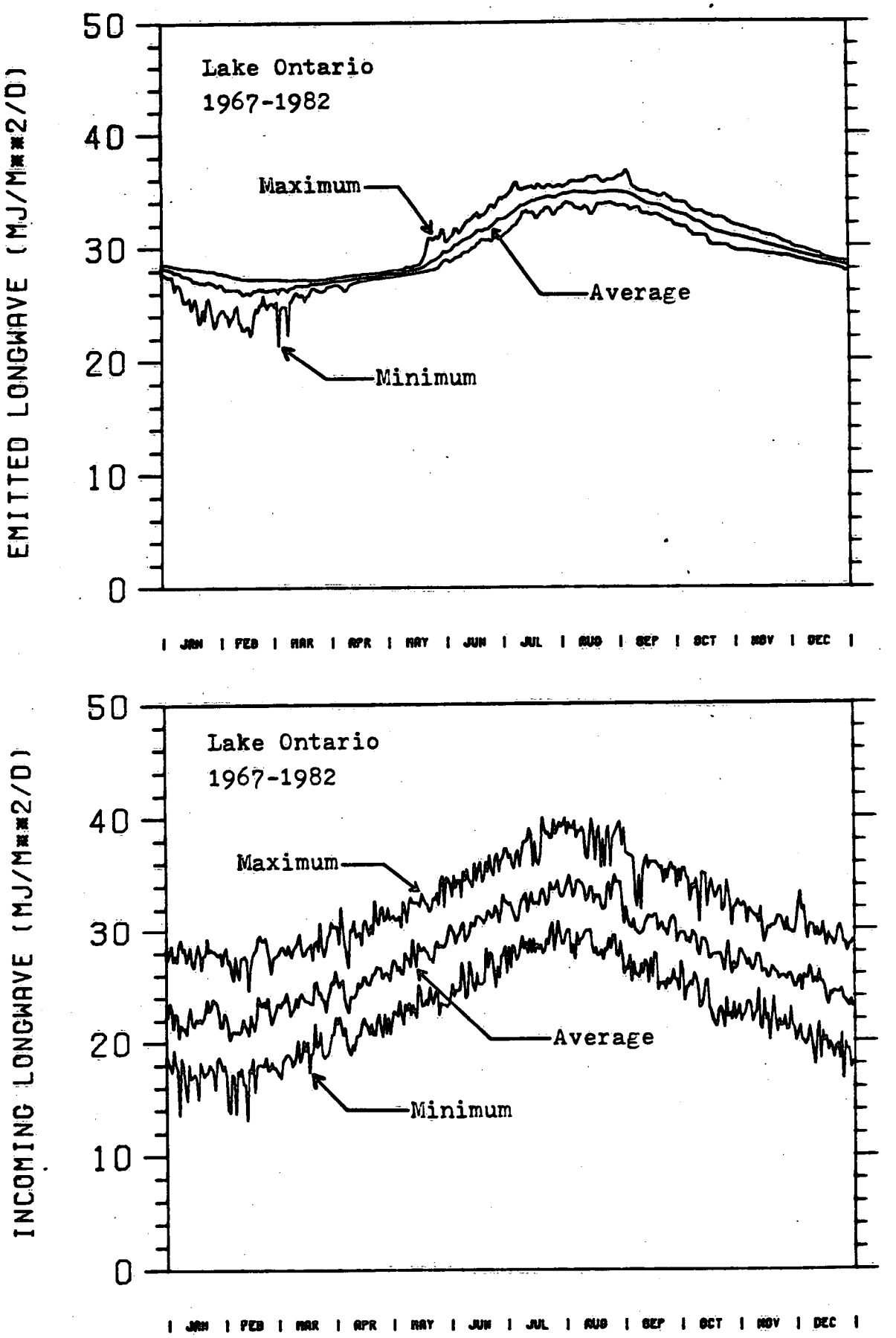

Figure 25. Lake Ontario long wave radiation fluxes longterm averages and ranges 1967 to 1982.

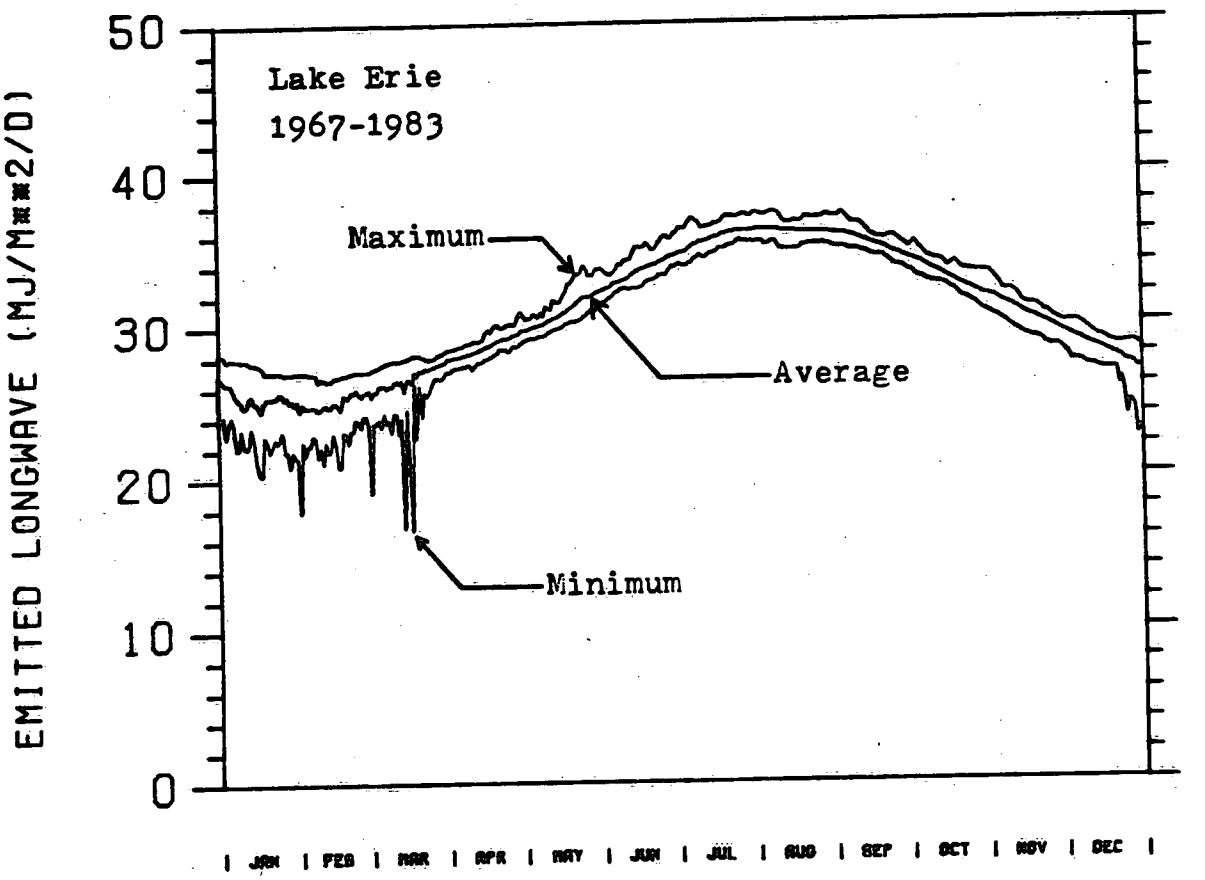

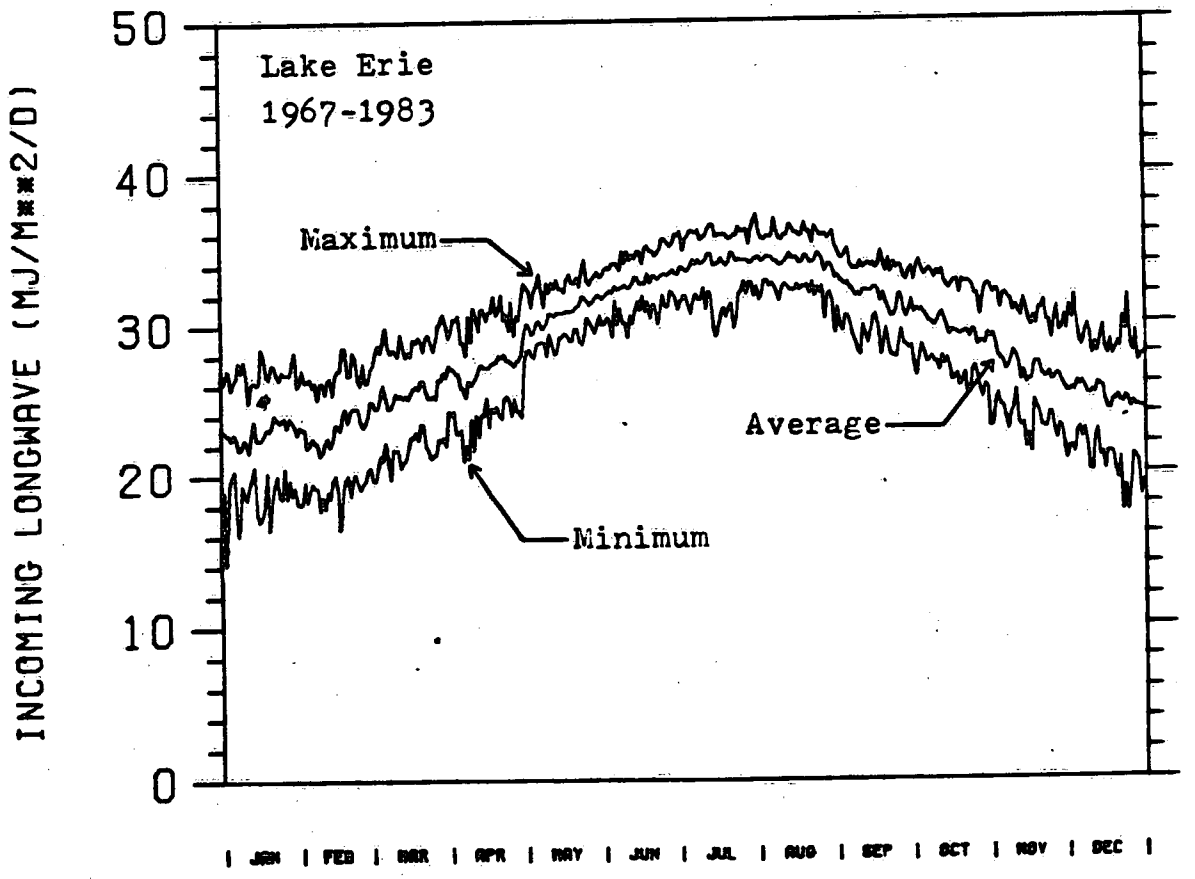

Figure 26. Lake Erie long wave radiation fluxes longterm averages and ranges 1967 to 1983.

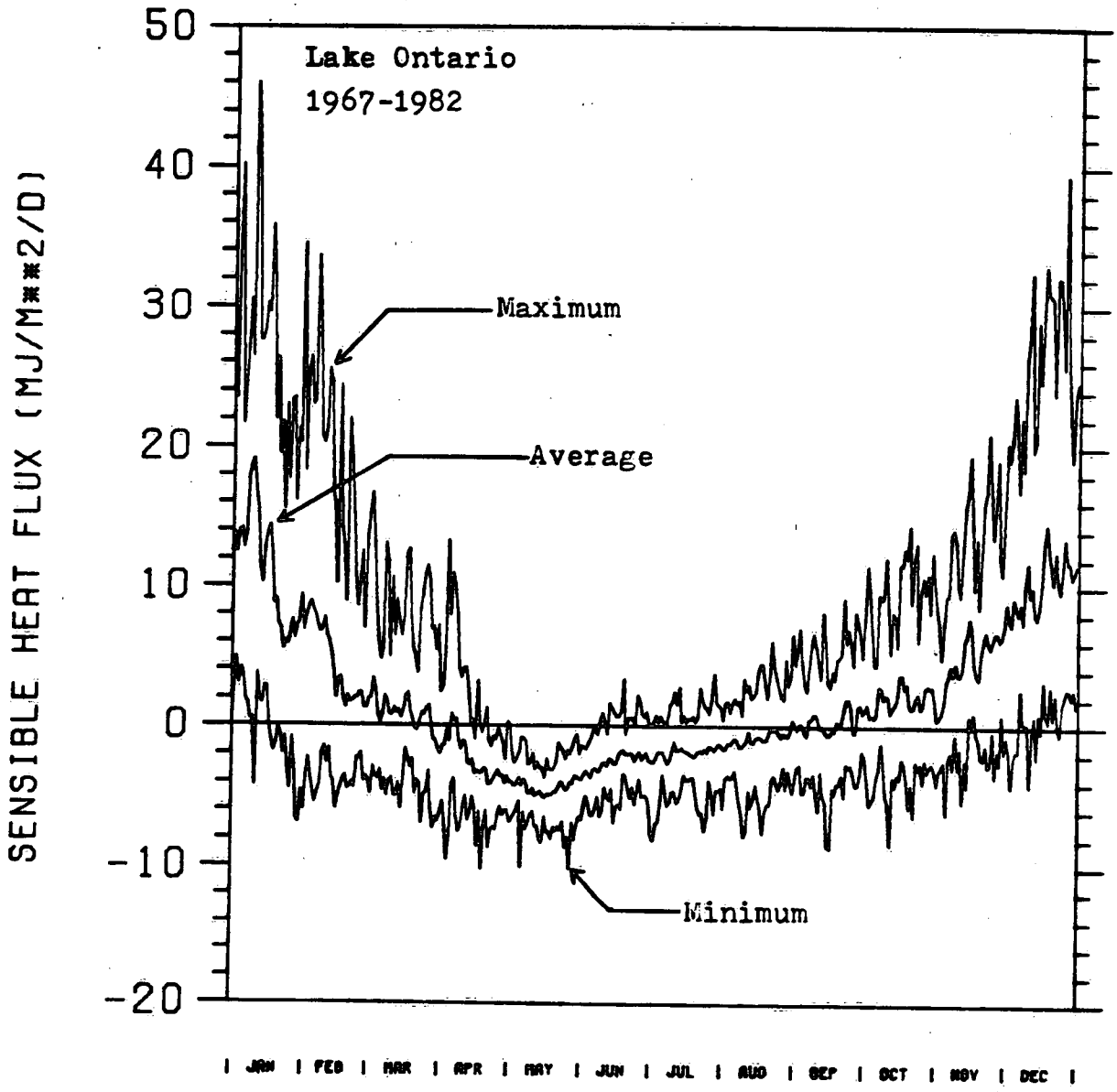

Figure 27. Lake Ontario sensible heat flux longterm average and range 1967 to 1982.

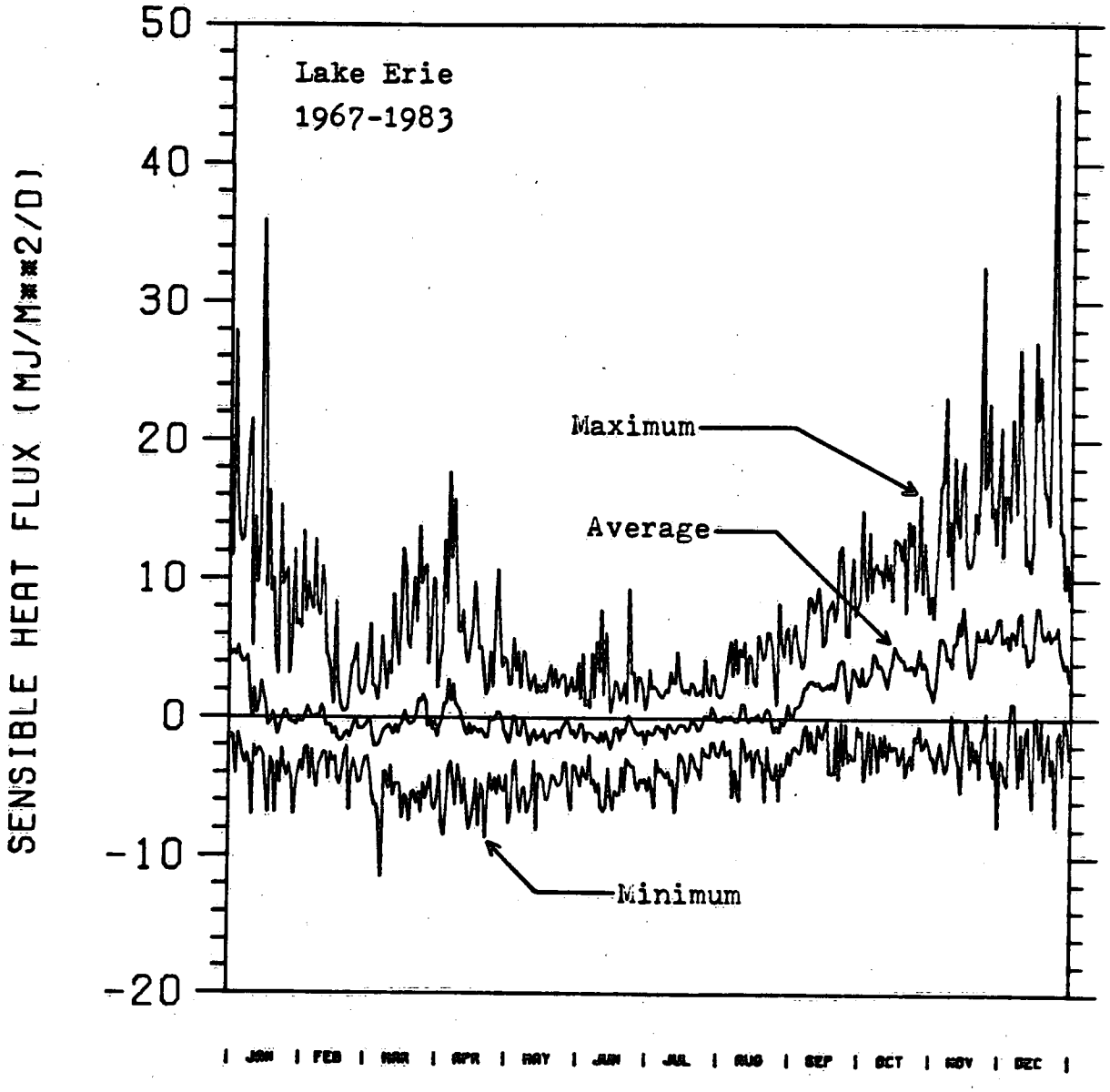

Figure 28. Lake Erie sensible heat flux longterm average and range 1967 to 1983.

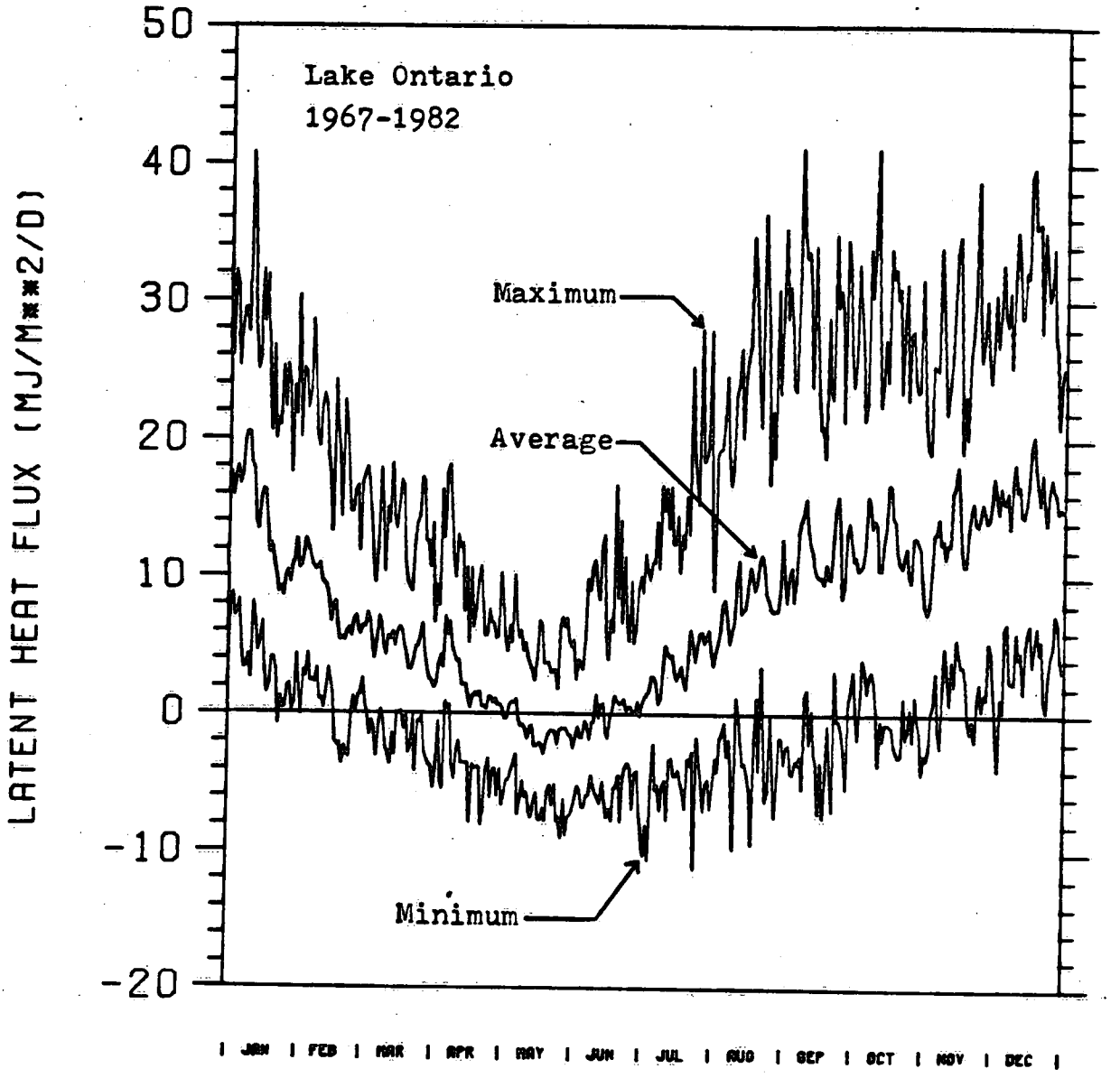

Figure 29. Lake Ontario latent heat flux longterm average and range 1967 to 1982.

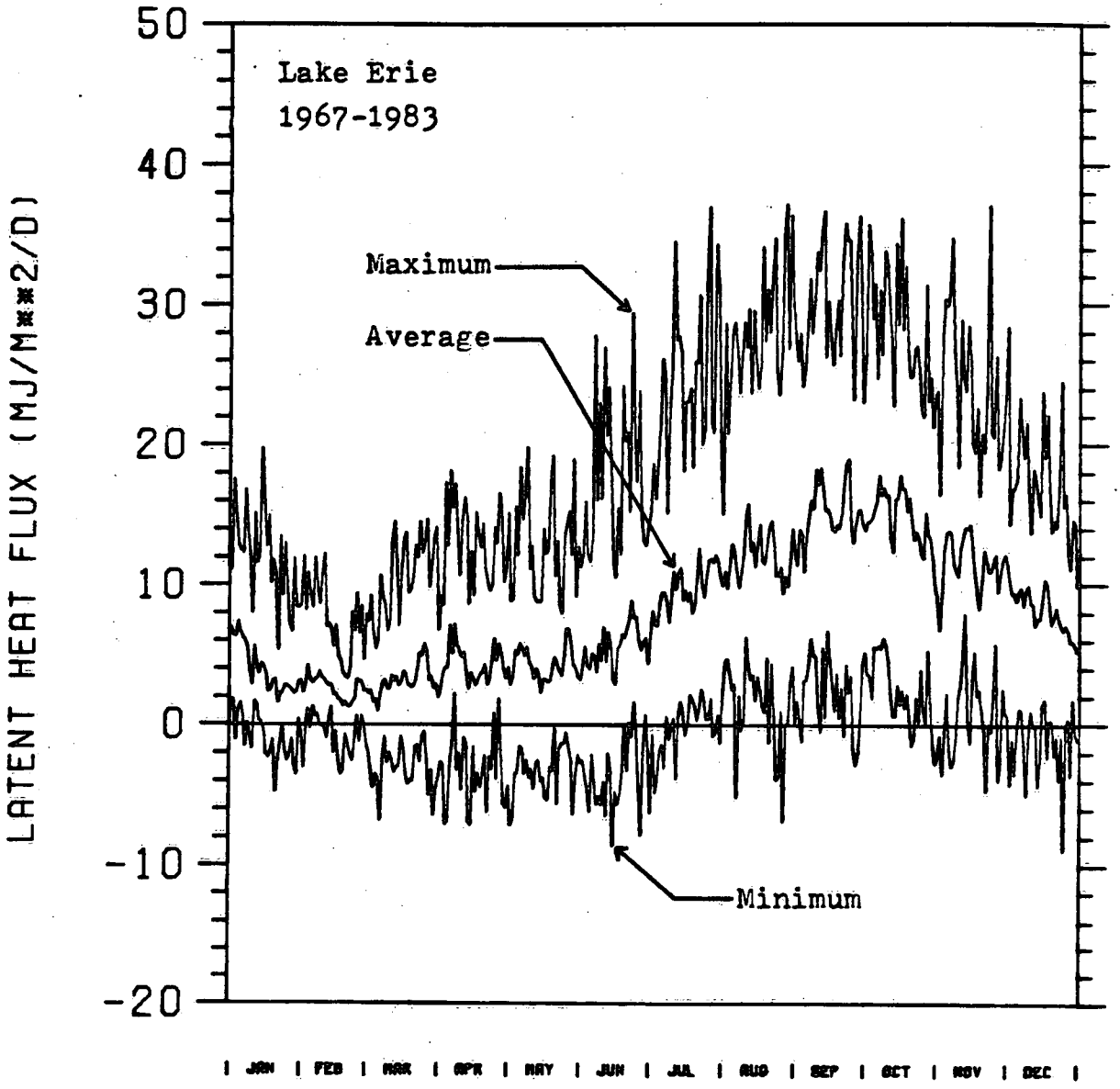

Figure 30. Lake Erie latent heat flux longterm average and range 1967 to 1983.

APPENDIX 1

Lake Ontario and Lake Erie two-day average wind speed departures from long-term mean.

APPENDICES

A1 Lake Ontario and Lake Erie two-day average wind speed departures from long-term mean.

A2 Lake Ontario and Lake Erie air temperature difference from long-term mean.

A3 Lake Ontario and Lake Erie vapour pressure difference from long-term mean.

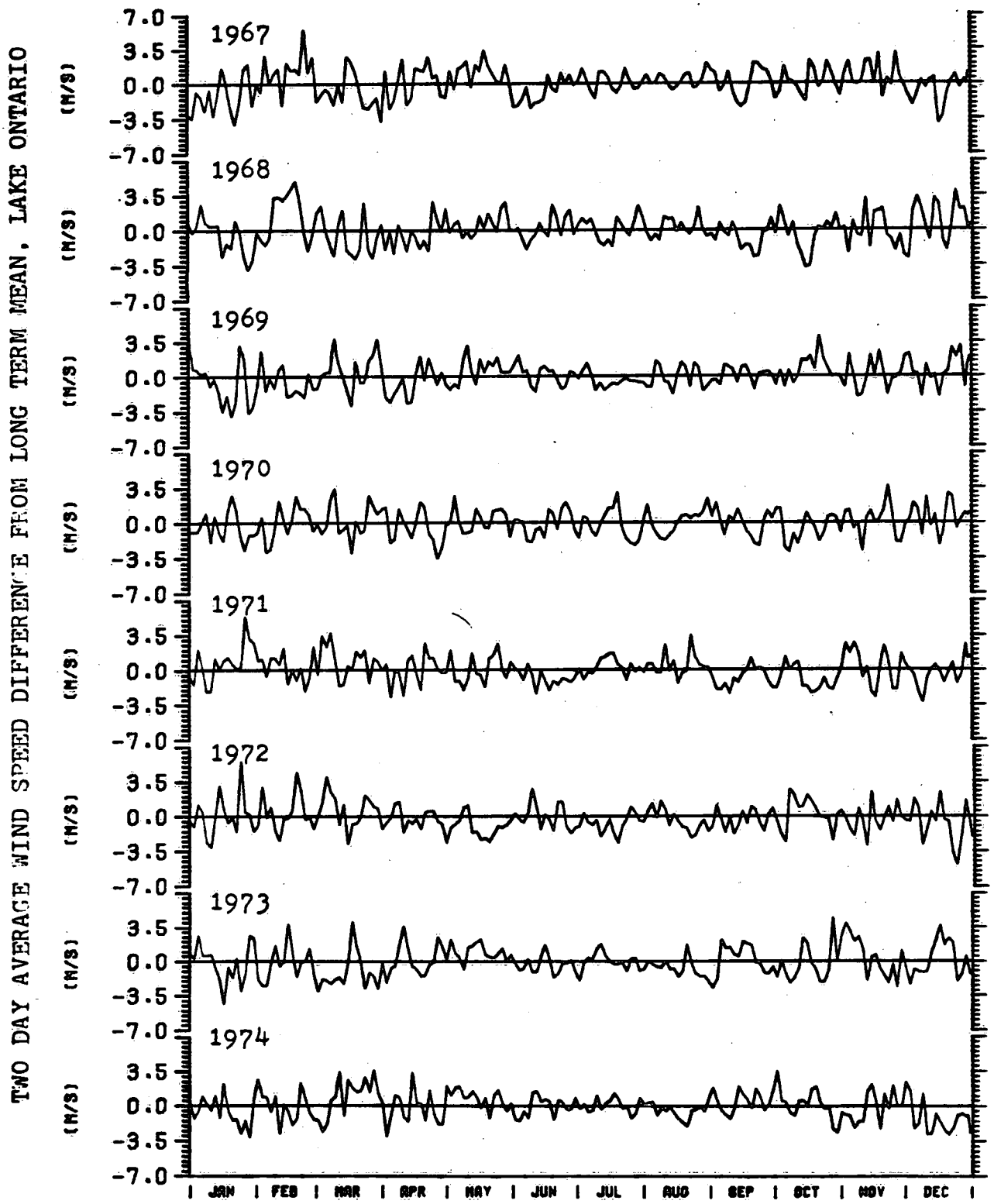
TWO DAY AVERAGE WIND SPEED DIFFERENCE FROM LONG TERM MEAN, LAKE ONTARIO
(M/S)
7.0
3.5
0.0
-3.5
-7.0
1967
1968
1969
1970
1971
1972
1973
1974
JAN
FEB
MAR
APR
MAY
JUN
JUL
AUG
SEP
OCT
NOV
DEC

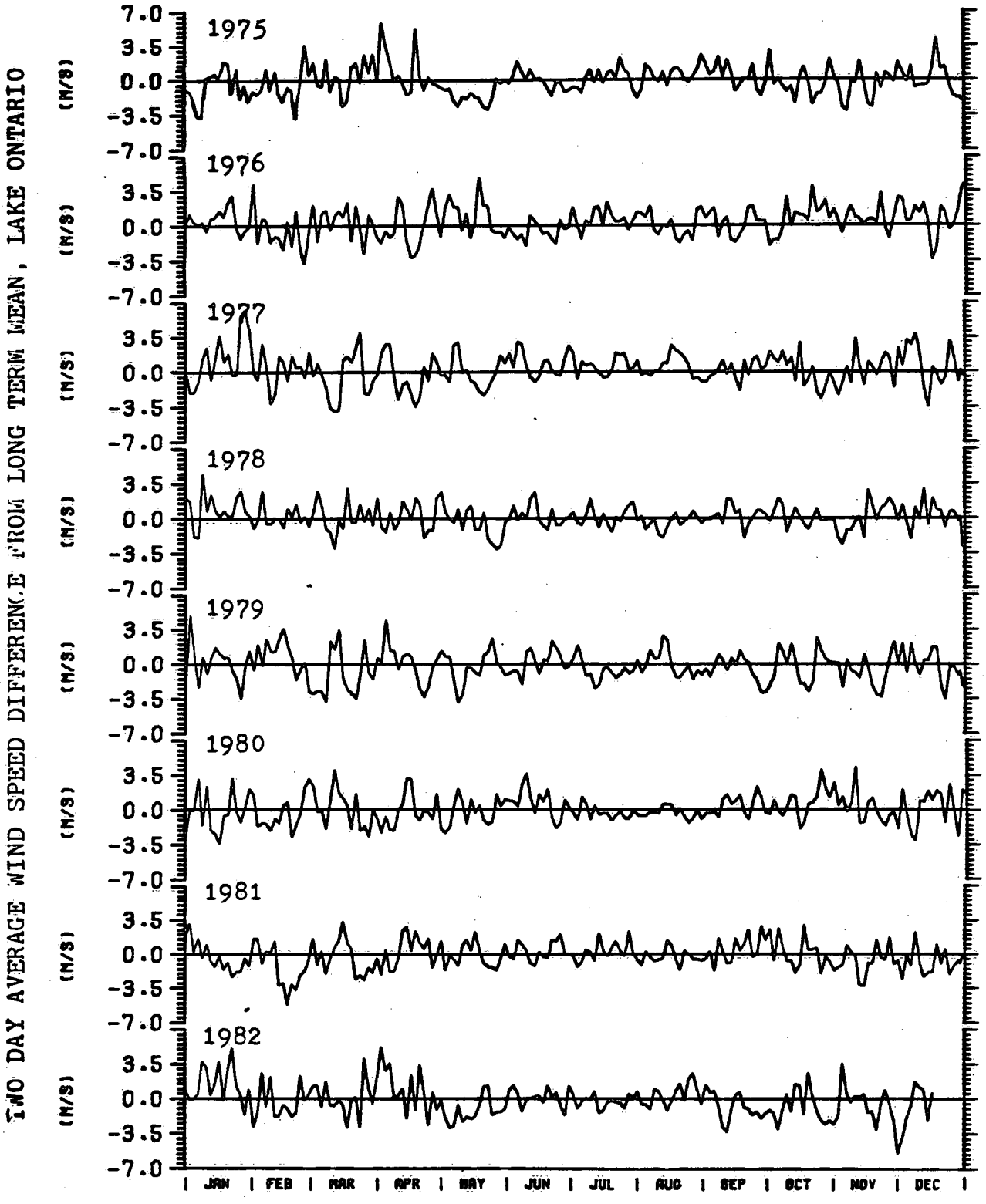
TWO DAY AVERAGE WIND SPEED DIFFERENCE FROM LONG TERM MEAN, LAKE ONTARIO
(M/S)
7.0
3.5
0.0
-3.5
-7.0
1975
1976
1977
1978
1979
1980
1981
1982
JAN
FEB
MAR
APR
MAY
JUN
JUL
AUG
SEP
OCT
NOV
DEC

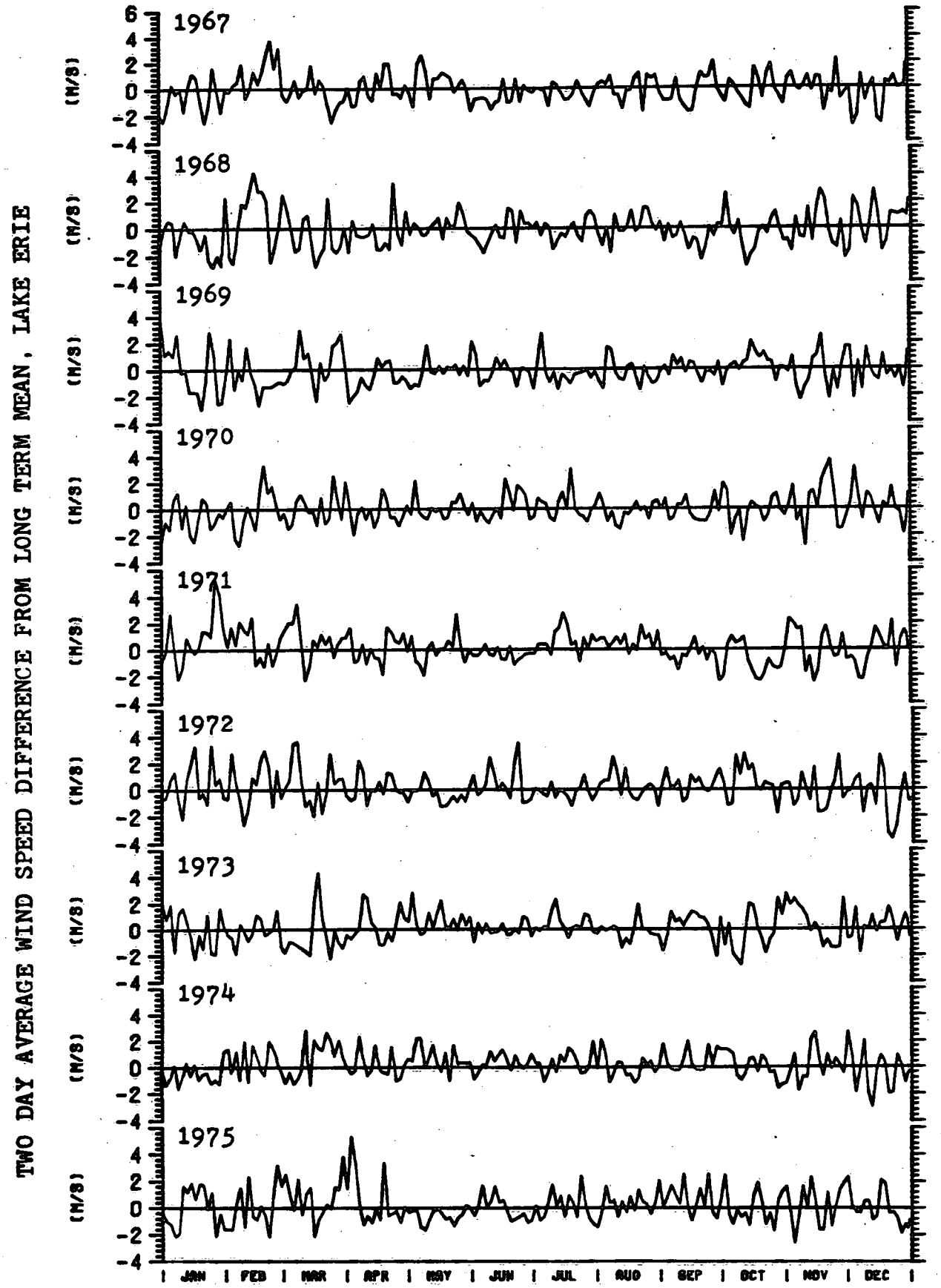
TWO DAY AVERAGE WIND SPEED DIFFERENCE FROM LONG TERM MEAN, LAKE ERIE
1967
1968
1969
1970
1971
1972
1973
1974
1975
(M/S)
6
4
2
0
-2
-4
JAN
FEB
MAR
APR
MAY
JUN
JUL
AUG
SEP
OCT
NOV
DEC

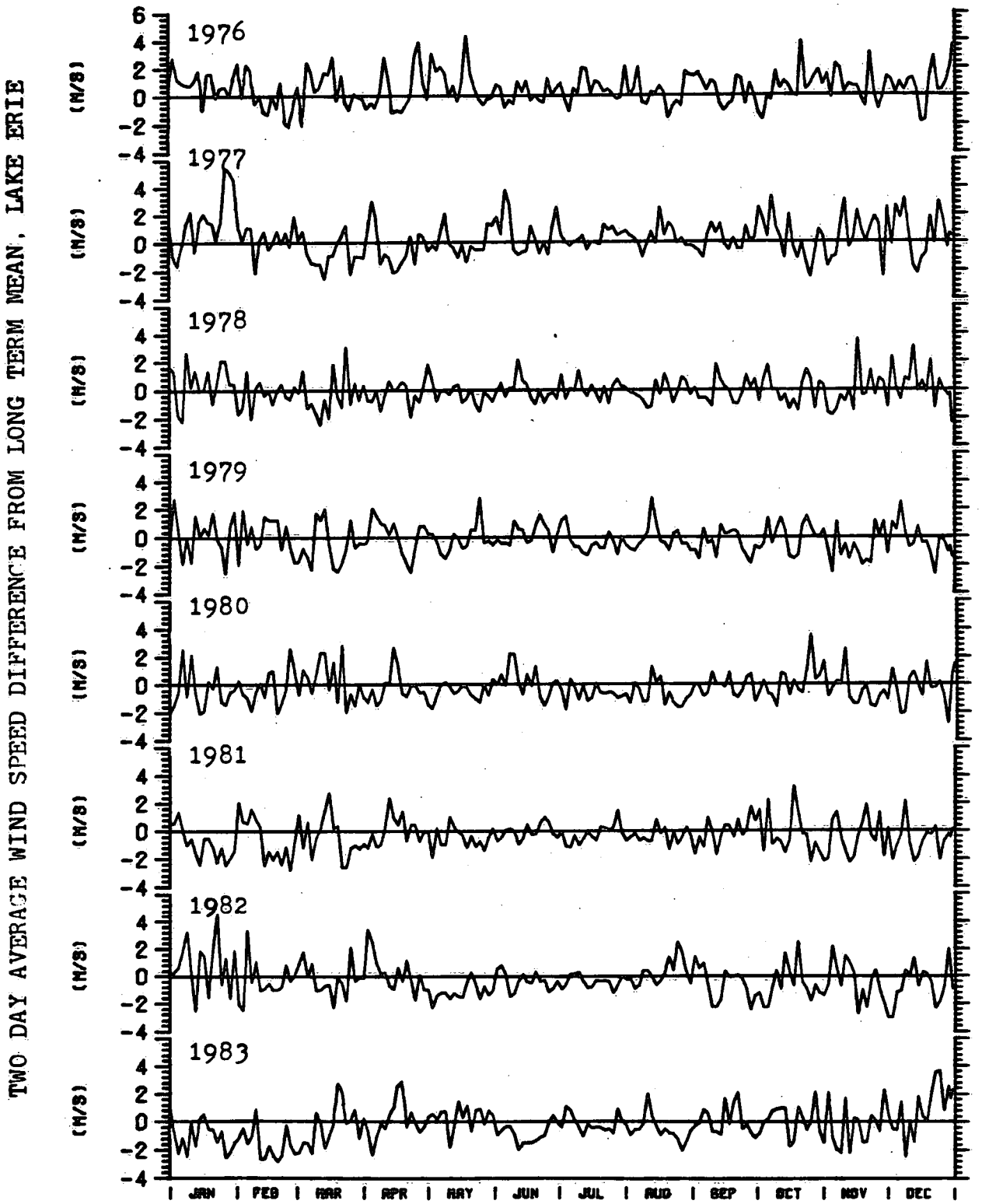
TWO DAY AVERAGE WIND SPEED DIFFERENCE FROM LONG TERM MEAN, LAKE ERIE
1976
1977
1978
1979
1980
1981
1982
1983
(M/S)
6
4
2
0
-2
-4
JAN
FEB
MAR
APR
MAY
JUN
JUL
AUG
SEP
OCT
NOV
DEC

APPENDIX 2

Lake Ontario and Lake Erie air temperature

difference from long-term mean.

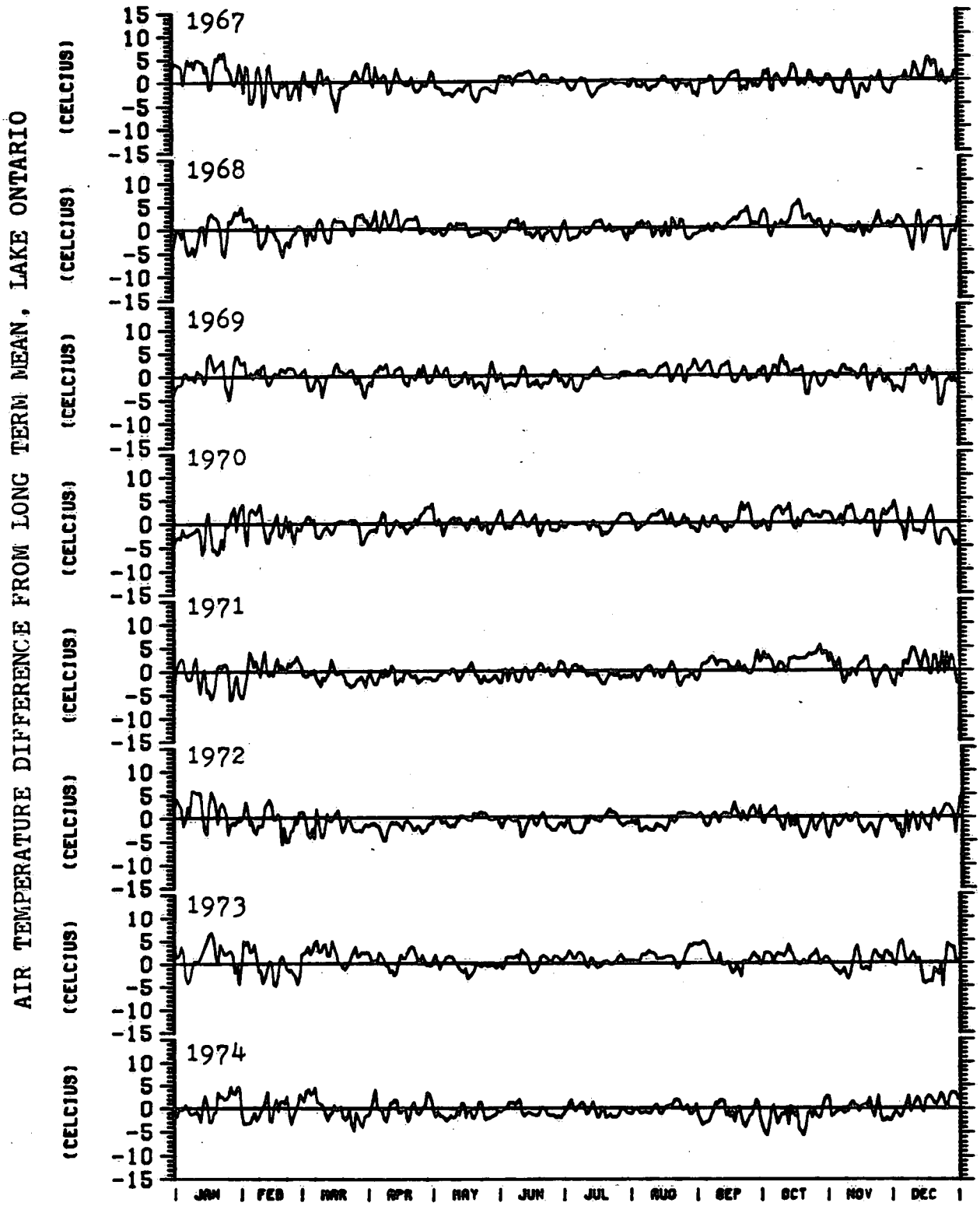
AIR TEMPERATURE DIFFERENCE FROM LONG TERM MEAN, LAKE ONTARIO
(CELCIUS)
1967
1968
1969
1970
1971
1972
1973
1974
15
10
5
0
-5
-10
-15
JAN
FEB
MAR
APR
MAY
JUN
JUL
AUG
SEP
OCT
NOV
DEC

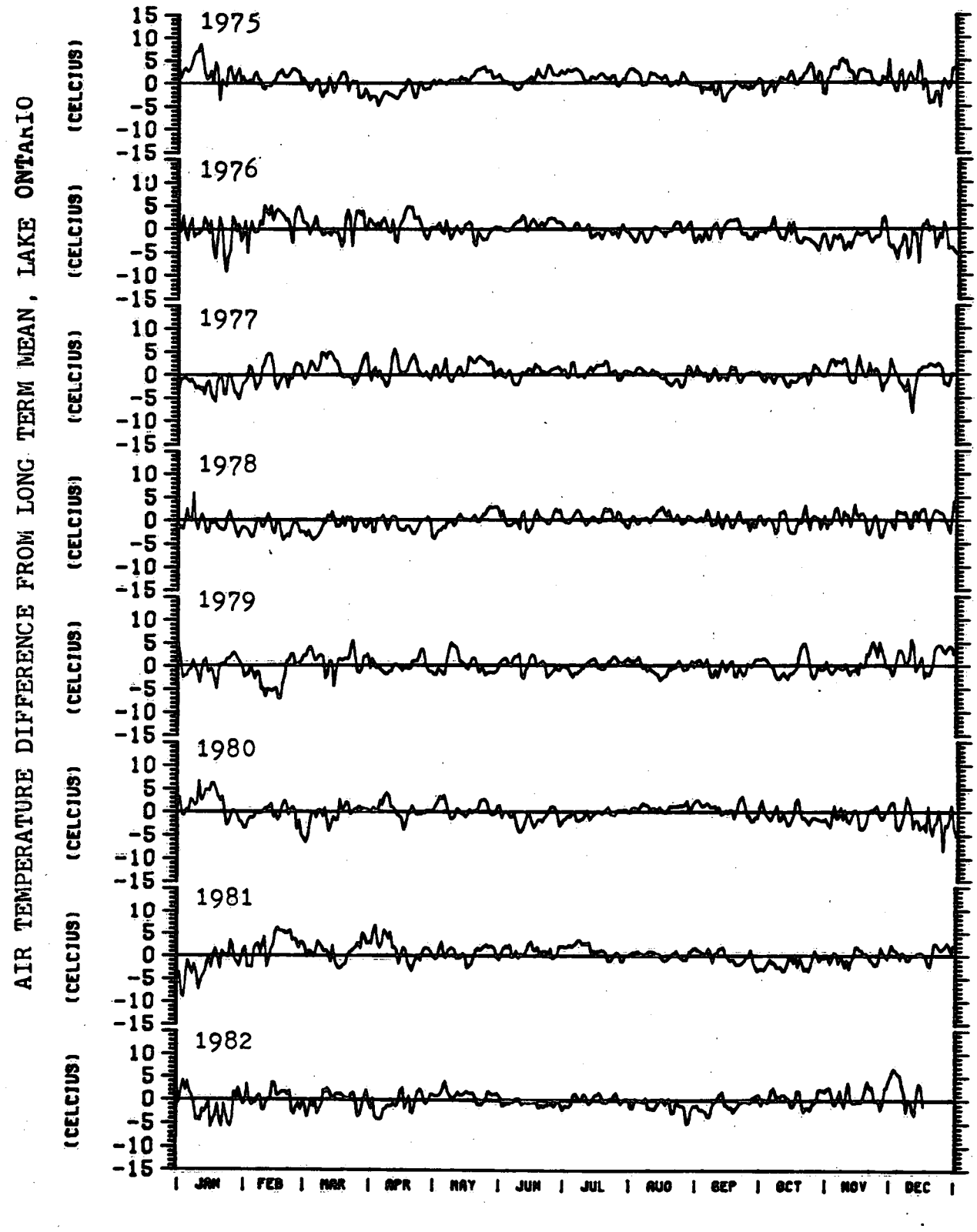
AIR TEMPERATURE DIFFERENCE FROM LONG TERM MEAN, LAKE ONTARIO
(CELCIUS)
1975
1976
1977
1978
1979
1980
1981
1982
15
10
5
0
-5
-10
-15
JAN
FEB
MAR
APR
MAY
JUN
JUL
AUG
SEP
OCT
NOV
DEC

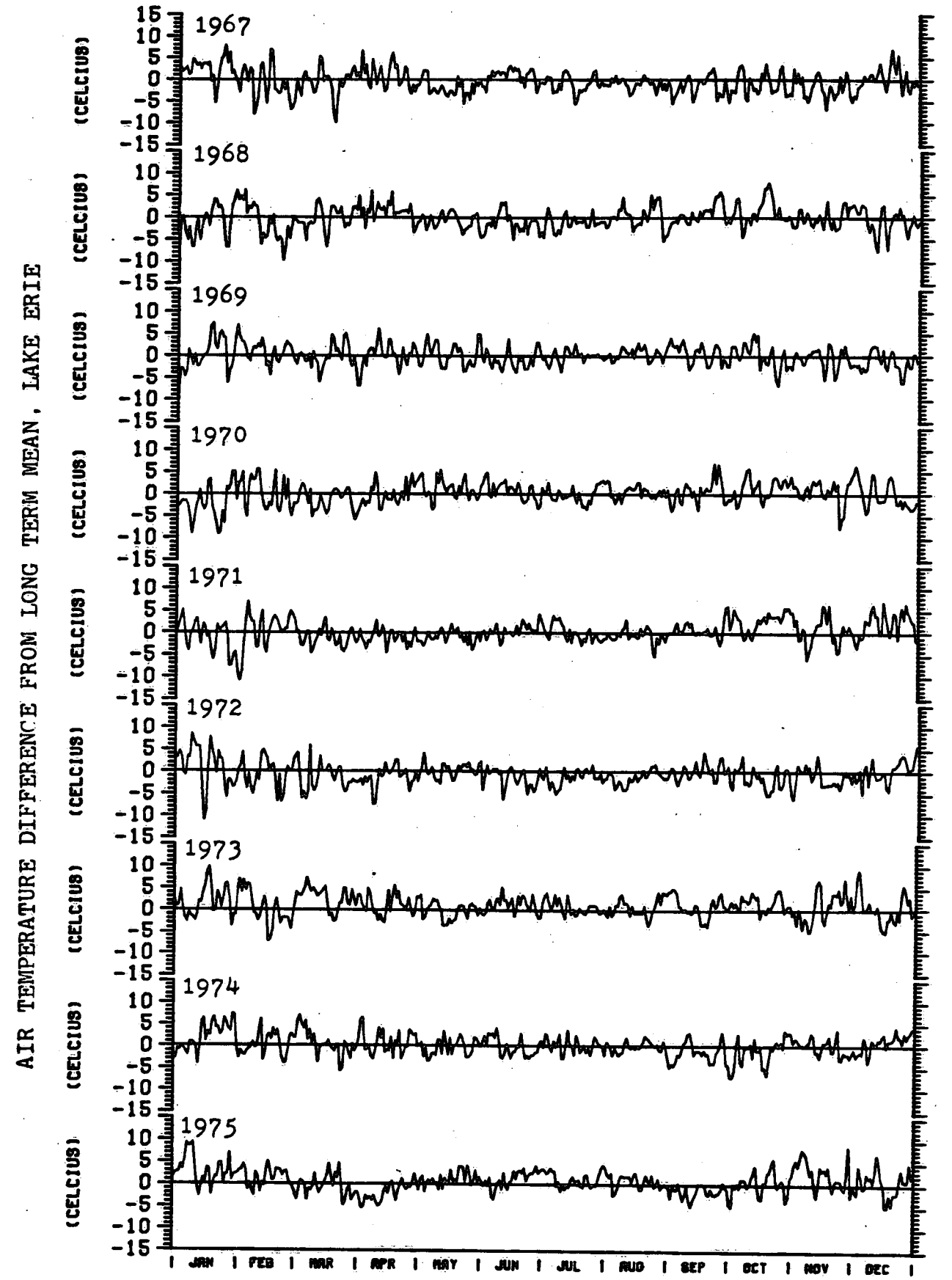
AIR TEMPERATURE DIFFERENCE FROM LONG TERM MEAN, LAKE ERIE
(CELCIUS)
1967
1968
1969
1970
1971
1972
1973
1974
1975
15
10
5
0
-5
-10
-15
JAN
FEB
MAR
APR
MAY
JUN
JUL
AUG
SEP
OCT
NOV
DEC

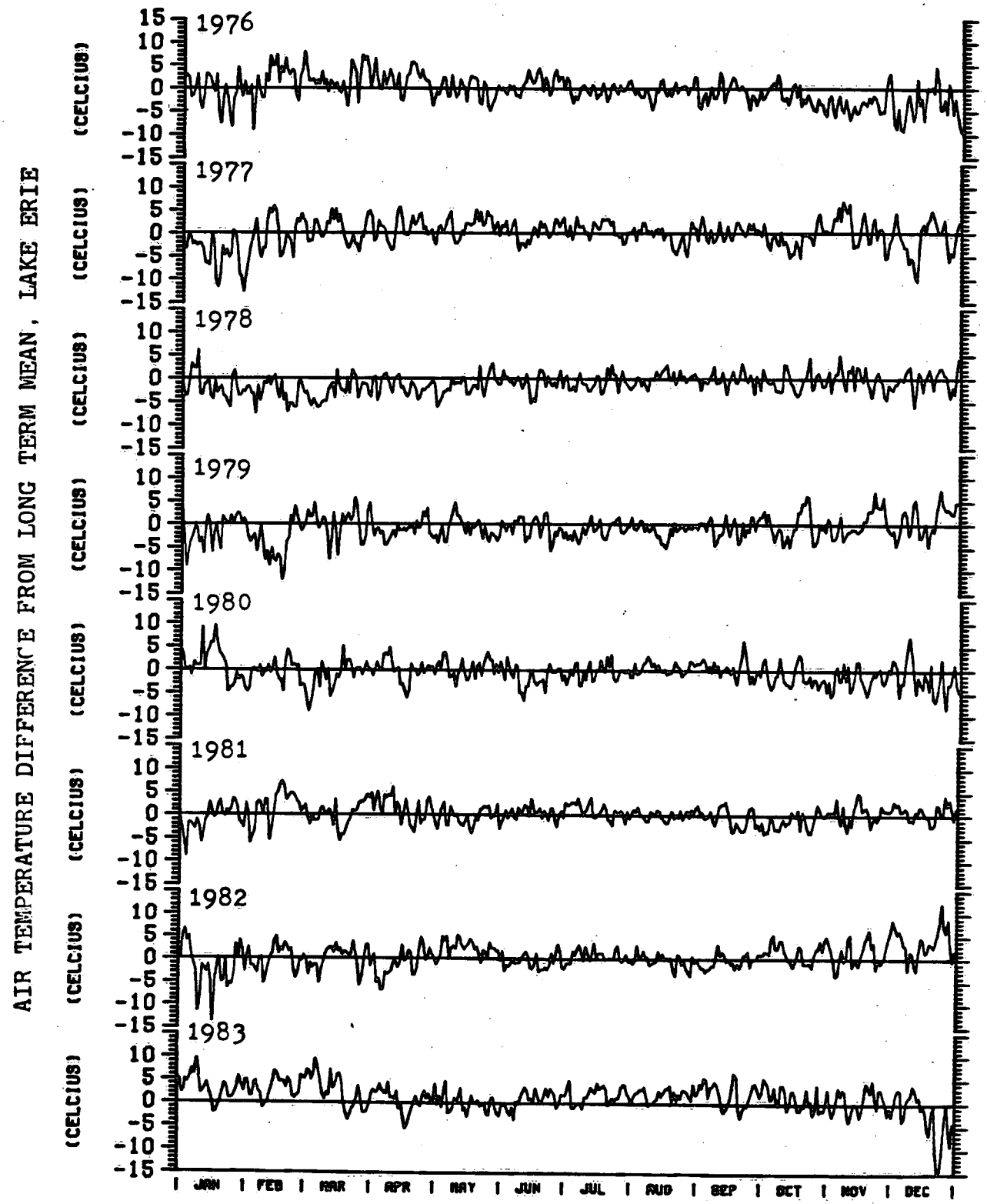
AIR TEMPERATURE DIFFERENCE FROM LONG TERM MEAN, LAKE ERIE
(CELCIUS)
1976
1977
1978
1979
1980
1981
1982
1983
15
10
5
0
-5
-10
-15
JAN
FEB
MAR
APR
MAY
JUN
JUL
AUG
SEP
OCT
NOV
DEC

APPENDIX 3

Lake Ontario and Lake Erie vapour pressure

difference from long-term mean.

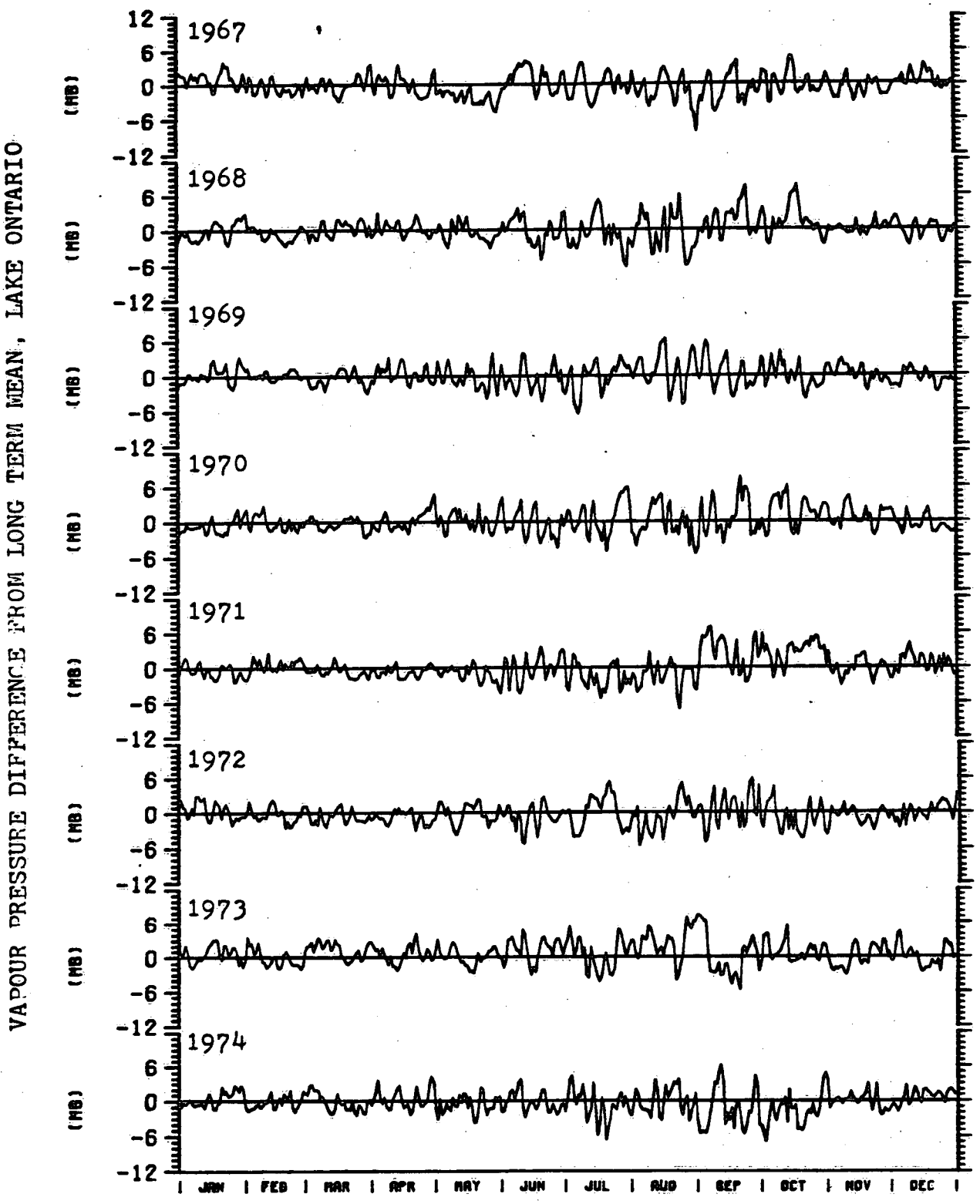
VAPOUR PRESSURE DIFFERENCE FROM LONG TERM MEAN, LAKE ONTARIO
1967
1968
1969
1970
1971
1972
1973
1974
(MB)
12
6
0
-6
-12
JAN
FEB
MAR
APR
MAY
JUN
JUL
AUG
SEP
OCT
NOV
DEC

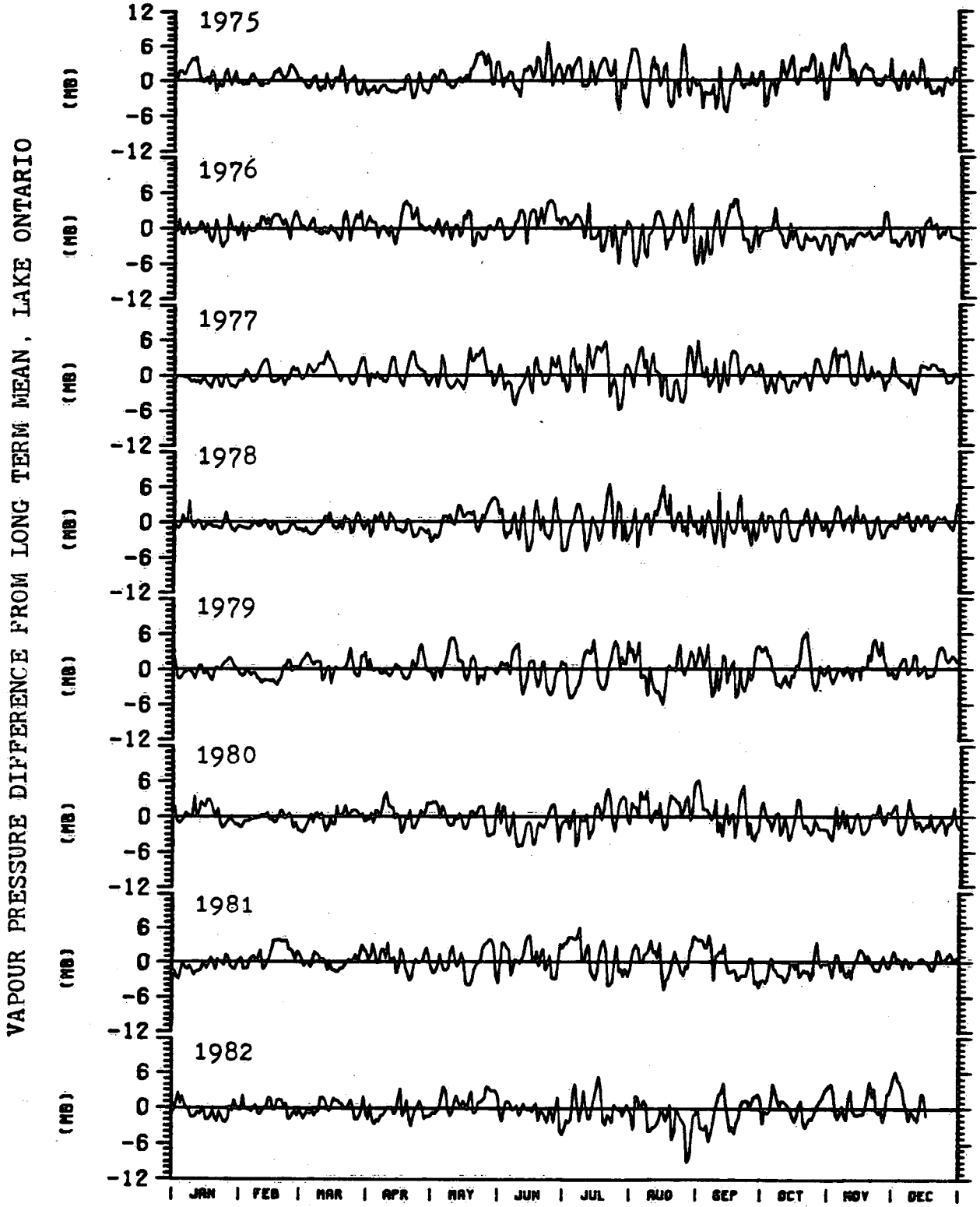
VAPOUR PRESSURE DIFFERENCE FROM LONG TERM MEAN, LAKE ONTARIO
1975
1976
1977
1978
1979
1980
1981
1982
(MB)
12
6
0
-6
-12
JAN
FEB
MAR
APR
MAY
JUN
JUL
AUG
SEP
OCT
NOV
DEC

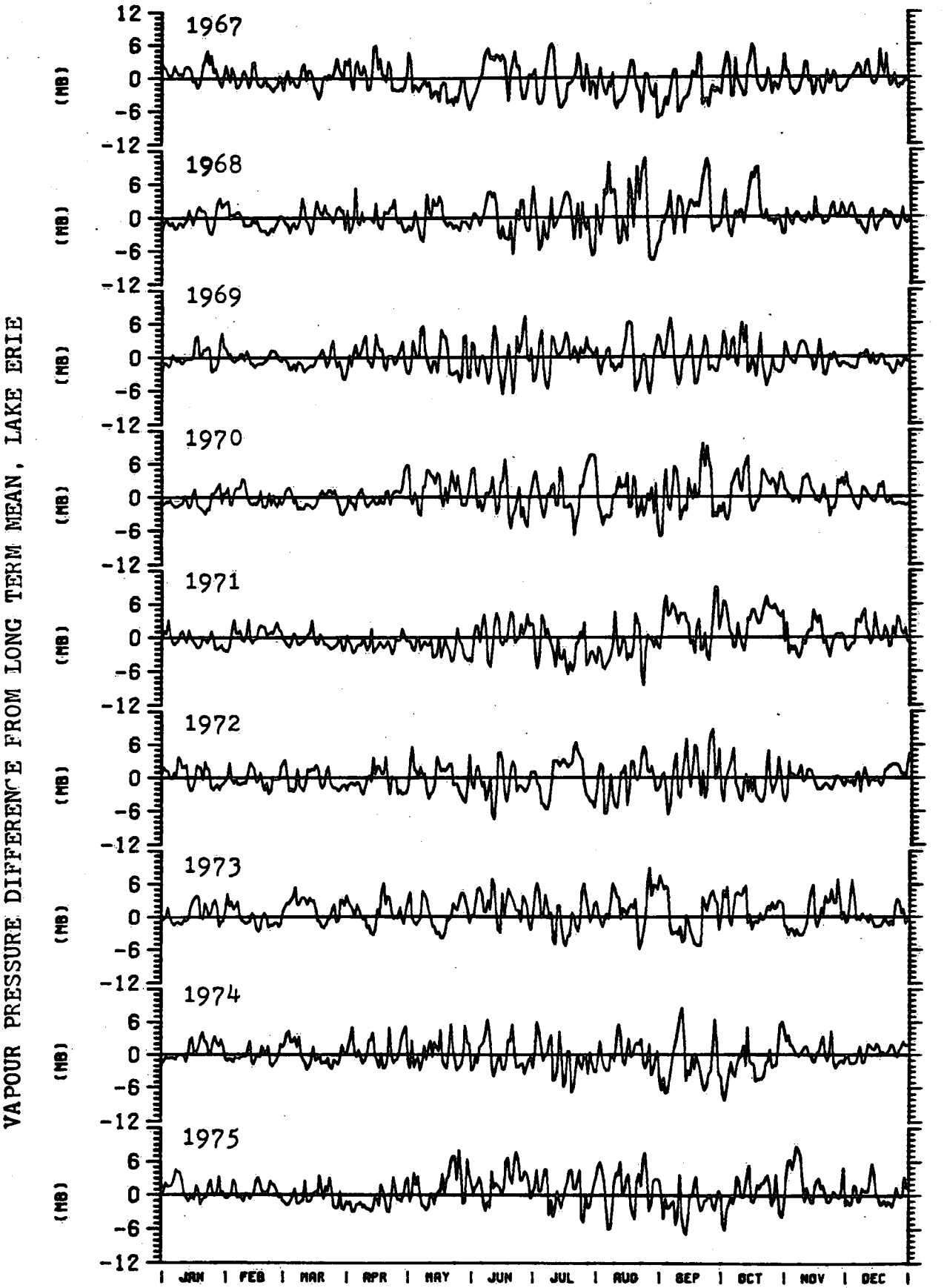
VAPOUR PRESSURE DIFFERENCE FROM LONG TERM MEAN, LAKE ERIE
1967
1968
1969
1970
1971
1972
1973
1974
1975
(MB)
12
6
0
-6
-12
JAN
FEB
MAR
APR
MAY
JUN
JUL
AUG
SEP
OCT
NOV
DEC

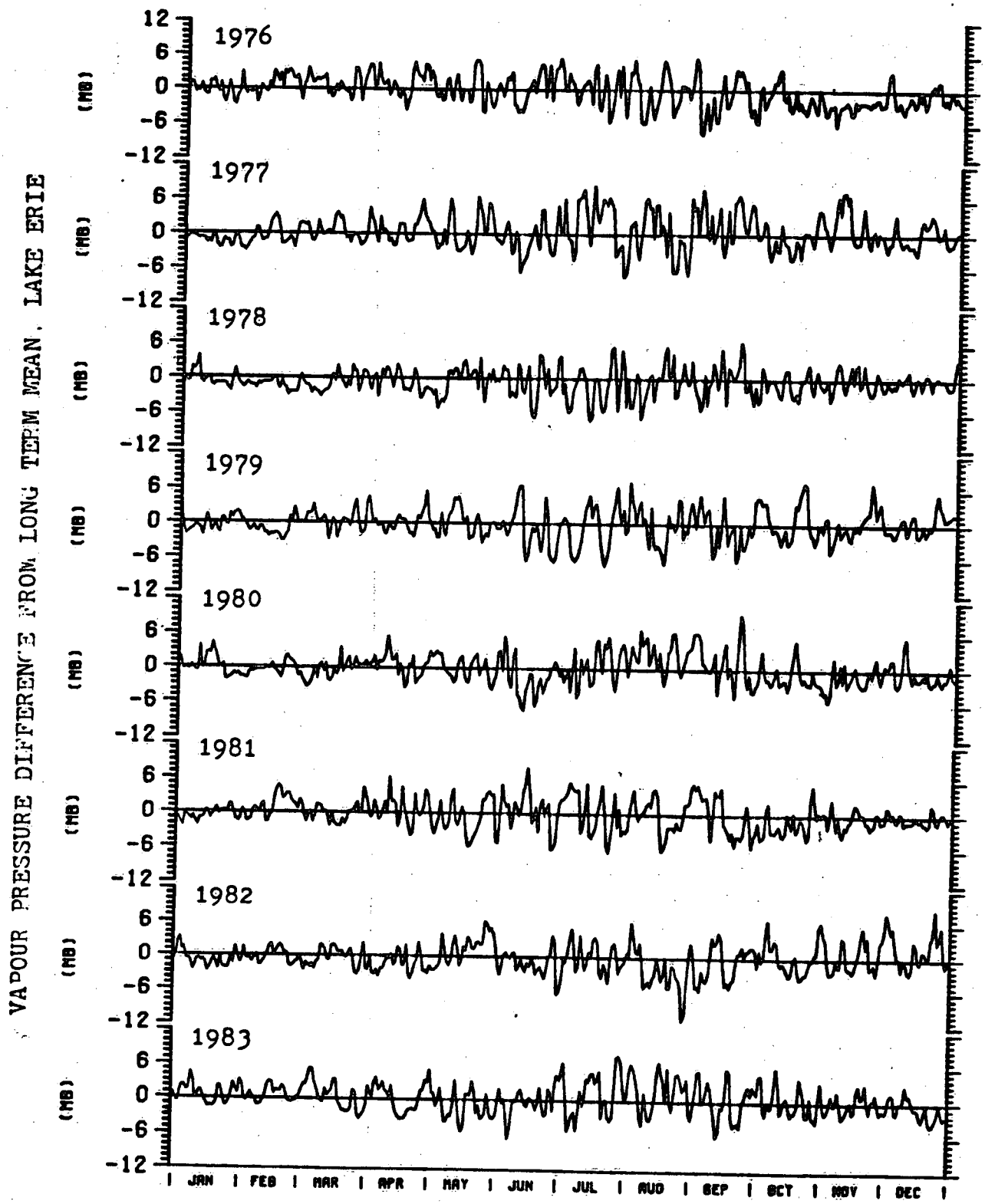
VAPOUR PRESSURE DIFFERENCE FROM LONG TERM MEAN, LAKE ERIE
1976
1977
1978
1979
1980
1981
1982
1983
(MB)
12
6
0
-6
-12
JAN
FEB
MAR
APR
MAY
JUN
JUL
AUG
SEP
OCT
NOV
DEC